Studies Towards The Synthesis of Novel Tridentate Ligands For Use In Ruthenium Metathesis Catalysts

A THESIS

Submitted in fulfilment of the requirements for the degree of

MASTER OF SCIENCE

of

RHODES UNIVERSITY

By

Tanya Millward

B.Sc. Hons. (Rhodes University)

January 2008

ABSTRACT

This work has focussed on the preparation of a variety of tridentate ligands, designed to form ruthenium complexes as potential metathesis catalysts. Various approaches to the tridentate, malonate-tethered imidazolidine system have been investigated, and a promising route to accessing ligands of this type is discussed. A tridentate malonate-tethered pyridine ligand has been successfully prepared and its dithallium salt has been accessed by hydrolysis with thallium carbonate; approaches to a longer-chain analogue have also been investigated. A thallium pyridine-2,6-dicarboxylate ligand has been has been successfully prepared, as have a range of pyridine diamine ligands, with various alkyl and aromatic substituents on the amine donor atoms. Preliminary investigations into the potential of these compounds as ligands for alkylidene ruthenium complexes are reported using molecular modelling techniques. The geometries and steric energies of the ligands and their corresponding complexes have been analysed, and results obtained from two different software packages are compared. Finally, some preliminary complexation studies have been undertaken.

CONTENTS

ACKNOWLEDGEMENTS

My extreme gratitude to my superviser, Prof. Perry Kaye, must be sincerely expressed. Prof. Kaye has demonstrated the utmost patience during the course of this study, and gently encouraged me to keep on path when I've been tempted to stray. His kind guidance and encouragement have been sincerely appreciated, without which I would not have made it through.

Many thanks to all those in the Rhodes University Chemistry Department for their time, expertise and friendship. Dr. Rosa Klein has been instrumental in her guidance and encouragement, particularly with the organometallic investigations. Likewise, the guidance, encouragement and support provided by Dr. Gary Watkins were invaluable. His help with organometallic studies and IR interpretation has been greatly appreciated. Mr. Kevin Lobb and Mr Emmanuel Lamprecht have given much of their time to help me with the computational work. Similarly, Dr. Zeni Tshentu sacrificed his time to help me with the ICP analyses. Many thanks to Mr. Sonneman for the mass spectrometry results, and to Mr. Albert van Wyk and Mr. Sunny Sunnassee for proof-reading parts of this thesis. To quote Prof. Mike Davies-Coleman, the chemistry department can only function as a team, and without the help and friendship of all the students and staff this work would not have been possible.

The support and love of friends and family was the most priceless contribution. Thanks to all my friends in the department for entertaining tea-time discussions, their understanding and empathy of the trials of research made these trials manageable. Lastly, I could not have completed this study without David's unwavering emotional support.

Final thanks to Dr. Wolfgang Meyer from Sasol, for valuable contributions to this study, and to Sasol R&D for financial support.

LIST OF ABBREVIATIONS

CM	Cross metathesis
COSY	^{1}H-^{1}H shift-correlated spectroscopy
DEPT	Distortionless enhancement by polarization transfer
DFT	Density functional theory
DMF	Dimethylformamide
DMSO	Dimethylsulfoxide
IR	Infrared
HMBC	Heteronuclear multiple bond coherence
HSQC	Heteronuclear spin quantum correlation
LAH	Lithium aluminium hydride
Mes	Mesityl
MM	Molecular mechanics
MS	Mass spectrometry
NMR	Nuclear magnetic resonance
NHC	*N*-heterocyclic carbene
PCy_3	Tricyclohexyl phosphine
PPh_3	Triphenyl phosphine
RCM	Ring closing metathesis
ROM	Ring opening metathesis
ROMP	Ring opening metathesis polymerization
TBAF	*Tert*-butylammonium fluoride
TBDMS	*Tert*-butyldimethylsilyl
TFA	Trifluoracetic acid
THF	Tetrahydrofuran
TLC	Thin layer chromatography
TMSCN	Trimethylsilyl cyanide

LIST OF FIGURES

LIST OF TABLES

1. INTRODUCTION

1.1. CATALYSIS IN INDUSTRY

1.1.1 From art to science

The phenomenon of catalysis has been recognised since the 19th century. Hubert[1] cites publications from 1823 on the combustion of alcohol in the presence of platinum, and of hydrogen in the presence of palladium and iridium wires. At this stage, catalysis was more of an art than a science, and the concept of catalysis was first formally proposed by Berzelius and Emmett in 1836.[1,2] The first really scientific observations of catalysis began in the last half of that century, notably with Ostwald's thermodynamic studies,[1,2] from which he proposed that catalysis may not influence the thermodynamics of the reacting system, but only the kinetics by increasing the rate of the reaction. The development of the Langmuir isotherm in 1912[1] introduced the concept of chemisorption and its role in early catalytic reactions. This sparked interest and debate amongst scientists, leading to the introduction of the concept of active sites by Talyor.[1-3]

While further progress in catalysis in the first half of the 20th century was focused on gas phase studies,[1] some of the most significant developments were made in the second half of that century, driven by the need for the production of motor oil from naptha[2] and the oil crisis of the 1970's.[4] The rapid progress made in the petrochemical industry around this period led to the development of new technologies, such as steam cracking, which provided feedstocks for the chemical industry.[4] Major progress in catalysis within the chemical industry has followed developments in the petrochemical industry, and many catalytic processes important to the chemical industry found their origins in the petrochemical industry.[4]

1.1.2. Classification of catalysts

Catalysts have been classified according to their function, as for example, redox catalysts, acid-base catalysts and polyfunctional catalysts.[5] A more common classification is based on solubilities, with catalysts being described as either heterogeneous or homogeneous catalysts.[5,6] Some authors consider biological catalysts as separate from these two classes of catalysts.[7]

1.1.3. Heterogeneous catalysis

In heterogeneous catalysis, the catalysts, reactants and products are in different phases. The different forms in which the catalyst may be used include powders, pellets or small-sized particles.[5] Today, most industrial applications of catalysis still use heterogeneous catalysts, as they offer important cost advantages. The primary advantages of heterogeneous catalysts typically include greater thermal stability than their homogeneous counterparts[8] and easy separation from the reaction products, permitting cost-effective regeneration of the catalyst.[8] They are, however, not without their limitations. Great difficulty is often encountered in controlling the temperature of the reaction, particularly with exothermic reactions. There are also often problems associated with mass transfer of reactants and products, with the requirement that the catalysts exhibit high mechanical resistance.[5]

1.1.4. Homogeneous catalysis

Homogeneous catalysis, on the other hand, involves reactions in which all the components are in the same phase, commonly the liquid phase. The catalyst may be a soluble acid, base, salt or organometallic compound.[5] The major advantages presented by this class of catalyst are higher selectivity than is generally achieved with heterogeneous catalysts,[9-11] and better control of the reaction conditions.[5] It is also generally easier to investigate the catalytic mechanism[5,7] using established kinetic[12,13] and spectroscopic methods.[7] This, in turn, allows for the rational design of homogeneous catalysts, making them very interesting from a research perspective. However, their appeal is partially diminished due to difficulties encountered in scaling these catalytic reactions up to an industrially useful level.[5,7,8,10,11,14]

Homogeneous catalysts usually comprise a central transition metal atom and one or more coordinated ligands, which allow for versatility in terms of metal-complex architecture, electronic properties and steric demand. The interplay of these ligand properties allows extremely large scope for ligand design.[7] Although heterogeneous catalysts still dominate the industrial scene, homogeneous catalysts are employed successfully in many industrial processes, and their importance is increasing continuously.[12]

1.1.5. Important catalytic properties

The industrial potential of a catalyst depends on a number of properties, including activity, selectivity, stability, lifetime and recovery.[5] The toxicity of the catalyst and the components in the reaction play an important role in determining the feasibility of large scale industrial application, as does the price of the catalyst!

Catalytic activity is usually the first, and perhaps most obvious requirement for any potential catalyst.[15] Such activity may be expressed in terms of rate, turnover number (moles product per mole catalyst) or conversion (moles transformed reactant per mole of inlet reactant).[5] However, the selectivity of the catalyst, be it chemo-, stereo- or regioselectivity,[7] is fast becoming a major focus for catalyst optimization, as it has important cost implications for the use of energy,[4,16] the ease of separation and purification and the relative quantity of reactants needed.[5]

1.1.6. Current and future industrial trends

In determining whether a given catalytic process is suitable for industrial application, it is important to consider the profitability, and whether the required technologies can be developed within the given time frame.[17] While the activity and selectivity of the catalyst are critical factors in determining profitability, it is also important to consider the availability and cost of the ligands and starting materials, as well as intellectual property rights.[17]

Catalysis is now applied in many different industries, including the petrochemical and refining industries,[4,16] the chemical industry (both commodity and fine chemicals),[9,13,18] and the pharmaceutical,[9] food[9] and agrochemical industries.[9,18] Catalysis is also important in environmental remediation. The refining and petrochemical industries are the largest employers of catalytic processes. Much research has been done on the development of materials used in different processes,[13] and the preparation of catalysts has seen significant technological breakthroughs.[13] Future trends will undoubtedly be directed by the growing focus on the environment, global warming, and the need to reduce dependence on fossil fuels.[4,16] Catalysis may play a very important role in the design of more energy efficient processes that will ultimately help cut emissions of greenhouse gases and the production of biofuels.[16]

Combinatorial chemistry may well become increasingly important in the search for new homogeneous catalysts. The rapid screening approach afforded by combinatorial chemistry has been widely explored in the pharmaceutical industry in the search for new drugs,[15] and there is significant interest in the use of this approach in the tailoring and fine-tuning of homogeneous catalysts.[7,15]

The difficulties of catalyst recovery in homogeneous processes have prompted interest into the immobilization of catalysts, permitting recovery of the catalyst with relative ease and minimal contamination of the product by the catalyst.[9] The success of immobilization strategies in enzyme catalysis lends hope for large-scale applications of immobilized of homogeneous catalysts,[9,19] particularly for enantioselective systems.[12,17,19] Another technology that is gaining interest is the use of two-phase catalysis, in which the catalyst is immobilized in a polar liquid in which the organic components are relatively insoluble.[10,11]

1.2. METATHESIS CATALYSIS

1.2.1. History and development

Olefin metathesis is a unique double-bond scrambling reaction that allows for the synthesis of new olefin products by the rupture and reforming of existing unsaturated C-C bonds.[8,20-24] The most important types of reaction accessed by metathesis catalysts are illustrated in Scheme 1.1 and include ring-closing metathesis (RCM), ring-opening metathesis (ROM), ring-opening metathesis polymerization (ROMP), acyclic diene metathesis polymerization (ADMET) and cross-metathesis (CM).[21-23,25]

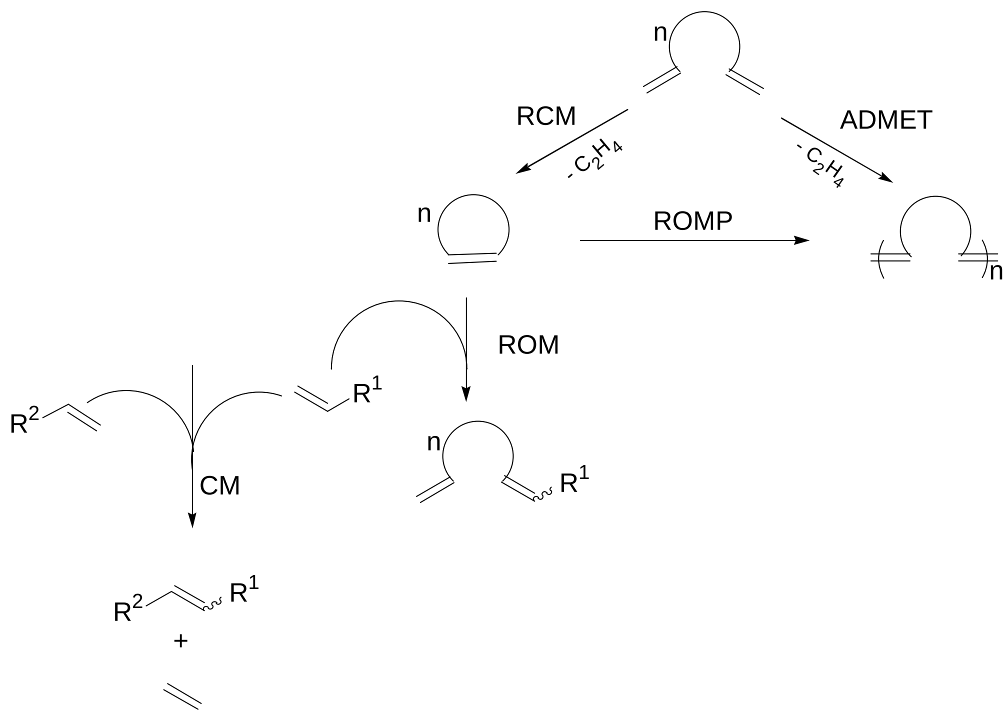

Scheme 1.1.

This versatile catalytic process is one of the truly novel reactions to emerge within the last 40 years.[26] It was discovered serendipitously in the 1950's during polymerization studies with a range of transition metals.[26,27] Ziegler and co-workers first observed the polymerization of ethylene under these conditions,[27,28] but the term *olefin metathesis* was only coined by Calderon and co-workers several years later.[20,21,29] By the late 1960's olefin metathesis had been commercialised by Phillips Petroleum Co. with their triolefin process.[26,27,30,31]

The usefulness of this reaction was initially limited to poorly defined transition metal salts as catalysts.[8,21,23] Frustration with the limitations of these ill-defined catalysts prompted intensive mechanistic studies aimed at understanding the catalytic process, triggering the development of well-defined homogeneous metathesis catalysts by Tebbe,[32] Schrock[33] and Osborn.[27] The bulky alkoxy imido molybdenum complex **1** developed by Schrock and co-workers became the first single-component metathesis catalyst to be used extensively. Such catalysts could be prepared on a moderate scale and were relatively stable,[27] thus providing a basis for detailed studies of metathesis reactions.[27]

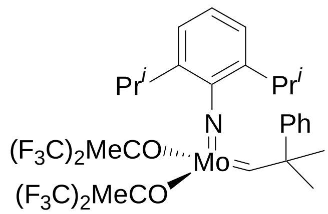

1

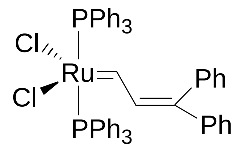

2

The usefulness of these catalysts in organic synthesis was nevertheless hampered by their oxophilicity and their consequent sensitivity to air, moisture and many oxygen-containing functional groups.[21] Efforts to develop catalysts with greater stability and functional group tolerance resulted in versatile ruthenium complexes which exhibit both functional group tolerance and good activity. Table 1.1 illustrates how ruthenium exhibits greatest activity with olefins, compared to other functional groups.

Table 1.1

Functional group reactivity of transition metal metathesis catalysts[21]

Titanium	Tungsten	Molybdenum	Ruthenium
Acids	Acids	Acids	***Olefins***
Alcohols, water	Alcohols, water	Alcohols, water	Acids
Aldehydes	Aldehydes	Aldehydes	Alcohols, water
Ketones	Ketones	***Olefins***	Aldehydes
Esters, amides	***Olefins***	Ketones	Ketones
Olefins	Esters, amides	Esters, amides	Esters, amides

Increasing activity

The observation that $RuCl_3$(hydrate) was a better metathesis catalyst in the presence of water[21,27,34] prompted more research into these ruthenium systems,[21] and it soon became clear that the active species was, in fact, a ruthenium alkylidene.[21,27,35] The alkylidene complex **2** subsequently synthesised from diphenylcyclopropene and $RuCl_2(PPh_3)_3$,[21] was found to polymerize norbonene both in the presence and absence of water and protic solvents,[8,21,27] and to show remarkable stability and functional group tolerance.[36,37] The metathesis activity was, however, limited to ROMP of highly stained cyclic olefins, and in an attempt to extend the activity of these ruthenium alkylidenes, the ligand sphere was systematically changed.[21] Introduction of the more basic tricyclohexyl phosphine ligand increased metathesis activity,[21,27] leading to the first-generation Grubbs catalyst **3** in 1992. The enhanced functional group tolerance and air-stability of the complex[8,21,27,38] triggered an avalanche of interest in metathesis reactions and to the development of the second-generation Grubbs catalyst **4** and the Hoveyda catalyst **5**. These catalysts are now used extensively and will be discussed in more detail later.

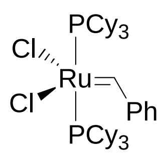

3

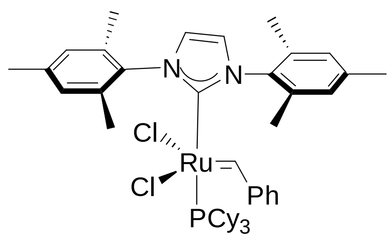

4

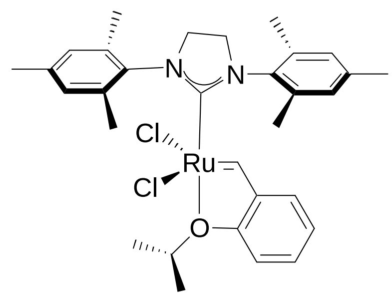

5

1.2.2. Types of metathesis reactions

The numerous types of metathesis reactions have been extensively reviewed[23,28,39-42] and consequently this section will provide only a brief overview with a few illustrative examples.

1.2.2.1. Ring-opening metathesis polymerization (ROMP)

Historically, ring opening metathesis polymerization (ROMP) has been the dominant application of metathesis[21,23] and several commercial products have been made using this reaction.[43] It provides an excellent route to polymers, as it allows for the maintenance of backbone unsaturation,[21,44] and the direct incorporation of functionality from the parent monomer.[21,44] ROMP, like other metathesis reactions, proceeds *via* chain processes in which the structures of the active entities alternate between metal alkylidenes and metallacyclobutanes.[28] Scheme 1.2 illustrates the accepted ROMP metathesis mechanism.

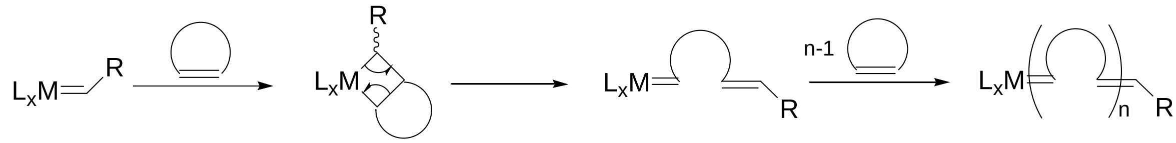

Scheme 1.2[21]

ROMP is thermodynamically favoured for strained ring systems, and is thus utilized extensively on ring systems incorporating 3, 4, 8 or more atoms.[23] For these strained cyclic systems, ROMP offers a means of "live polymerization", which refers to polymerization reactions that proceed in the absence of a termination step[21,45-47] When the rate of initiation is greater than the rate of propagation, polymers with specified molecular weights and narrow polydispersities, as well as block copolymers can be produced.[21,45,46]

Scheme 1.3 illustrates the synthesis of a block copolymer from monomer **6.** The polymerization takes place in an aqueous emulsion, in the presence of the Grubbs catalyst **3**. After polymerization has ended, monomer **7** is added to the emulsion, resulting in block polymerization.[45]

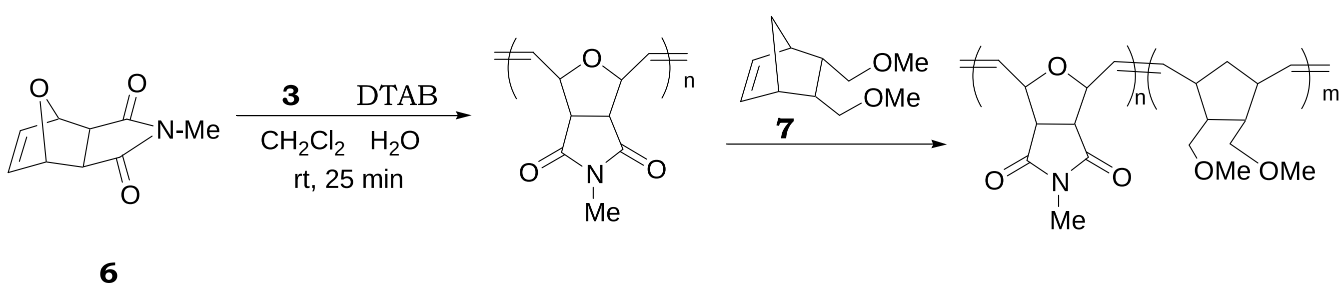

Scheme 1.3.

Living ROMP has also been developed for aqueous media,[35,48-50] utilizing robust ruthenium catalysts.[45,51-53] Although these systems are able to efficiently perform ROMP in aqueous media, the catalysts are insoluble, and reactions have to take place in the organic phase of an emulsion created in the reaction vessel.[46] The Grubbs group published the first record of an entirely aqueous ROMP system in 1998.[46] Although complex **8** had been shown to be able to ROMP water soluble monomers, the conversions were low, presumably due to enhanced decomposition by hydroxide ions present in the medium. To eliminate even small concentrations of hydroxide ions, DCl was added to **8**, generating a new alkylidene species, as shown in Scheme 1.4. This monophosphine alkylidine derivative is remarkably stable, and the presence of the acid allows for living polymerization, thus aiding the formation of block copolymers

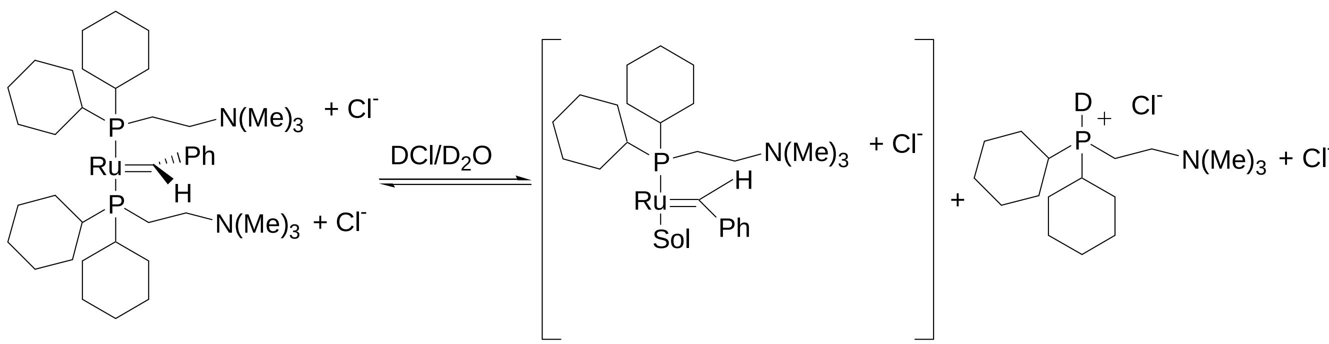

8

Scheme 1.4

1.2.2.2. Ring-closing metathesis (RCM)

Although the first reported example of ring closing metathesis (RCM) was only reported by Tsuji and Villemin in 1980, this is perhaps the area of olefin metathesis that has expanded most.[21,24] The great interest that this reaction has received in recent decades is due largely to the development of well-defined catalysts providing good functional group tolerance,[23,24,54] greater thermal stability,[54] and the ability to accommodate more substituents on the double bond formed in RCM.[54]

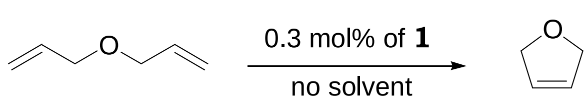

Scheme 1.5

The reaction generally involves low-molecular weight molecules, and a simple example is illustrated in Scheme 1.5, using Shrocks' molybdenum catalyst, **1**.[39] The reaction mechanism involves the interconversion of an olefin and metal alkylidene.

Mediated by a metallacyclobutane species, the reaction proceeds through alternating [2 + 2] cycloadditions and cycloreversions, as shown in Scheme 1.6.[39]

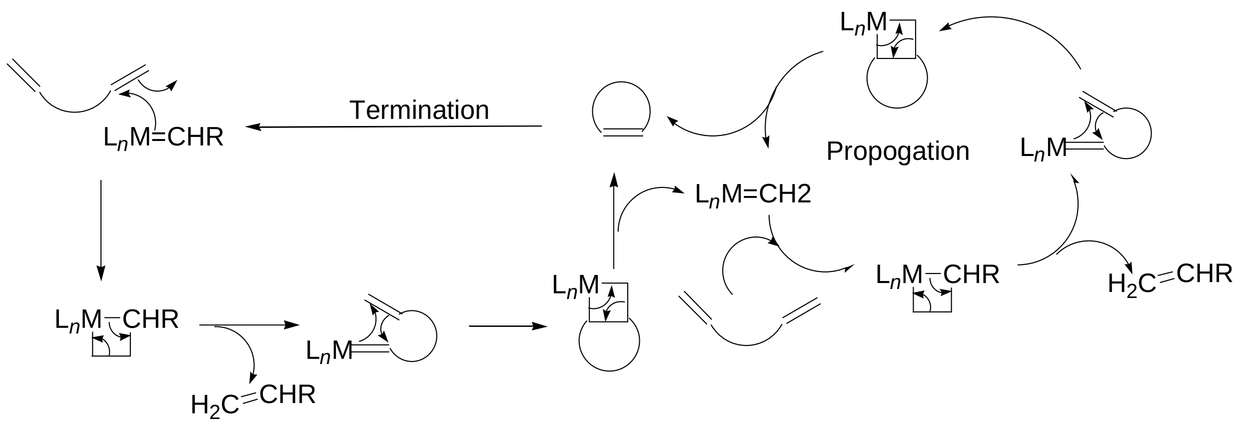

Scheme 1.6.

The reaction has enjoyed wide application in the field of organic synthesis, being employed for the synthesis of 5-8 membered cyclic systems and macrocyclic systems, and for mono-, bi- and polycyclic ring systems. It is also widely employed for stereoselective, peptide,[55] and natural product synthesis.[23,39,56] Catalysts **1**, **2**, and **3** have been used extensively in RCM, and the tungsten catalyst **8** and molybdenum catalyst **9** have also been used, among others, if somewhat less frequently.[39]

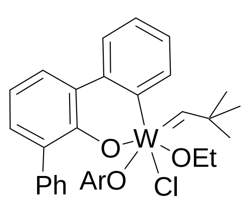

8

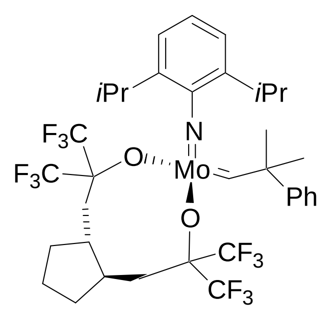

9

RCM has been used to synthesise chromenes with a variety of substituents on the chromene scaffold, as illustrated in Scheme 1.7;[57,58] The Grubbs catalyst **3** has remarkable tolerance to these functional groups.[23]

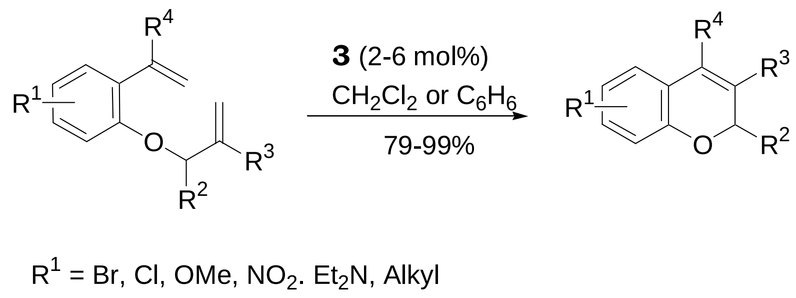

Scheme 1.7.

RCM is also useful for macrocyclization and may still be achieved with substrates lacking the conformation needed for metathesis, by the slow addition of the substrate.[23,59] Thus, slow addition of the α,ω-diene substrate affords the 16-membered lactone, after RCM with the ruthenium catalyst **2** (Scheme 1.8).

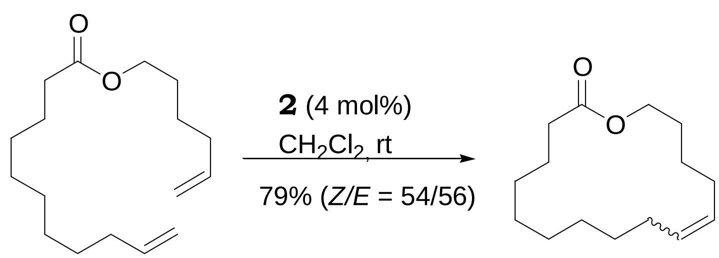

Scheme 1.8.

However, RCM does have its limitations, particularly regarding substitution on the double bond. For example, when the substituents are electron-withdrawing, the formation of tri- and tetra-substituted cyclic alkenes generally only occurs in low yield.[54,60,61] To a certain extent, these problems may be overcome by the use of microwave irradiation. Grigg *et al.*[54] have successfully used this technique in the formation of a range of tri-substituted, five- and six-membered heterocycles. One such example is provided in Scheme 1.9, where the product was formed in good yield.

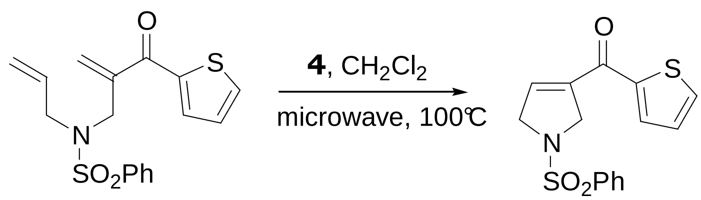

Scheme 1.9

1.2.2.3. Cross metathesis (CM)

CM is a unique method for the intermolecular formation of C-C bonds,[23,24] providing a convenient route to functionalised and higher olefins from simple alkene precursors.[62] However, CM has traditionally found only limited application due to a number of factors. The most important of these factors is the difficulty of ensuring high selectivity of the desired hetero-dimer CM product, relative to the unproductive homo-dimer self-metathesis products. Scheme 1.10 illustrates how CM of two different olefins may result in 3 possible products: the desired CM product, as well as two undesired homometathesis products.[23,24] In addition to the problems of regio- and stereoselectivity, CM is not only often characterised by lower activities than RCM or ROMP, but also lacks a major enthalpic driving force (such as ring strain in ROMP) or an entropic advantage (as is the case for intramolecular reactions like RCM).

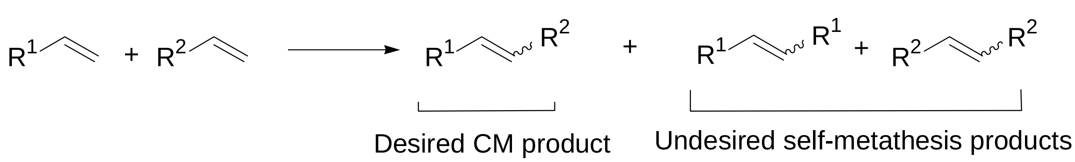

Scheme 1.10.

The advent of the well-defined Shrock molybdenum and Grubbs ruthenium catalysts prompted new interest in CM, and the above problems have, to some extent, been overcome with certain olefinic substrates.[21,24,62] For example, while substrates with electron-deficient double bonds show poor activity with the Grubbs first-generation catalyst **3**, a 90% yield is obtained with the second generation NHC catalyst **4**.[27,63] Indeed, the latter catalyst is able to CM cleanly a number of functionalised olefins that exhibit less selective metathesis with the bis(phosphine) ruthenium complexes.[24,27,64]

The vast majority of reported CM reactions have been performed using terminal olefin substrates, as internal olefins lead to very complex product mixtures.[24] However, in the late 1990's the Grubbs group developed a new methodology whereby unhindered terminal olefins with symmetrically disubstituted internal olefins could be successfully metathesised yielding the desired cross product in good yields using the first generation ruthenium catalyst, **3**.[21,24,65] Scheme 1.11 shows how this approach has been successfully applied to a number of functionalised olefins. It has been documented that sterically hindered terminal olefins can undergo clean metathesis reactions with catalysts **1** and **3**.[24,66] The rate of self metathesis may also be reduced by steric bulk in the allylic position, and alkyl substitution directly on the double bond.[27]

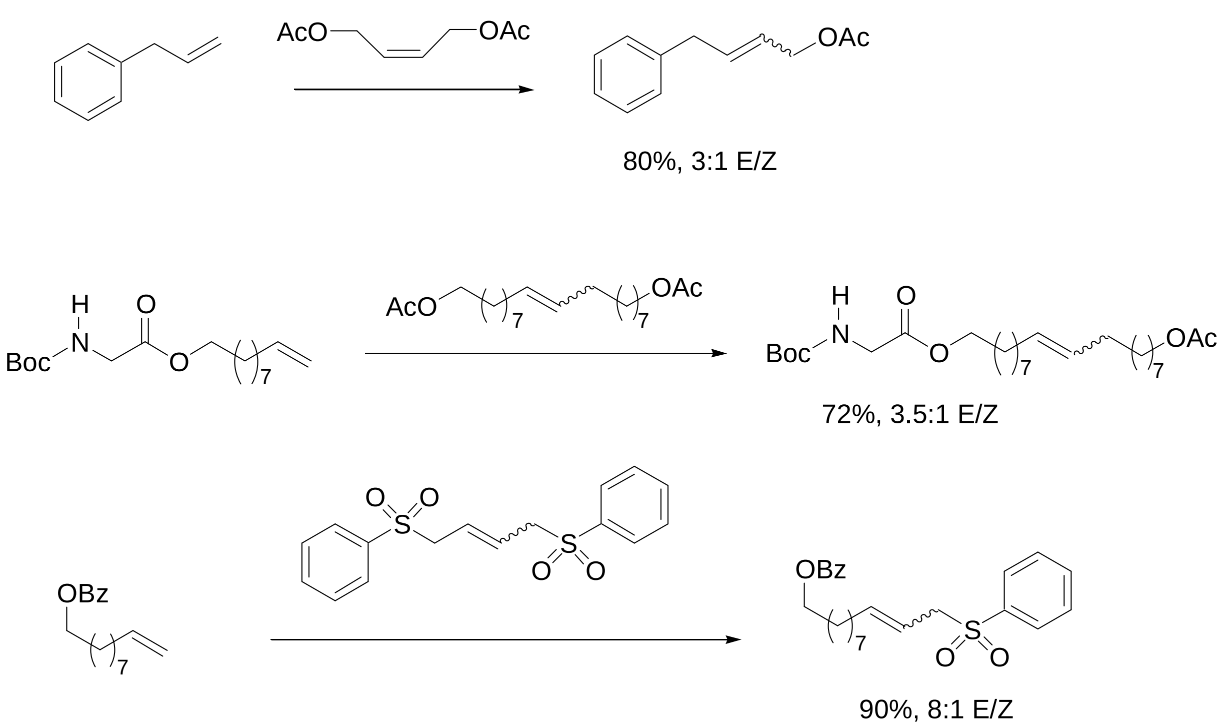

Scheme 1.11.[24]

One of the persistent problems with CM is the difficulty in predicting whether a given CM reaction will be selective or not.[62] In an attempt to overcome this problem, Chatterjee *et al.*[62] developed a general model for predicting both selective and non-selective CM reactions. This model is based on: the categorization of olefin reactivity; the relative ability of different olefins to undergo self-metathesis; and the susceptibility of these self-metathesis products to undergo further metathesis. This model now allows for selective CM with a variety of electron-rich, electron-deficient and sterically bulky olefins, provided a suitable catalyst is employed.

1.2.2.4. Other metathesis reactions

Other metathesis reactions include acyclic diene metathesis (ADMET), ring opening metathesis (ROM), and enyne metathesis. Tandem metathesis has also been widely applied, either combining different metathesis reactions, or combining metathesis with another catalytic process.[23,39,54,67-69]

ADMET is an intermolecular reaction between two alkenes, allowing for the synthesis of oligomers and polymers in a step-growth manner, with the liberation of volatile side products.[21,43,70] With the development of the functional group tolerant ruthenium catalysts, ADMET has been applied to olefins with various oxygen-containing functional groups,[43,71] and it has also been successfully used in the synthesis of liquid crystalline polymers.[43,72] Like all catalytic reactions, ADMET is not without its limitations, and there are some reactions for which ADMET is not suitable.[73]

When metathesis effects ring opening without polymerization, the reaction is called ring opening metathesis (ROM). Scheme 1.12 illustrates the difference between ROM and ROMP. Once strained ring systems have been opened by the metathesis activity, it is not unusual for the resultant olefins to undergo cross metathesis. ROM is therefore fairly commonly employed in tandem with cross metathesis reactions.[74,75]

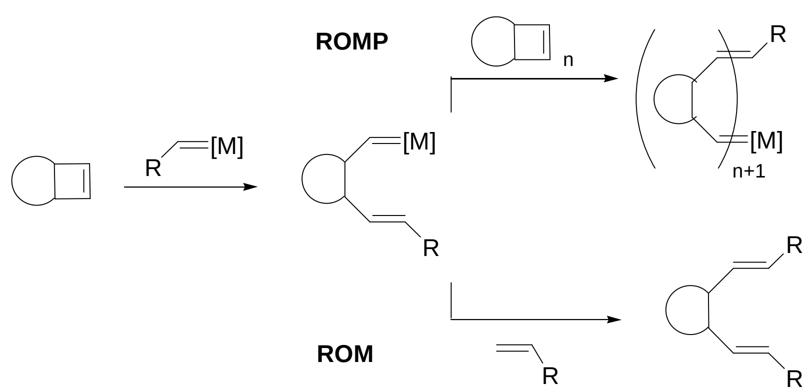

Scheme 1.12.[74]

Enyne metathesis has received less attention than alkene metathesis,[40,76] and involves either an inter- or intramolecular bond reorganization between an alkene and an alkyne, to form a 1,3-diene (Scheme 1.13).[40] Enyne metathesis is mechanistically similar to olefin metathesis, and the reaction may often be promoted by the same catalysts used in olefin metathesis. Of particular use are the ruthenium catalysts **3**-**5**,[40,77] but recent advances in catalyst design include new ruthenium catalysts,[70] tungsten alkylidyne catalysts[76] as well as homogeneous and supported molybdenum catatlysts.[76,78-81]

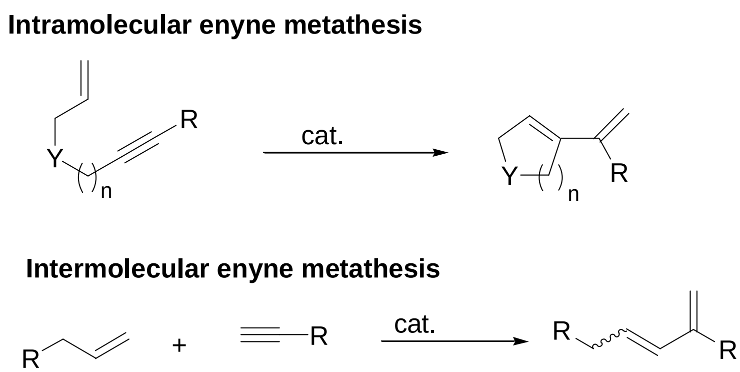

Scheme 1.13.[40]

1.2.3. Early transition metal catalysts

The ill-defined catalysts consisting of transition-metal salts are poorly understood in terms of their mechanism of activity[39] and there is thus little scope for design and improvement. This section will overview only those well-defined homogeneous catalysts that have been developed for metathesis activity.

1.2.3.1. Molybdenum catalysts

The development of Schrock's molybdenum catalyst **1** was the first to provide efficient and controlled ROMP, and ushered in an era of well-defined, active catalysts.[8,23,27,73,82] The exceptional activity of the catalyst enables it to perform some metathesis conversions that other catalysts seem unable to do.[39] It exhibits high activity with substrates having large electronic and steric differences in the ligand sphere.[23] Unfortunately, this exceptional activity is not without major cost. The catalyst is extremely sensitive to both oxygen and moisture, and, consequently, the most stringent controls need to be taken when handling it - ideally the complex should be made and stored in a refrigerated glove-box, limiting the use of the catalyst to a few specialised laboratories.[23,39,73,83] The limited functional group tolerance may be improved by modifying the ligand sphere.[8,23] For example, replacement of the alkoxy groups with silsequioxane (a silicon-oxygen cage-like structure) markedly improves the functionality tolerance, but only under anhydrous conditions.[8,84]

Catalysts of the Schrock type have been extensively used: many ROMP reactions; RCM of 5- and 6-membered ring systems with pendant ether and ester functionalities;[8,39] in RCM to form bicyclic systems;[8,39] in the formation of nitrogen-containing heterocycles;[8] asymmetric synthesis;[85-87] and the synthesis of natural products.[8,88,89] These catalysts have also been used for ADMET, particularly for the synthesis of polyesters[90] and polycarbonates.[8]

1.2.3.2. Other transition metals as metathesis catalysts

A number of tungsten carbene complexes have been developed for use in metathesis chemistry. Among these is the Tp'-oxotungsten carbene complex **10** developed as an air-stable precursor for ROMP.[8,91] The tungsten alkylidene **11** is remarkably tolerant of heteroatoms, such as S, Si, P, Sn.[92] Its significant steric bulk probably contributes to its success as a RCM metathesis catalyst,[39] and it may be used with comparatively concentrated substrate solutions, even in the absence of solvent.[39] Tungsten alkylidynes, the first of which was reported in 1981, have been developed for alkyne metathesis.[93] Complex **12** is one such alkylidyne catalyst used in alkyne metathesis.[76]

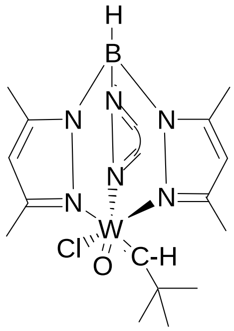

10

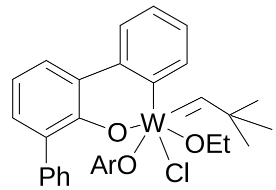

11

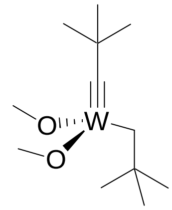

12

One of the rare osmium metathesis catalysts has been reported by Castarlenas *et al.*[94] **13**. This complex has been shown to be an efficient catalyst precursor.[95] The tantalum and rhenium systems **14** and **15** have been shown to produce living ROMP.[96-98]

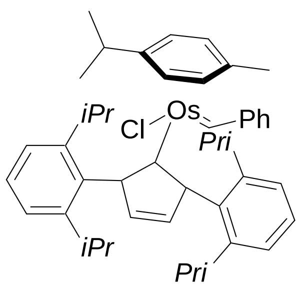

13

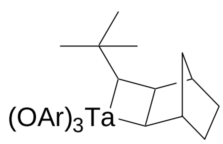

14

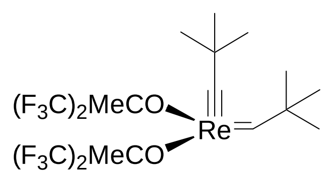

15

1.2.4. Ruthenium catalysts

Although ignored for quite some time, ruthenium alkylidene complexes have, ultimately, provided the synthetic chemist with active and user-friendly catalysts. The great advantage of these ruthenium catalysts over other transition-metal alkylidenes is that they are able to successfully metathesize many transformations, while exhibiting excellent functional-group compatibility. Despite the wealth of research currently devoted to the design of new ruthenium metathesis catalysts, the general structure has remained much the same; the central ruthenium atom is surrounded by five ligands, including two neutral electron-donating ligands, two monoanionic groups and an alkylidene moiety.[99]

The discovery of bis-phosphine complexes such as **2** and **3** has afforded a great deal of mechanistic insight into the metathesis cycle, prompting further studies into the rational design and synthesis of new catalysts. It is now well established that the primary catalytic pathway takes place *via* the initial loss of one labile phosphine ligand from the “pre-catalyst”, to form a catalytic 14 electron complex intermediate. This intermediate is then free either to coordinate to free phosphine, or to advance the metathesis cycle by coordinating to an olefinic substrate.[27,99-101] This initiation step prompted investigations into the use of *N*-heterocyclic carbenes (NHC’s) as an alternative to phosphine ligands. There is consequently a wide range of both mixed phosphine/NHC catalysts and phosphine-free catalysts reported in the literature.

The nature of the anionic and alkylidene ligands affects catalyst activity. Since the incoming olefin may sometimes initially bind *trans* to the halide, larger and more electron donating halides tend to decrease metathesis activity[99,101-105] due to the resultant increase in electron density in the π–bond. In contrast, complexes with smaller alkylidene moieties tend to initiate more slowly:[21,99] the larger the alkylidene substituent, the greater the activity.

1.2.4.1.Mechanism

When the metathesis reaction was first discovered, it was clear that the mechanism would be unusual.[27] One of the first mechanisms to be proposed was a pair-wise exchange of alkylidenes through a “quasi-cyclobutane” mechanism;[29] it was envisioned that two olefin molecules coordinate to the metal centre and are then exchanged through a symmetrical intermediate.[27] This hypothesis had some shortcomings, and to counter these, Hérisson and Chauvin proposed a non-pair-wise mechanism in the early 1970’s.[106] The mechanism involved the fragmentation of the olefin, as shown in Scheme 1.14, and later became known as the carbene mechanism.[27]

$$M{=}CHR^1 + CH_2{=}CHR^2 \rightleftharpoons M{=}CHR^2 + CH_2CHR^1$$

$$M{=}CHR^1 + CH_2{=}CHR^2 \rightleftharpoons M{=}CH_2 + CHR^1{=}CHR^2$$

Scheme 1.14.

Solution studies by Grubbs' group in 1997 provided evidence for two competing pathways, a dissociative and an associative pathway.[102] The former was postulated to involve loss of a phosphine ligand upon coordination of the olefin substrate to the metal. Conversely, it was proposed that the associative mechanism involves the coordination of the olefin to the catalyst to form an intermediate 18 electron complex. The associative pathway was originally more attractive, as all of the intermediates have either 16 or 18 electrons (Scheme 1.15). The kinetic data, however, proved that the dissociative mechanism was in fact the dominant mechanism - contrary to expectations!

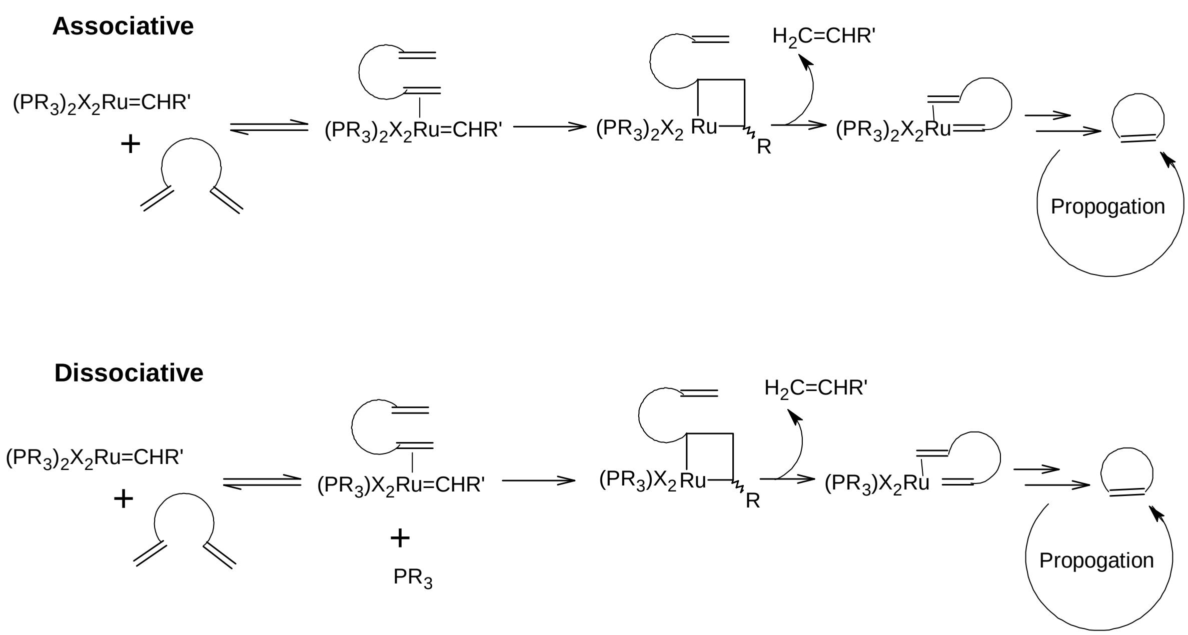

Scheme 1.15.

There has since been a wealth of data indicating that metathesis does indeed proceed by a dissociative mechanism involving alternating [2 + 2] cycloadditions and cycloreversions.[101,102,106-110] The first step involves the dissociation of a labile phosphine ligand to produce a 14 electron intermediate of the general form LX_2Ru=CHPh. Assuming the intermediate is not trapped by free phosphine, this electrophilic intermediate is free to coordinate with the olefin substrate, usually *trans* to L.[100] The resultant π-complex then rearranges by migratory insertion of the olefin into the metal carbene bond, yielding a metallacyclobutane. This intermediate is cleaved to form an isomeric π-complex, and the final products are released upon dissociation of the olefin.[106] This mechanism is illustrated in Scheme 1.16.

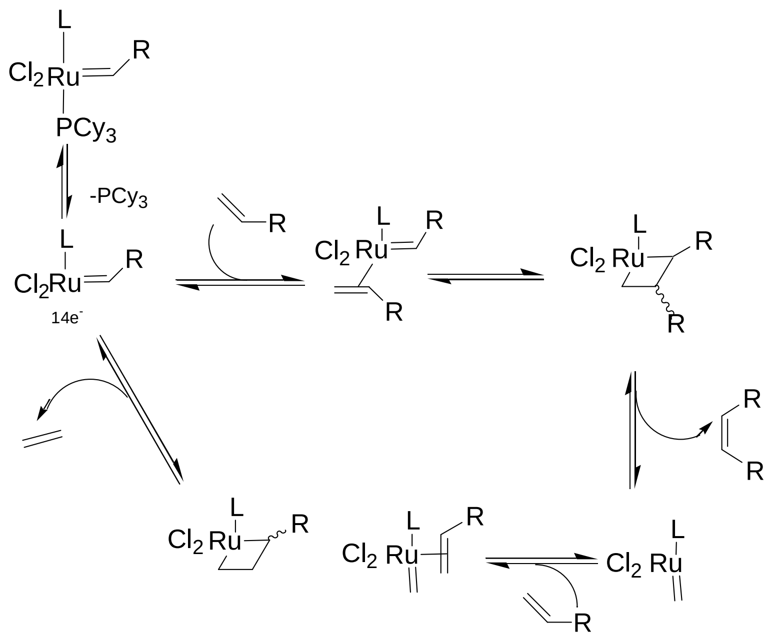

Scheme 1.16.[106]

Although this mechanism is widely accepted today, it must be noted that the details of the mechanism are affected by variations in the ligand sphere,[106,111,112] and computational techniques are increasingly being used to examine these variations. For the second generation NHC catalysts, there is much debate as to whether the olefin coordination occurs *trans* or *cis* to the NHC. The latter is accompanied by a shift in the halide ligand to a *trans* position[111] and crystal structure of complex **16**, in which the olefin is side-bound, has been offered as evidence for this geometry.[113-115] Other studies report a bottom-bound approach.[116-122] A recent DFT study[121] of structures **16**, **17** and **18** (incorporating the saturated mesityl ligand, SIMes), indicates that, with solvent effects, the side-bound geometry may be favoured for the coordination intermediate but, in the transition-state complex, the bottom-bound geometry is favoured. Structure **17** is a simplified model, whereas the more sterically encumbered complex **18** is a more representative metathesis catalyst. In this case (**18**), even the coordination intermediate favours the bottom-bound geometry, although the side-bound analogue competes quite strongly when solvent effects are taken into account.

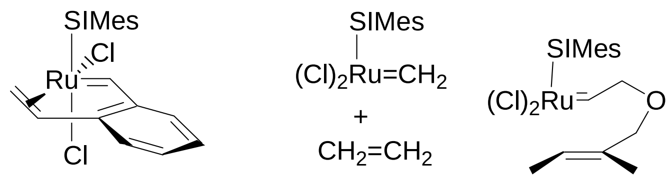

16 **17** **18**

Such theoretical studies may provide valuable insight into the catalytic mechanism when used in combination with experimental studies.[101,112,116,118,121,123-127] One example is a comparative study between first and second generation catalysts **3** and **4**, and the Sasol "Phobcat" catalyst **19**.[128] In this study, complete DFT level Gibbs free energy surfaces for the catalytic cycles of the three catalysts are constructed. The full ligand set was used, but the alkylidene moieties were reduced to methylidene moieties, and ethylene was used as the olefinic substrate. The computational results agree neatly with the experimental data, and illustrate the power of computational techniques as a tool for predicting the potential metathesis activity of a given ruthenium-alkylidene.[129-131]

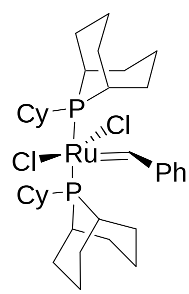

19

The following sections will provide only a brief overview of the 3 main variations of the ruthenium alkylidene catalysts, namely the bis-phosphine catalysts, the mono-phosphine catalysts and the phosphine-free catalysts.

1.2.4.2. Bis-phosphine ruthenium catalysts

Commonly referred to as first generation catalysts, these bis-phosphine complexes of the type $L_2(PR_2)Ru=CHR$ were the first metathesis catalysts to be widely used, owing to their attractive functional group tolerance and handling properties. While complex **3** is commercially available, these bis-phosphine complexes are readily prepared synthetically, as outlined in Scheme 1.17[8] The more active catalysts tend to have alkyl-substituted phosphine ligands, and are generally more soluble in common organic solvents.[8] Tricyclohexyl phosphines (PCy_3) provide the best balance between stability and activity,[27,102] and these more active catalysts may easily be generated by phosphine exchange, [27,53,102,132-134] as illustrated in Scheme 1.17.[8]

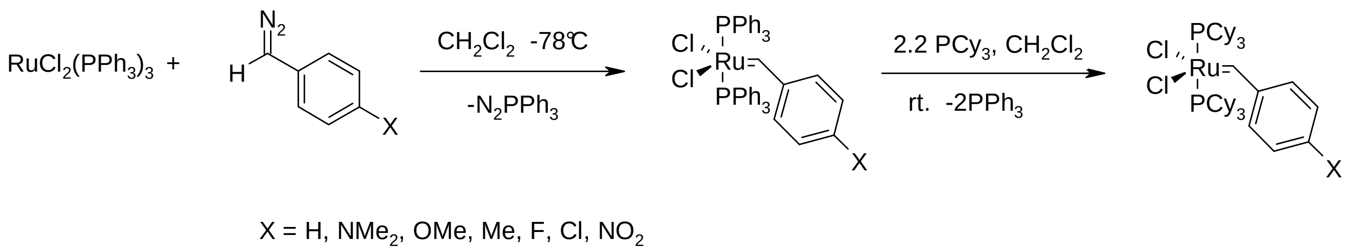

Scheme 1.17.[8]

These first generation catalysts have been effectively used to catalyse a wide array of living ROMP,[8,36,45,51,134-136] RCM[8,38,137-142] and ADMET[8,72] reactions, as well as ethenolysis,[126,143] CM[5] and enyne metathesis reactions.[77,99] They have important applications in the biofuels[126] and pharmaceutical industries,[99,144] but have yet to be used for large, industrial-scale synthesis.

The bis-phosphine catalysts have major limitations. They exhibit activities that are much lower than those reported for the early transition metal catalysts of Schrock,[30,99] and generally are only able to ROMP highly strained monomeric systems.[21] They are also not suitable for RCM approaches to tri- and tetra-substituted cycloalkenes, and fail to CM sterically hindered or deactivated alkenes.[99] These limitations have been largely overcome by the second-generation metathesis catalysts.

1.2.4.3. Mono-phosphine catalysts

N-Heterocyclic carbenes (NHC's) are used extensively in organometallic chemistry. They are better σ-donors than phosphine ligands,[21,131,145,146] and the first ruthenium metathesis catalyst **20** to make use of these ligands was reported in 1998.[27,99,100,147] In complex **20**, both phosphine ligands have been substituted by the the unsaturated mesityl ligand, IMes, the rationale being that initiation should be faster, due to the greater σ-donation of electron density to the ruthenium centre. Contrary to expectations, however, complex **20** only showed activity comparable to the first-generation catalyst **3**, possibly as the NHC is less labile than the phosphine ligand.[145-149]

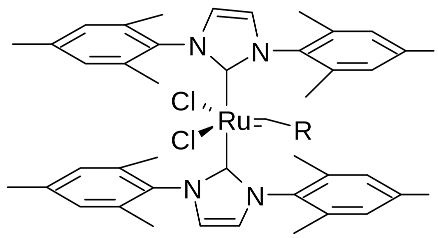

20

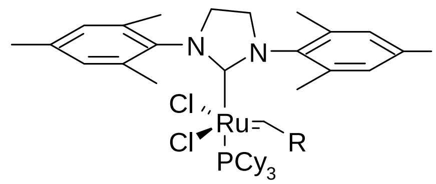

21

In 1999 and 2000, the Grubbs and Nolan groups reported the synthesis of the mixed NHC/phosphine complex **4**.[21,123,147,150,151] This catalyst did indeed exhibit far greater metathesis activity than the first generation catalyst, but for unexpected reasons. Again, the rationale was that dissociation of the labile phosphine ligand *trans* to the σ-donating NHC would be more rapid than for the first generation catalysts. However, it was found that initiation is actually slower,[21,99-101,106] and the enhanced activity was attributed to the greater affinity of the 14 electron species for the incoming olefinic substrate, relative to the first-generation analogues.[99,100,106] NHC's are also less susceptible to decomposition than most phosphine ligands, which tend to undergo P-C bond degradation at elevated temperature.[100] The ability of the NHC's to mimic the electronic effects of phosphine ligands in the absence of thermal decomposition makes this class of ligand a superior choice for a longer-lived catalyst. The bulky NHC ligand is thus able to stabilize the catalytically relevant intermediates, protecting against uni- and bimolecular decomposition pathways.[27,82,100]

Catalysts such as complex **21**, incorporating the saturated NHC ligand, SIMes, exhibit even greater activity.[21,99,101,152,153] Many mixed ruthenium complexes have been developed with variations on the NHC moiety. Generally, larger NHC ligands tend to produce catalysts that initiate faster[101,153] and, overall exhibit more enhanced metathesis activity.[99] Other recent developments involve mixed ruthenium complexes with unsymmetrical NHC's, including mixed methyl mesityl and ethyl mesityl systems.[99,154] Significant steric hindrance within the NHC may serve to impede metathesis activity, as is the case with the bulky adamantyl ligand in complex **22**.[99,155] Much attention is currently being devoted to the development chiral second-generation catalysts,[85,99] of which complex **23** is a good example.[99,156,157]

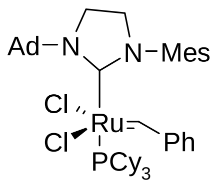

22

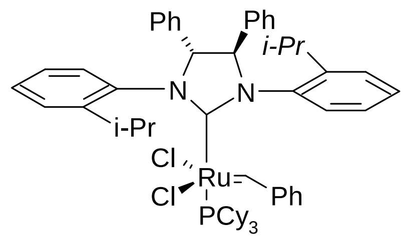

23

As was the case with the first generation catalysts, the alkylidene moiety has an important influence on metathesis activity.[101] The ruthenium benzylidene (as in complexes **22** and **23**) offers the best balance of activity and stability, while a ruthenium indenylidene[158,159] complex has been shown to exhibit similar reactivities.[159] In contrast, the vinylidene moiety exhibits reduced activities relative to benzylidene, and allenylidene complexes are completely inactive.[99,160] In general, sterically bulky and electron-donating alkylidenes increase initiation by facilitating dissociation of the phosphine ligand.

The phosphine ligands may also be varied, depending on the purpose for which the catalyst is designed. For example, slower-initiating catalysts are often desirable for ROMP of highly strained olefin monomers.[99] Complex **24** has an initiation rate 170 times slower than complex **21**,[161] and may be useful for such ROMP reactions.[99] Conversely, in situations where metathesis is required to proceed at low temperatures, faster initiating catalysts such as complex **25** are desirable[99] (e.g. Complex **25** initiates 60 times faster than complex **21**).[99,161]

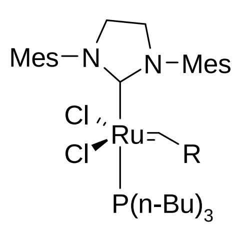

24

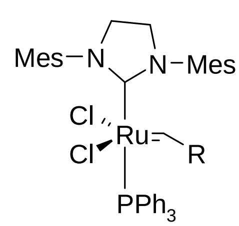

26

Both the NHC and the alkylidene moieties allow for the possibility of anchoring the complex to a support.[22,99,162,163,163-166] The supports used may include silica,[23,100,167,168] polymeric supports,[14,166,168-172] or monolithic supports.[23,100,173] In the case of anchorage through the alkylidene moiety, the immobilization is not a permanent fixture, but it may allow for controlled release of the homogeneous catalyst into the reaction medium.[99,174] Attempts to anchor this class of catalyst through the anionic ligands have also been reported.[172]

Recent variations on the NHC second-generation catalysts include the design, synthesis and evaluation of *P*-heterocyclic carbenes (PHC's),[106,175] as candidates to compete with and complement NHC's. While these ligands provide for interesting comparisons, computational studies have shown that both initiation and π-coordination of the olefin are slower than those for the NHC analogues. The ruthenacycle that forms is, however, more stable than the NHC analogues, and future developments in this area may hold interesting possibilities.

The applications of the second-generation catalysts are numerous, and include the metathesis of sterically demanding or deactivated olefins,[99] challenging CM reactions,[21,99,151,176-178] ROMP of sterically hindered substrates,[21] chiral RCM,[27, 85] RCM of tetra-substituted cycloalkenes,[21,147,179,180] the synthesis of macrocyclizations,[99,152,176,177,181] ring opening insertion metathesis polymerization (ROIMP),[99] as well as enyne metathesis.[21,77,99]

1.2.4.4. Phosphine-free catalysts

In the mid-nineties the Hoveyda group developed a new class of ruthenium alkylidene catalysts, incorporating the saturated mesityl ligand (SIMes) with a chelating benzylidene ether ligand.[168] These catalysts exhibit similar activity to the second-generation catalysts,[99] but provide unique selectivity levels.[99,100,173,182] Apart from the many transformations that this class of catalyst is able to effect, they have good stability and handling properties, and are easily recovered after metathesis by column chromatography.[168] They are especially useful for the metathesis of electron-deficient substrates, presumably due to easier release of the ether ligand.[99,156,174,181,183] Chirality introduced within either of the neutral ligands provides catalysts that efficiently metathesize with good diastereo- and enantioselectivity.[156,168,173,184]

This class of catalyst is activated by the dissociation of the Ru-O coordination *via* a release/return mechanism.[100,173,174] Scheme 1.18 illustrates the initiation, propagation and termination steps involved. The absence of free phosphine in the reaction mixture affords unique catalytic properties, as the catalyst is free of the decomposition implications associated with interaction between the activated complex and the free phosphine.[27,82,100,101,173] The release/return mechanism also makes it possible to immobilize these catalysts on to a solid support, offering the benefits of truly homogeneous catalysis, as well as the advantage of catalyst recovery *via* heterogeneous methods.[167,168,185] Tagging the isopropoxy benzylidene ligand to an ionic liquid has also provided unique recovery levels.[186]

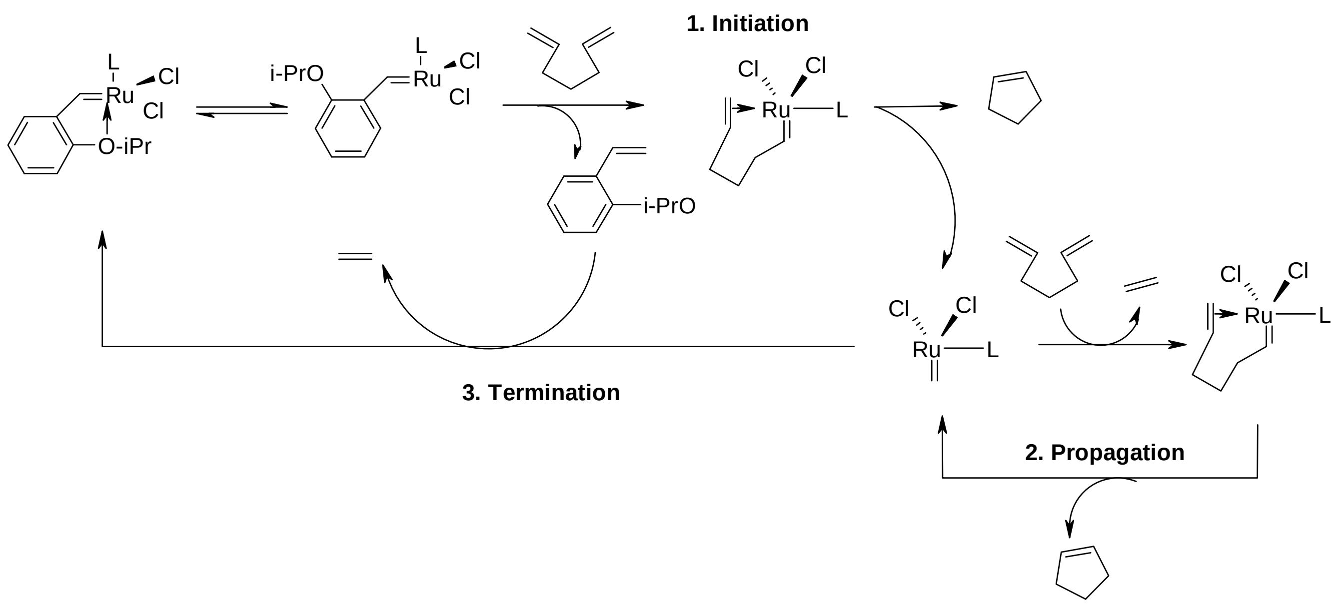

Scheme 1.18.[100]

The nature of the ether chelate has profound consequences for the activity and utility of the complex as a metathesis catalyst.[168,187] A greater rate of decomposition is observed when the ether functionality is a methoxy moiety rather that an isopropoxy group. The methoxy ether is also thought to render a less active catalyst as it is less sterically encumbered. It is thought that the bulky isopropoxy group facilitates dissociation of the ether chelate.[168]

Other catalysts of this type have been developed with different substitution patterns on the chelating benzylidene ether ligand.[99,185,188] These range from being sterically hindered (**26**),[99,189] to those bearing electron-withdrawing groups (**27**).[99,185,188-190] Both steric and electronic variations appear to influence the initiation rate of the catalyst.[99]

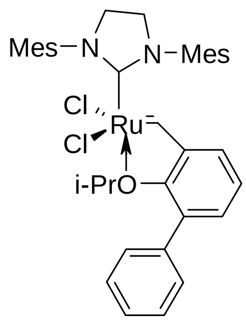

26

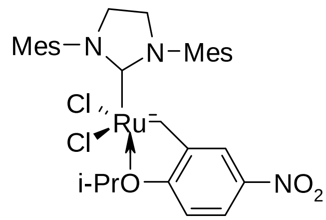

27

1.2.5. Metathesis applications

The practical applications of metathesis have traditionally been limited to organic and polymer synthesis.[21] Recently, however, the scope of the reaction has been extended, as many different research groups have applied the reaction to new synthetic challenges. This section serves to highlight different applications of metathesis.

While metathesis offered new and efficient routes to macrocycles,[23,59,67,104,168,191-195] bicyclic diaza compounds,[23,196] unsaturated alcohols and amides[23,138,197-199] carboxylic nucleosides,[23,200,201] and has contributed substantially to peptide chemistry,[23,139,202-208] its application is not limited to the organic chemist at the bench in a laboratory. It has also caught the attention of industrial chemists.[30] One of the first industrial applications was the triolefin process used by Phillips Petroleum (1966-1972). This process converted propylene to ethylene and 2-butene *via* CM in the presence of a heterogenous catalyst.[26] The catalysts used are typically oxides of Cr, W, Re and Mo.[209] Since the reaction is reversible and the demand for propylene is high,[26] ABB Lummus Global, Houstan (USA) licence this reverse reaction to make propylene from 2-butene and ethylene. The process is known as olefins conversion technology (OCT), and uses a fixed-bed reactor with WO_3/SiO_2 as catalyst.[26,30,210]

Neohexene is used as an intermediate in the synthesis of Tonalide® and Terbinafine®, a synthetic musk perfume and anti-fungal agent, respectively. Chevron Phillips Chemical Company have manufactured this intermediate since 1980, utilizing CM of 2,4,4-trimethyl-2-pentene with ethane (Scheme 1.23).[26]

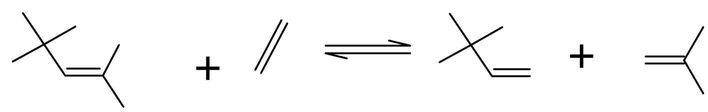

Scheme 1.23.[26]

Shell incorporates metathesis in the Shell Higher Olefin Process (SHOP), converting ethylene into higher olefins. The last of the three steps in the process is a CM reaction using an aluminium-supported molybdate metathesis catalyst.[26,210] In this manner, Shell is able to produce 1.2 million tons of linear higher olefins per year.[30]

The above industrial processes make use of cheap, ill-defined, heterogeneous catalysts, but in the polymer industry there are examples of the application of well-defined homogeneous catalysts. These include the production of polymers such as polyoctenamer, polynorbornene, and polydicyclopentadiene (PDCP),[26,30] a tough, rigid, thermoset polymer of excellent impact strength. Due to these remarkable characteristics, PDCP has marine, recreational vehicle and heavy-vehicle applications.[26] Technology for its synthesis on a larger scale has been licensed to other interested companies from its founding company, Materia, who is spearheading the application of metathesis to the fine chemicals industry.[30,211] Their technology utilizes metathesis catalysts to form new polymers for sporting goods, as well as the synthesis of natural products and pharmaceuticals.

Pheromones can be synthesised using metathesis technology, often at a lower cost than traditional synthetic methods. Materia have patented the synthesis of six pheromones using this technology,[212] and have registered three of these with the USA Environmental Protection Agency, for use in environmentally friendly pest control methods. They have commenced field and laboratory tests of a mosquito oviposition pheromone that could aid in trapping and killing mosquitoes of the *Culex* genus that transmit the West Nile virus.[30] Other examples of the application of metathesis to natural product synthesis include the synthesis of epithilone A and its derivatives.[213,214] An enantioselective synthesis of the natural alkaloid (-)-indolizidine 167B (naturally found in the skin of a neotropical frog from Panama) has been described,[215] and the natural products castanospermine, ciguatoxin and various cyclic ethers have also been synthesised using metathesis technology.[23,88,216-221]

In a pharmaceutical application, Materia use metathesis to synthesise α,β-unsaturated aldehydes, which are then employed by MacMillan as a substrate for a metal-free catalytic process.[30] This process employs asymmetric organic molecules as catalysts to synthesise medically useful chiral products. An example is the production of (*S*)-ketorolac, an anti-inflammatory drug that has been produced by MacMillan using these two complimentary processes. Other examples include the search for a generic route to GlaxoSmithKline's anti-depressant, Paxil; Materia have successfully produced a key intermediate to the pharmacophore using CM.[30]

1.2.6. Current and future trends

There is a great need to increase the stereo- and enantioselectivities of certain metathesis processes. There have been reports describing as an existing chiral centre in the substrate can control the direction of cyclization of prochiral dienes in RCM.[23,87] There is, however, more effort being devoted to the design and synthesis of new chiral catalysts[23,30,39,85,87,156,172,184,222,223] that provide good stereoselectivity in metathesis reactions. The challenge for the future is to develop a robust chiral catalyst that meets the challenges of stereoselectivity without compromising on activity or stability.

As far as catalyst design and development is concerned, one area that is expected to receive more attention is the immobilization of homogenous catalysts on to solid supports. Although there have been numerous reports in the literature of such efforts,[23,100,166-173] the application of these catalysts at an industrially useful level has yet to be observed. Other current aspects of catalyst design include modifying the catalyst to minimise the rate of decomposition[82,104,128,173,224,225] and reduce the number of side reactions that may occur, particularly in the case of CM.[159,225]

The future will undoubtedly hold more opportunities for the use of well-defined homogenous metathesis catalysts in industrial processes, as companies become increasingly interested in using metal carbenes in catalytic processes.[30] J.C. Mol[26] predicts that oleochemistry stands to benefit from olefin metathesis technologies, as this would provide routes to new and existing products from unsaturated natural fats and oils.[26,30] It is also likely that greater emphasis will be placed on green catalysis, and the development of environmentally friendly metathesis technologies. Such developments may involve the use of ionic liquids[14,186] and water.[21,45,46,73,83,103,226]

K.C. Nicolaou has been quoted as saying "Today, this powerful reaction provides solutions to many synthetic puzzles and has the potential to do so in the future for myriad others".[30] This may be pre-emptive of Grubbs' own anticipation for the future of olefin metathesis, when in 2004 he mused, "A number of times along the way, I thought the journey was complete. However, the reaction keeps fooling me. It will be interesting to see what happens next."[27]

1.3. PREVIOUS WORK IN THE GROUP AND AIMS OF THE PRESENT STUDY

In the past there have been numerous studies in the group on the design and synthesis of ligands for their potential to chelate to various metals. One such study involved the design of complexes as biomimetic models for the active site of the enzyme tyrosinase, and consisted of novel diamido, diamino and diimino ligands complexed to Cu(II), Co(II), Ni(II) and Pt(II).[227,228] Molecular modelling was employed to explore the potential of these novel complexes.

Metal-selective bidentate, tridentate and tetradentate sulfur-containing ligands were designed for the selective extraction of Pt(II) and Pd(II) in the presence of base metals, for use in the mining industry.[229] In addition, highly selective polydentate malonamide ligands for chelation to Ag(I) were developed and silver selectivity in excess of 96% was achieved for one such ligand.[230] Bidentate ligands with amine and pyridyl nitrogen donors were also synthesised for the formation of metal-selective molecularly-imprinted polymers (MIP's); ICP-MS analysis showed a clear selectivity for Ni(II) over Fe(III).[231,232]

More closely related to the current study, novel tridentate camphor-derived ligands for use in ruthenium metathesis catalysts have been investigated.[233,234] Molecular modelling at the DFT level was used to determine both the chelating potential of these ligands and the catalytic potential of the ruthenium chelates.

In the present study, attention has been focussed on the development of various ligand systems, designed to chelate to ruthenium. More specifically the research has involved:-

i) exploring routes for the synthesis of the tridentate malonate-derived ligand **31** initiated in previous work;

ii) the synthesis of tridentate malonate-tethered pyridine systems;

iii) the synthesis of tridentate, branched pyridine systems;

iv) the use of modelling techniques to assess the potential for forming Grubbs-type ruthenium complexes; and

v) preliminary metal complexation studies.

2. DISCUSSION

The work presented here stems from previous research in the group aimed at the synthesis of novel halide-free ruthenium metathesis catalysts using tridentate, chelating ligands.[234,235] There is evidence for the involvement of a chloride-bridged dimer in the decomposition of Grubbs-type catalysts[224,236-238] and it was thought that replacing the chloride ligands would afford more stable complexes, not only by removing this decomposition pathway, but also by the stabilizing effects of chelation. Other benefits associated with the use of chelating ligands include the provision of a point of anchorage for immobilizing the ligand on to a solid support.[234]

There have been several reports in the literature on the synthesis of halide-free ruthenium metathesis catalysts, including the use of carboxylate, heterobifunctional silicylaldimine, and alkoxide or aryloxide ligands as pseudohalides.[156,224,237,239-242] These examples, some of which have promising metathesis activity,[237] have prompted us to explore this class of catalyst further, with an emphasis on ligand design. The current project has been concerned with three parallel lines of investigation, *viz*.; i) the extension of previous attempts to access a malonate-derived imidazolidine tridentate system (Section 2.1); ii) the synthesis of a tridentate, malonate-tethered pyridine system (Section 2.2), and (iii) the synthesis of a variety of branched tridentate pyridine systems, involving either carboxyl or amine ligand donor groups (Section 2.3). Finally, some preliminary complexation studies have been undertaken (Section 2.4).

2.1. TRIDENTATE MALONATE-TETHERED SYSTEMS

Sabbagh[234] initiated work within the group on malonate-derived systems, based on the chelation potential of the malonate system and the possibility for structural elaboration of the malonate moiety. In the ruthenium metathesis catalysts, malonate systems may coordinate to metals in unidentate (a) or bidentate (b) fashions (Figure 2.1).[234,243] While little attention has been given to the use of malonate species as dianionic ligands in ruthenium alkylidene complexes, there has been substantial research into the synthesis of ruthenium complexes bearing other carboxylate ligands.[105,170,242,244] These studies have generally aimed to immobilize the catalysts on to solid supports.

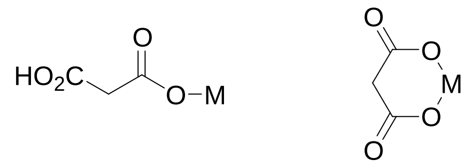

a unidentate   **b** bidentate

Figure 2.1. Binding modes of the malonate anion.[234]

2.1.1. Design rationale

Complex **28** was geometry-optimized at the DFT level by Sabbagh[234] who found that the ruthenium-phenoxy bond length (2.36Å) was comparable to that of the Hoveyda catalyst **5** (2.37 Å), suggesting that initiation rates for this complex could be similar to that of catalyst **5**. This bond length was also found to be significantly shorter than for the untethered analogue **29** (2.44 Å), suggesting that the tethering of the malonate moiety to the NHC could relieve steric crowding around the substrate coordination site,[234] thus facilitating coordination of the olefinic substrate. In the present study it was decided to extend this earlier work into the synthesis of the tridentate ligand **31** (Scheme 2.1), required to form the Grubbs-type complex **30**.

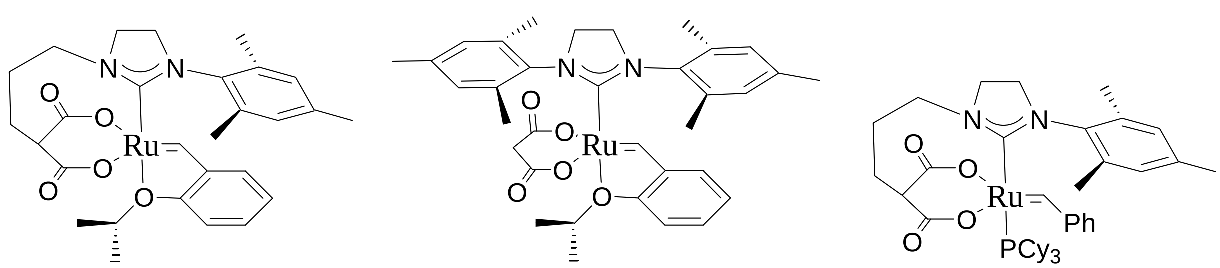

28   **29**   **30**

Complex **30** was modelled at the molecular mechanics level (Figure 2.2). Previous studies have shown that molecular mechanics gives a good approximation of the geometry of these systems,[234,245] justifying our use of this rapid and convenient approach for initial design purposes. These calculations indicate a ruthenium-phosphine bond length of 2.604 Å, compared to 2.419 Å for the analogous Grubbs second generation catalyst **21**[123] (Figure 2.2). The longer bond length in the case of complex **30**, suggests that initiation (loss of the labile phosphine) might occur more readily than for the Grubbs second-generation catalyst. However, the Ru-NHC bond length (3.00 Å) is longer than the Ru-P bond length, suggesting that the latter is stronger. This may have negative implications in terms of the dissociation of the phosphine moiety. As with the Hoveyda-type complex **28**, the O-Ru-O bond angle (74.6°) has *cis* geometry, deviating from the standard *trans* geometry of the anionic ligands. The effect of this has not, to our knowledge, been examined in the literature.

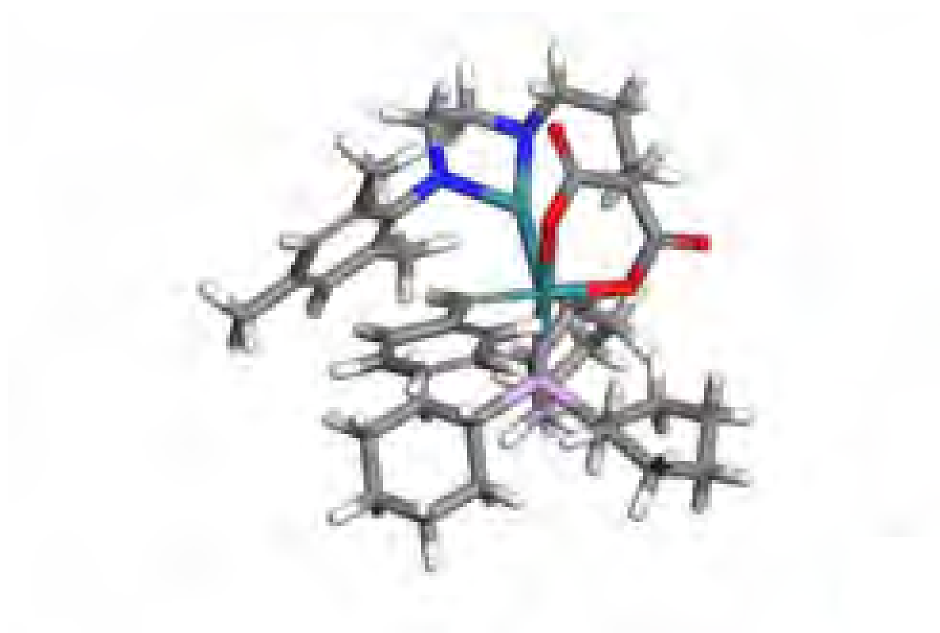

Figure 2.2. Complex **30**: conformation of global minimum from molecular mechanics calculations.

The retrosynthetic strategy initially developed[245] for the preparation of the target complex **30** is outlined in Scheme 2.1. The target ligand **31** is a cyclic derivative of compound **32**, which in turn may conceivably be synthesized *via* a condensation reaction between two synthons, the aldehyde **33** and the amine **34**. However, previous attempts to access the diacid **34** were unsuccessful (Scheme 2.2).[245]

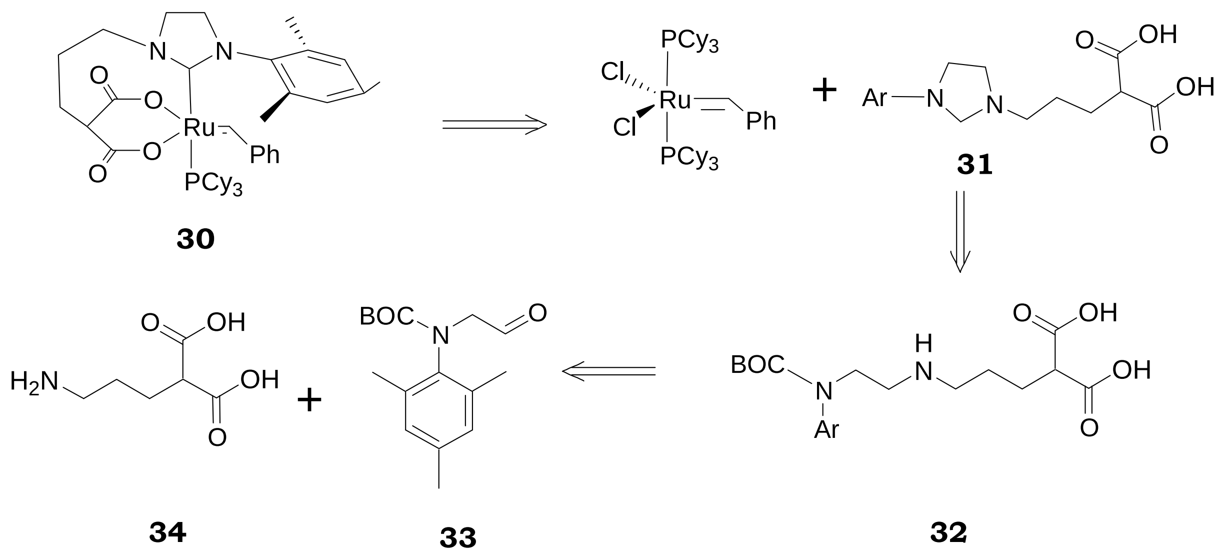

Scheme 2.1

Earlier attempts to access synthon **34**[234] were directed at the synthesis of the ammonium tosylate **35**. While α-alkylation of diethyl malonate **36** with allyl bromide **37** successfully yielded the desired malonate derivative **38**, attempts to prepare the bromo-diester **39** using aqueous HBr gave the carboxy lactone **41** (Scheme 2.2). Better results were obtained when gaseous HBr was employed, but the conversion to the desired ammonium tosylate **35** was unsuccessful. In light of these synthetic difficulties, the current project has focussed on the synthesis of synthon **34** using different approaches.

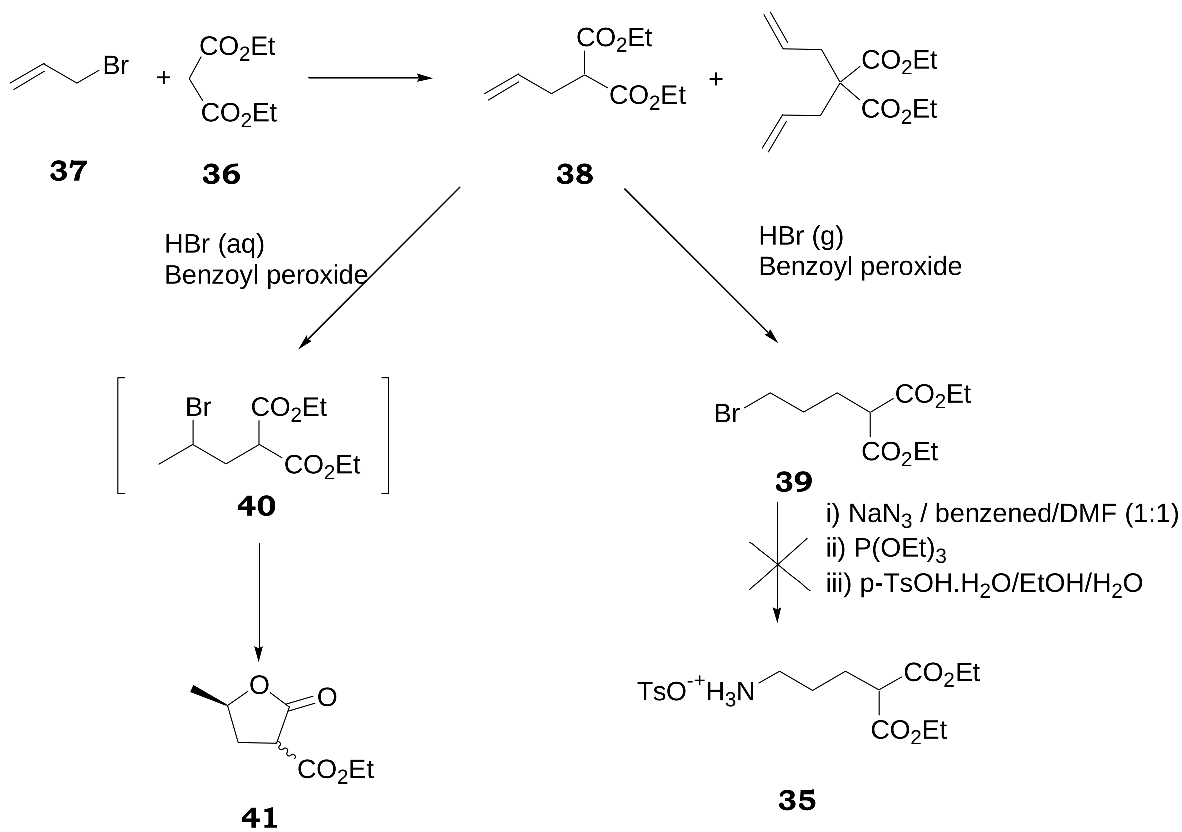

Scheme 2.2[234]

2.1.2. Synthetic approach

The aldehyde **33** was prepared following the method outlined in Scheme 2.3.[246] Thus, after protecting the amine moiety of 2,4,6-trimethylaniline **42** as the Boc amide **43**, *N*-alkylation was effected in good yield using potassium hydride and 3,3-dimethylallyl bromide. The structure of olefin **44** was confirmed by the presence of the expected proton signals in the ^{1}H NMR spectrum, including the vinylic methine signal as a multiplet at 5.28 ppm. The olefin **44** was readily converted to the desired aldehyde **45** by ozonolysis; this was confirmed by the disappearance of the two olefin methyl signals at 1.50 and 1.62 ppm, and the appearance of the aldehyde multiplet at 9.80 ppm in the ^{1}H NMR spectrum. The carbonyl carbon of aldehyde **45** resonates at 199.5 ppm in the ^{13}C NMR spectrum.

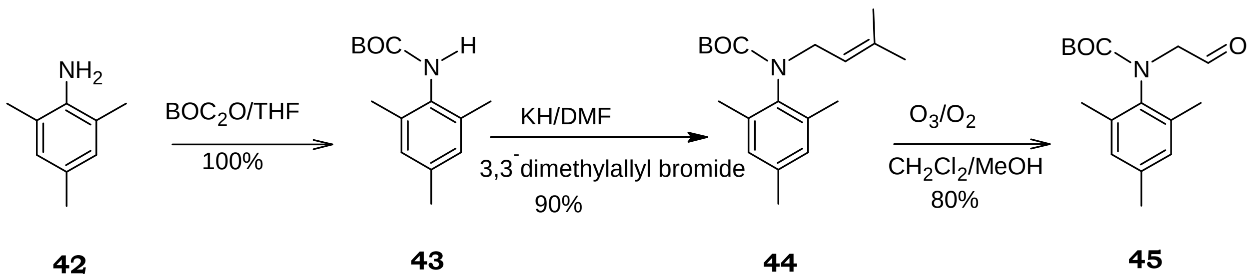

Scheme 2.3

In a new approach to the amine **34**, 3-aminopropanol **46** was treated with NaH and *p*-toluenesulfonyl chloride (Scheme 2.4). However, the *N*-tosylated isomer **47** was obtained instead of the desired *O*-tosylated product **48**. This was confirmed by ^{1}H NMR analysis and IR spectroscopy; Table 2.1 shows the predicted chemical shifts for the NCH_2 moiety in the *O*-tosylated **48**, *N*-tosylated **47** and ditosylated system **49**, using the NMR predict tool in the ChemDraw software package.[246] The NH protons are predicted to resonate at lower field in the *N*-tosylated compounds isomers **47** and **49**, compared to the NH_2 protons in the *O*-tosylated compound **48**. ^{1}H NMR analysis of the material obtained from this reaction gives a signal closer to that predicted for the *N*-tosylated isomer, with an observed chemical shift of 3.04 ppm.

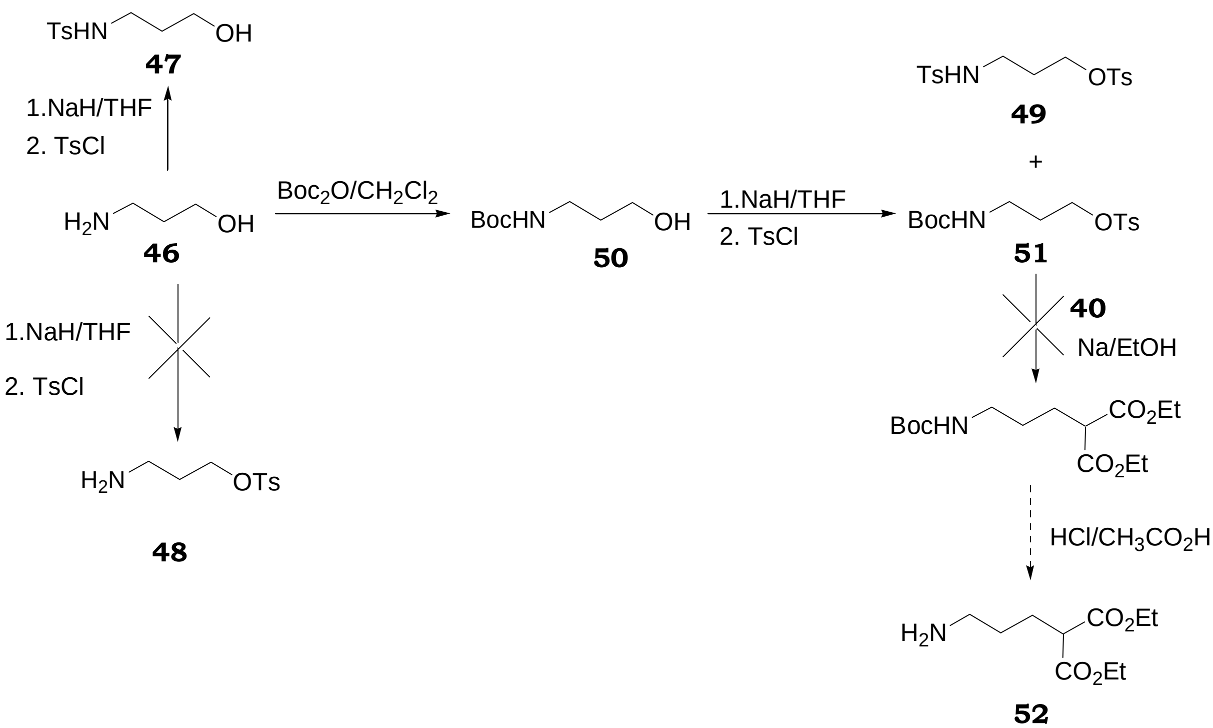

Scheme 2.4

In addition to the NMR analysis, IR analysis of the material clearly shows overlapping OH and NH absorption bands (Figure 2.3). Such a strong OH band should not be observed for the *O*-tosylated isomer. Thus, with the aid of ^{1}H NMR and IR analysis, we were able to conclude that the *N*-tosylated isomer **47** was obtained, rather than the desired *O*-tosylated isomer **48**.

Table 2.1. Predicted and observed NH ^{1}H NMR chemical shifts (δ/ppm) in compounds **48**, **47**, and **49**.

Compound		**Predicted**	**Observed**
48	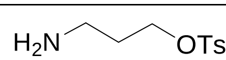	2.65	-
47	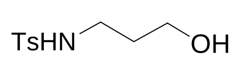	3.16	3.04
49	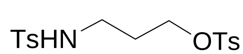	3.16	3.08

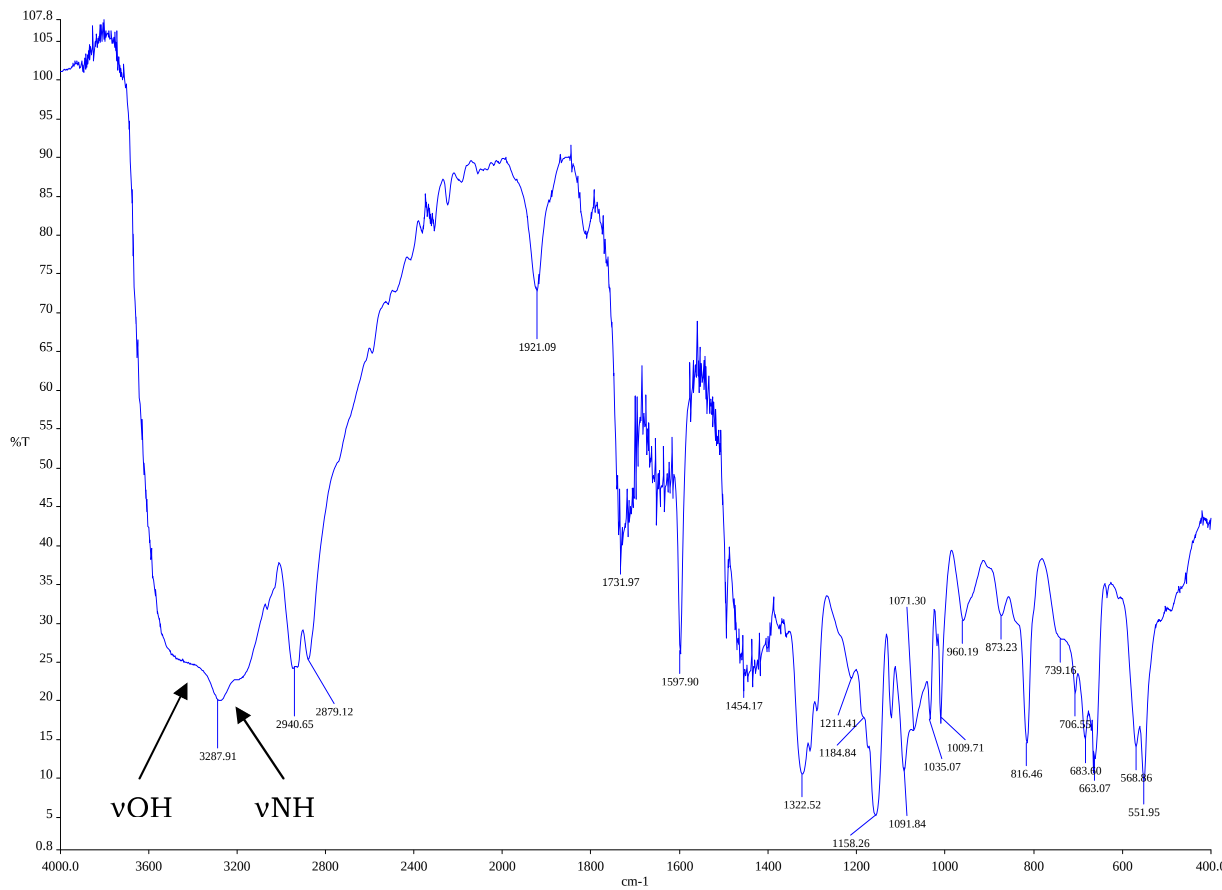

Figure 2.3. IR spectrum of *N*-tosylated **47**, illustrating overlapping νOH and νNH absorption bands.

It was then decided to first protect the amine moiety of 3-aminopropanol **46** (Scheme 2.4), following a standard procedure using di-*tert*-butyl dicarbonate in dichloromethane. The Boc amide **50** was obtained in quantitative, and was subsequently tosylated to form the *O*-tosylated Boc amide **51** in 53% yield. Isolation of the ditosylated product **49**, in approximately 13%, yield suggests some displacement of the Boc group during the reaction. The ^{1}H NMR spectrum for the ditosylated product **49** (Figure 2.4) clearly indicates the presence of two sets of tosyl signals, both with regards to the aromatic proton signals and the tosyl CH_3 signals. Unfortunately, attempts to selectively displace the OTs moiety in the monotosylated compound **51** by diethyl malonate enolate proved unsuccessful.

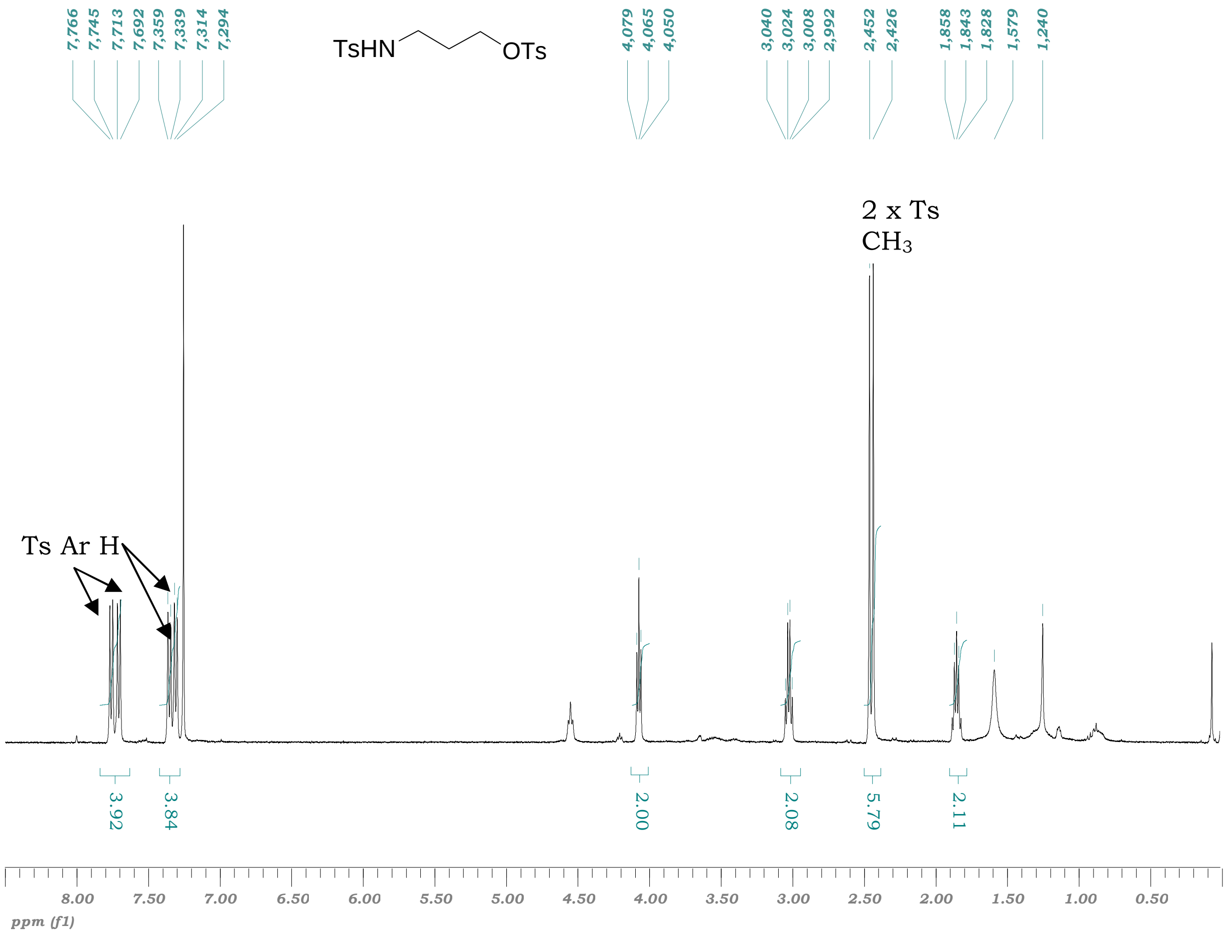

Figure 2.4. 400 MHz [1]H NMR spectrum of the ditosylated product **49** in $CDCl_3$.

An alternative approach to diester **52** involved the alkylation of 3-bromopropylamine **53** with diethyl malonate **36**, using sodium ethoxide as base (Scheme 2.5). Small amounts (*ca* 30-33% yield) of the diester were obtained, as evidenced by the methylene quartet at 4.22 ppm, and the methyl triplet at 1.28 ppm in the [1]H NMR spectrum. However, numerous attempts to prepare the imine **54** in an aldehyde condensation reaction were unsuccessful (Scheme 2.5). Similarly, attempts to reductively aminate the aldehyde **45** with the amine **52** using sodium cyanoborohydride were unsuccessful.

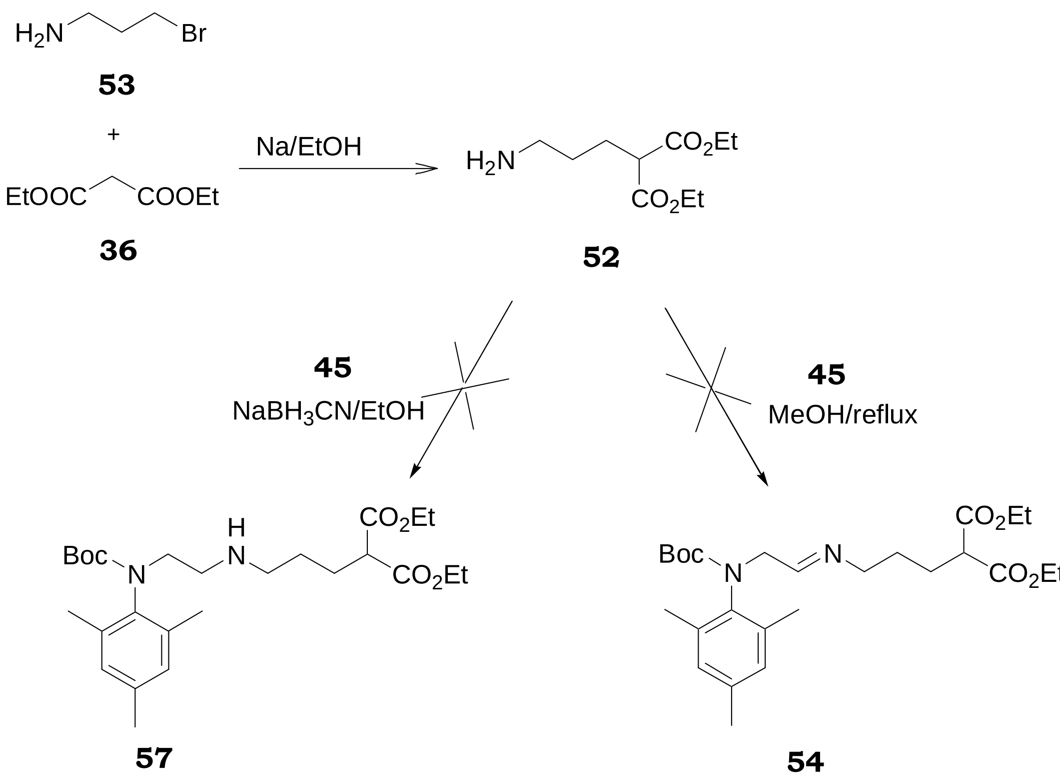

Scheme 2.5

Consequently, we decided to prepare the pseudohalide **55** (Scheme 2.6). This was achieved by reducing the aldehyde **45** to the alcohol **56** using $NaBH_4$ (confirmed by a shift in the NCH_2 signal in the ^1H NMR spectrum from a doublet at 3.96 ppm to a triplet at 3.78 ppm). Reduction was followed by tosylation to form the tosyl derivative **55**, confirmed by the presence of the tosyl aromatic doublets at 6.86 and 7.41 ppm, and the tosyl CH_3 singlet at 2.49 ppm in the ^1H NMR spectrum. The tosylate **55** proved unstable, and chromatography resulted in the hydrolysis of the tosyl moiety. The crude product **55** was therefore taken through to the next step without purification, but attempts to prepare the amine **57** from the tosylate **55** and the diester **52** were unsuccessful (Scheme 2.6).

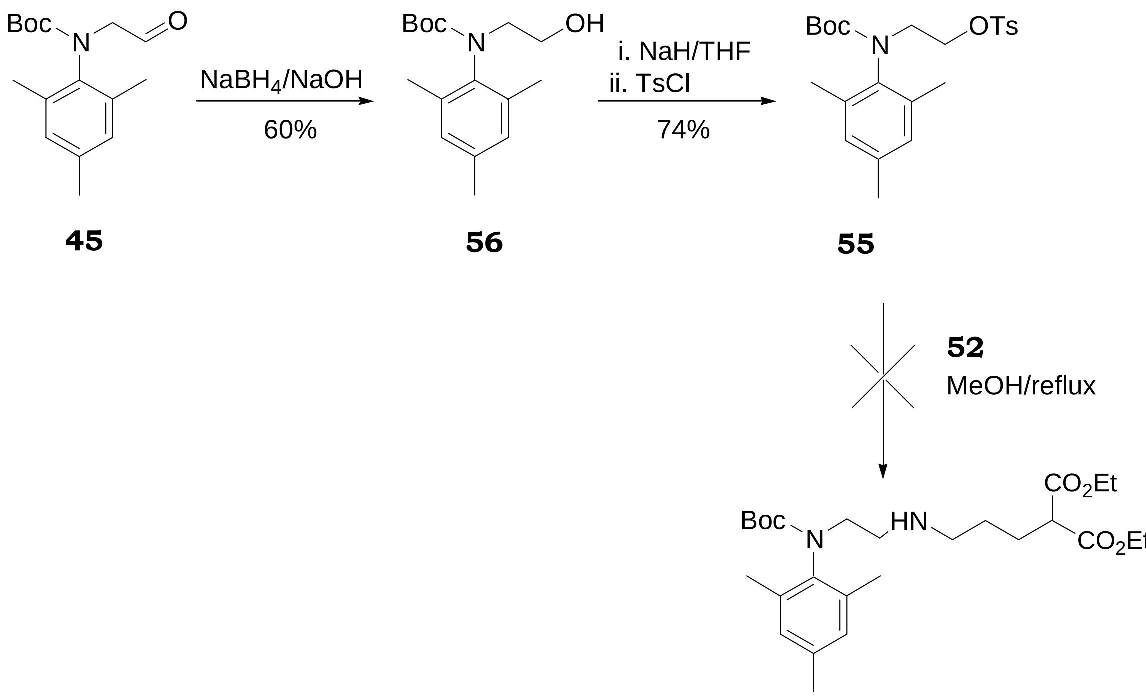

Scheme 2.6

Given the difficulties encountered with the above approaches, it was decided to investigate a third approach. Using a method adopted from Vougiokalakis *et al.*[247] oxalyl chloride was reacted with 2,4,6-trimethylaniline **42**, in the hope of obtaining the asymmetrically-substituted mono-amide **58**. From this it might be possible to access the disubstituted amide **59**, as illustrated in Scheme 2.7. Reduction of the amide functionalities, followed by cyclization, would thus afford a good precursor **60** to the desired ligand **31**.

The reaction afforded a white precipitate, and NMR analysis of this material indicated that it was, in fact, the bis-substituted diamide **61**. This was confirmed by the presence of only one carbonyl signal in the ^{13}C NMR spectrum (Figure 2.5), suggesting symmetry in the isolated product. The IR carbonyl absorption band was observed in the IR spectrum, as indicated in Figure 2.6. MS analysis confirmed this unequivocally, indicating the presence of the molecular ion of the bis-substituted diamide **61**.

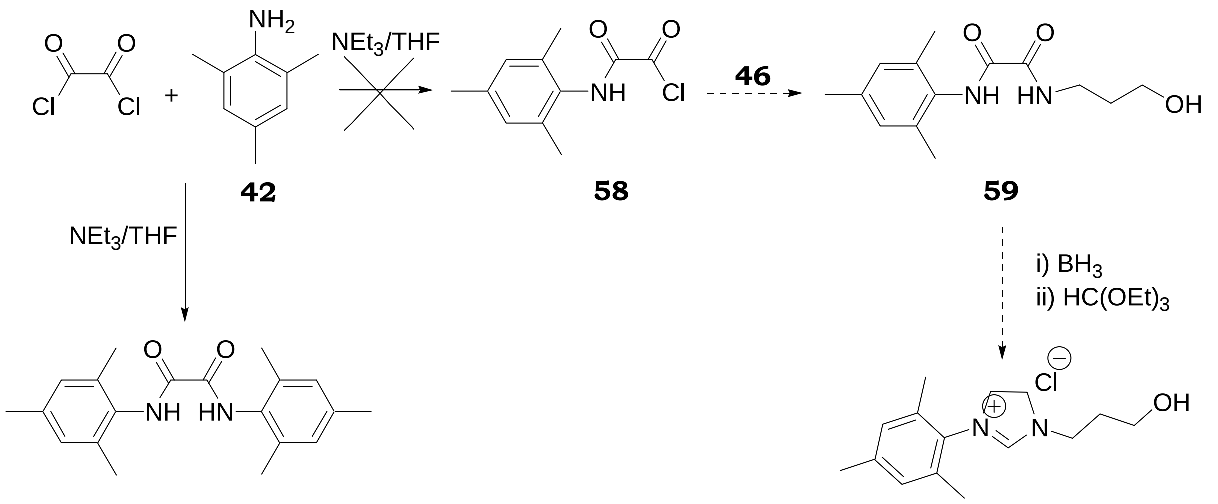

42 58 59 61 60

Scheme 2.7

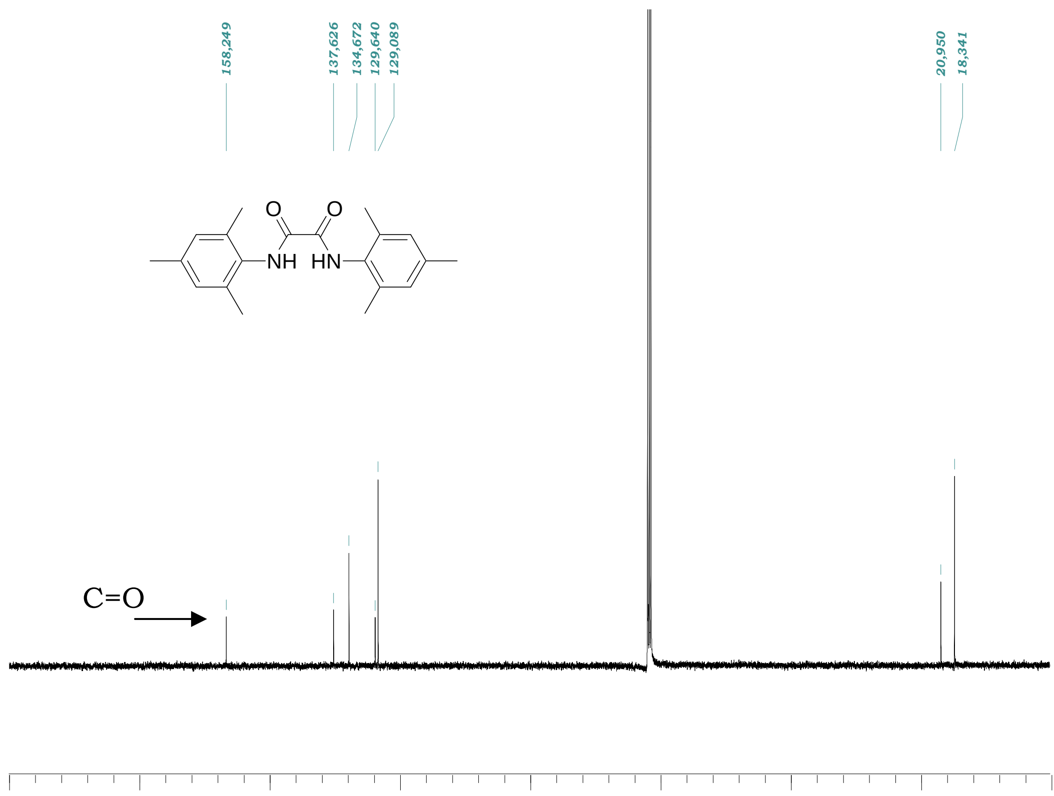

Figure 2.5. 100 MHz ^{13}C NMR spectrum of **61** in $CDCl_3$, indicating the presence of only one carbonyl signal.

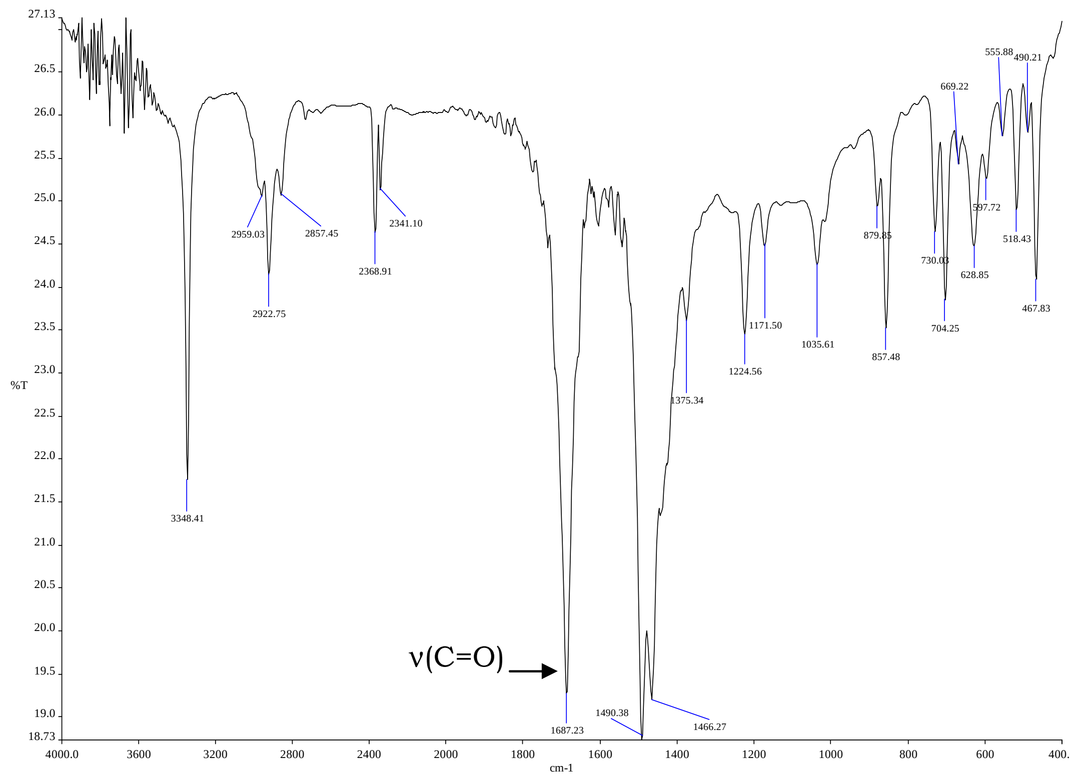

Figure 2.6. IR spectrum of **61** (KBr disk), indicating the presence of the C=O absorption band.

As we were unable to isolate the desired mono-substituted amide **58** using this approach, we decided to react the mono-chloro derivative, ethyl chlorooxoacetate **62** with 2,4,6-trimethylaniline **42** (Scheme 2.8). From the reaction products, it was clear that the desired monoester **63** was present in the mixture. MS analysis of the crude mixture showed the presence of the molecular ion at *m/z* 236. Similarly, NMR analysis confirmed the presence of the aniline moiety, with the aryl hydrogen signals at 6.90 ppm, and the *o*- and *p*-CH_3 signals at 2.25 and 2.28 ppm respectively (Figure 2.7). The ethyl signals are also present. ^{13}C NMR analysis confirmed the presence of two chemically non-equivalent carbonyl carbons, resonating at 154.7 ppm and 160.9 ppm. IR analysis also indicated two separate carbonyl absorption bands, at 1731 and 1677 cm^{-1}.

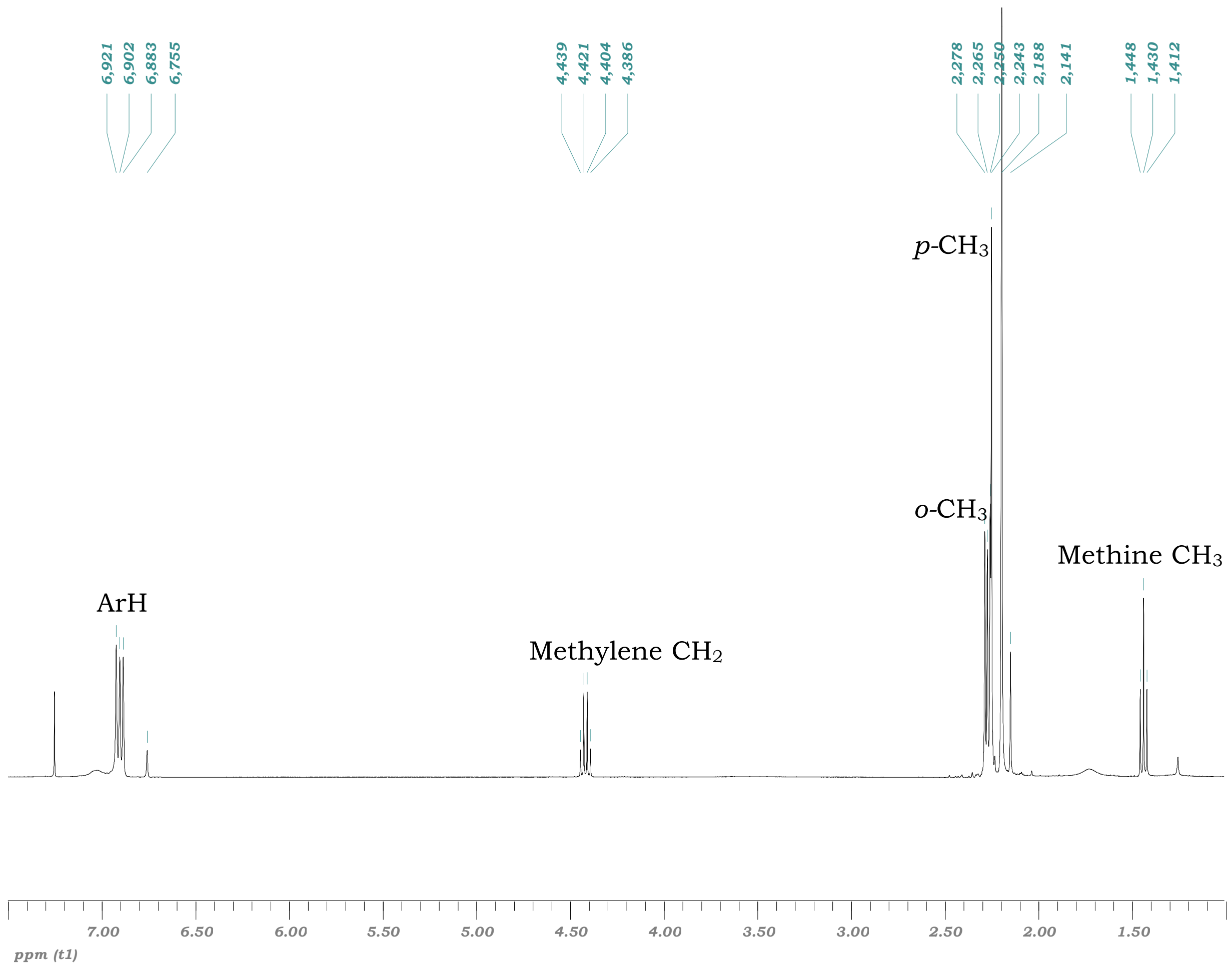

Figure 2.7. 400 MHz NMR spectrum of the crude monoester **63** in $CDCl_3$.

When the crude ester **63** was refluxed in excess 3-amino-1-propanol **46** for 8 hours, ^{1}H NMR analysis of the crude material suggested that the desired diamide **59** had indeed formed, as reflected in presence of alkyl CH_2 signals in the ^{1}H NMR spectrum, and two carbonyl signals in the ^{13}C NMR spectrum, with chemical shifts different to those of the starting materials **46** and **63**. In addition, two carbonyl absorption bands were observed in the IR spectrum. Unfortunately, time constraints prevented further investigation of this approach to the desired ligand. Scheme 2.7 shows how, if successful, only two further steps are required to the desired ligand. The reduction of the carbonyl functionalities and cyclization using ethyl orthofomate have been reported by Vougiokalakis *et al.*[247] for a different system, and the desired ligand **60** should thus be readily accessible using this approach.

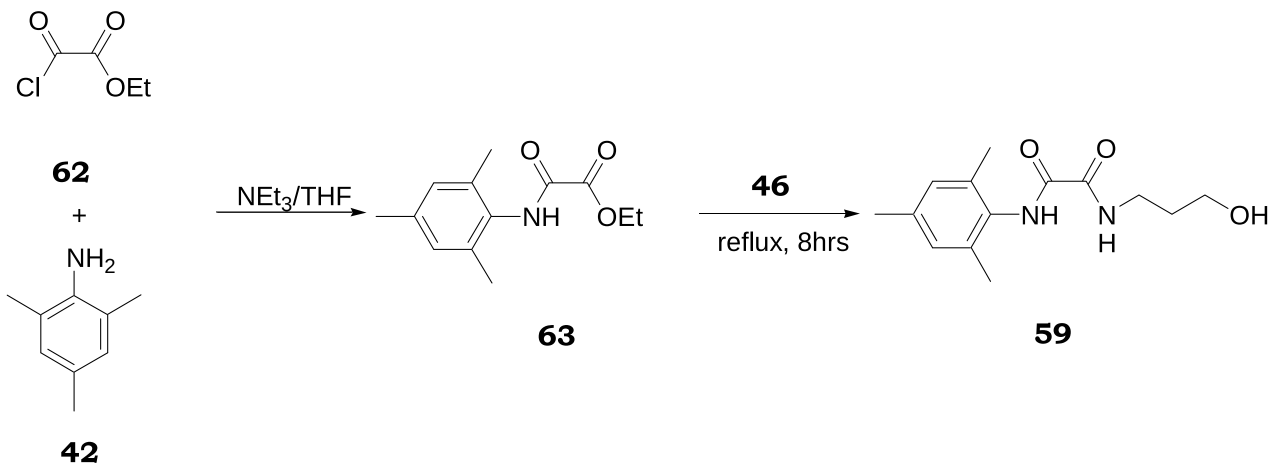

Scheme 2.8

2.2. MALONATE-TETHERED PYRIDINE SYSTEMS

Given the advantages of the malonic system mentioned in Section 2.1, we decided to design a class of pyridine ligand that could incorporate the malonate moiety. In this class of ligand, the malonate moiety is tethered to the pyridine ring at position 2, through a carbon chain of variable length, *e.g.* compounds **64** (n = 1) and **65** (n = 2).

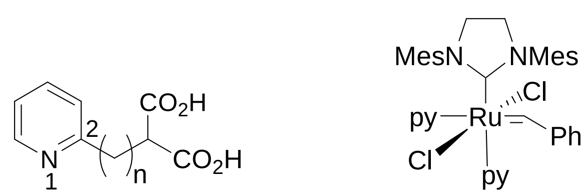

64: n = 1 **66**

65: n = 2

Pyridine systems have long been used as ligands in organometallic chemistry, and examples of their use in metathesis catalysts are well established in the literature. For example, the ruthenium metathesis catalyst **66** is cited as a third-generation catalyst with moderate activity.[188,248] The lability of the pyridine moiety ensures faster initiation.

One potential advantage of tethering the malonate moiety to a pyridine ring rather than to the imidazolidine system (as in compound **31**) may be attributed to the relative basicity of two ring systems. The pyridine system is expected to be more basic than its NHC counterpart, as the lone pair of electrons on the nitrogen is not involved in π-bonding in the aromatic ring,[249] thus contributing to the overall basicity of the system. As was noted in the Section 1, the more basic ligands tend to increase metathesis activity, albeit at the expense of catalyst lifetime. However, in the proposed ligand systems, an expected advantage of the chelating effect would be to increase complex stability, and hence, the catalyst lifetime. While increased lifetime is a desirable property in any catalyst, the metathesis activity of the complex may be adversely affected. It is hoped that the combination of a more basic ligand with the stabilizing effects of chelation may result in a more favourable metathesis catalyst. The structural features of modelled ruthenium complexes incorporating the tridentate ligands **64** and **65** are modelled in the next section.

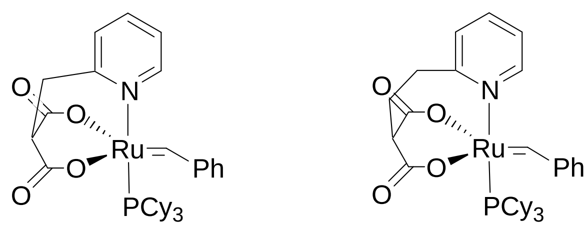

67 **68**

2.2.1. Computational comparison

Figure 2.8. Complexes **67** (left) and **68** (right) with malonate-tethered pyridine ligands.

When comparing the two putative complexes **67** and **68** (containing ligands **64** and **65** respectively) at the molecular mechanics level (conformational search using the Cerius^2 software package),[266] there is remarkably little difference in the relative geometries (Figure 2.8). Table 2.2 lists the Ru-ligand bond lengths for the two complexes. The Ru-PCy_3 and Ru-N bond lengths in each system are comparable, but the Ru-PCy_3 bond is longer in each case, indicating this to be the weaker bond. This suggests that initiation may be achieved more readily with these tethered pyridine systems than with the imidazolidine complex **30**, where the Ru-NHC bond appeared to be weaker than the Ru-PCy_3 bond (Section 2.1). One similarity between these pyridine systems and the imidazolidine system **30** is the O-Ru-O bond angle. A *cis*-arrangement of the anionic ligands is again observed, with the O-Ru-O bond angle at 92.9° for the smaller chelate **67**, and 90.2° for the longer chelate **68**.

Table 2.2. Geometrical data for malonate-tethered systems **30**, **67** and **68**.

Parameter	30	67	68
	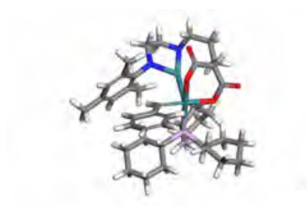		
Ru-PCy$_3$	2.60 Å	2.608 Å	2.607 Å
Ru-N/	3.00 Å	2.149 Å	2.189 Å

As with the imidazolidine system **30**, the Ru-P bonds of the tethered systems **67** and **68** are longer than for the Grubbs second-generation catalyst **21** (2.419Å), suggesting that initiation may proceed faster in these malonate tethered systems. However, this longer bond length may not be attributed to the more basic pyridine ring *trans* to the phosphine ligand, as a comparable bond length (2.604 Å) is observed for the imidazolidine complex **30**. This observation may therefore be a result of the tethered malonate moiety common to all three systems.

2.2.2. Synthetic approaches

The shorter-chained system **64** presented fewer synthetic challenges than its longer-chained analogue **65**. Scheme 2.9 illustrates the synthetic approach to the diester **69**, precursor to the desired diacid **64**. 2-(Bromomethyl)pyridine **70** was alkylated using diethyl malonate **36**, with sodium ethoxide as base. Both the desired diester **69** and its dialkylated analogue **71** were isolated from the reaction mixture, in varying amounts, depending on the amount of sodium ethoxide used. When a large excess of the base was used (*ca* 5 eq) the monoester **69** was isolated in 50% yield, and the diester **71** in 20% yield. The ratio of monoester to diester could be increased with a smaller excess of sodium ethoxide. For example, a 70% yield of the monoalkylated product **69** was obtained when only a slight excess of sodium ethoxide was used.

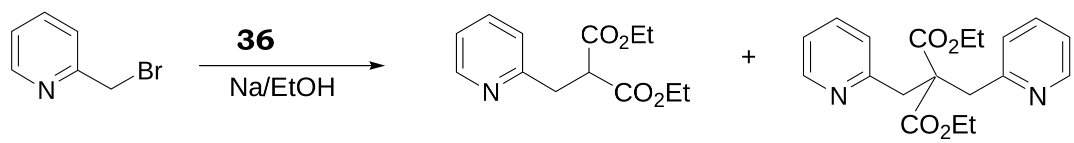

70 **69** **71**

Scheme 2.9

NMR spectroscopy was used to differentiate between the mono- and dialkylated products **69** and **71** respectively. Figure 2.9 shows the ^1H NMR spectrum for the monoalkylated product **69**. The most significant of the signals is the triplet at 4.07 ppm (see insert in Figure 2.9). This triplet corresponds to the 8-methine proton, as confirmed by 2-D NMR analysis. Furthermore, in Figure 2.10, the C-8 signal is clearly observed at 51.2 ppm in the DEPT 135 spectrum (supported by the relevant 2-D NMR analyses). However, the ^1H NMR spectrum for the dialkylated product **71** (Figure 2.11) does not exhibit a triplet immediately adjacent to the ethyl CH_2 signal, indicating that the proton at C-8 has been replaced; moreover the integral ratios indicate the presence of two pyridyl methyl groups. Figure 2.12 confirms that C-8 (resonating at 58.1 ppm in ^{13}C NMR spectrum) in the dialkylated **71** is a quaternary carbon, as this signal is not present in the DEPT 135 spectrum.

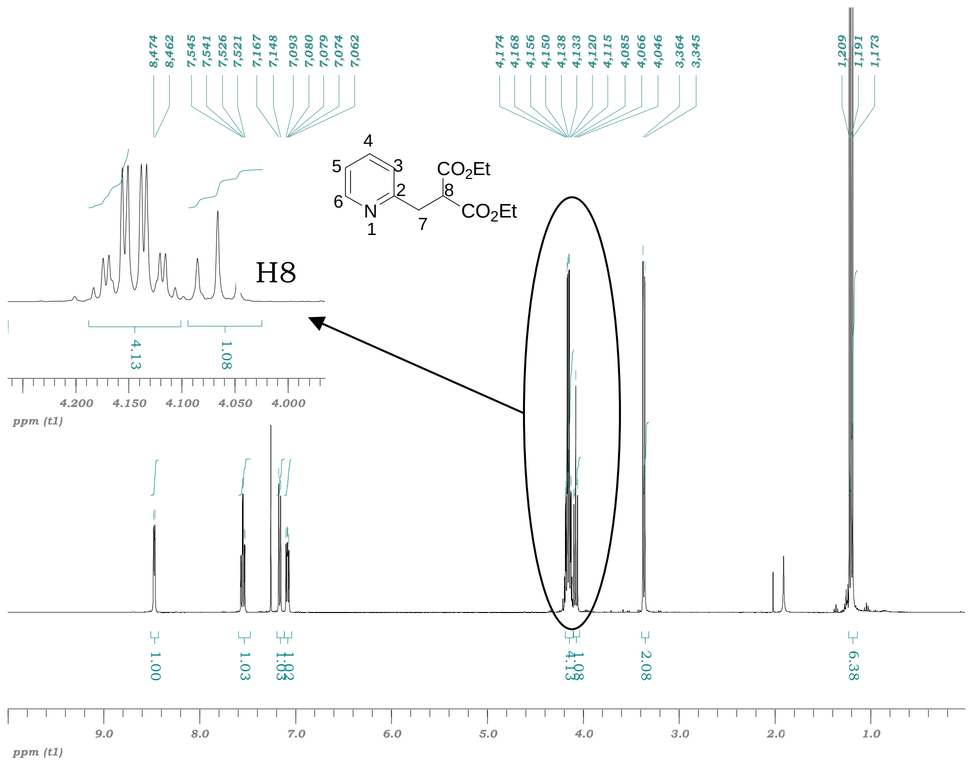

Figure 2.9. 400 MHz ¹H NMR spectrum of the monoalkylated diester **69** in $CDCl_3$.

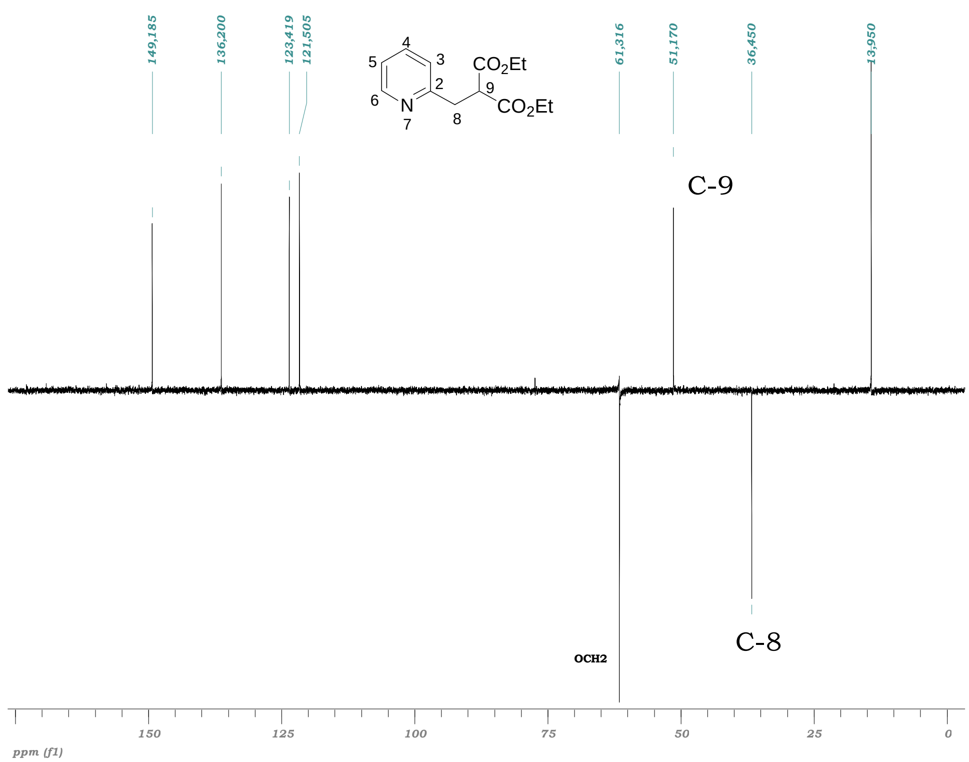

Figure 2.10. DEPT 135 spectrum of the monoalkylated diester **69** in $CDCl_3$.

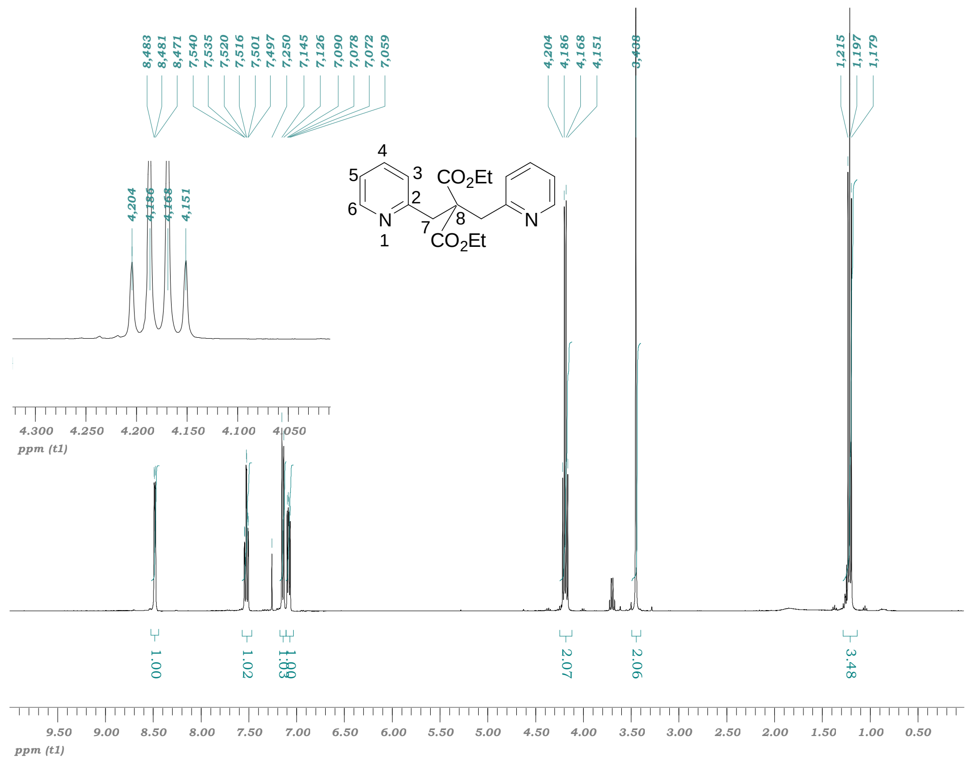

Figure 2.11. 400 MHz ^{1}H NMR spectrum of the dialkylated diester **71** in $CDCl_3$.

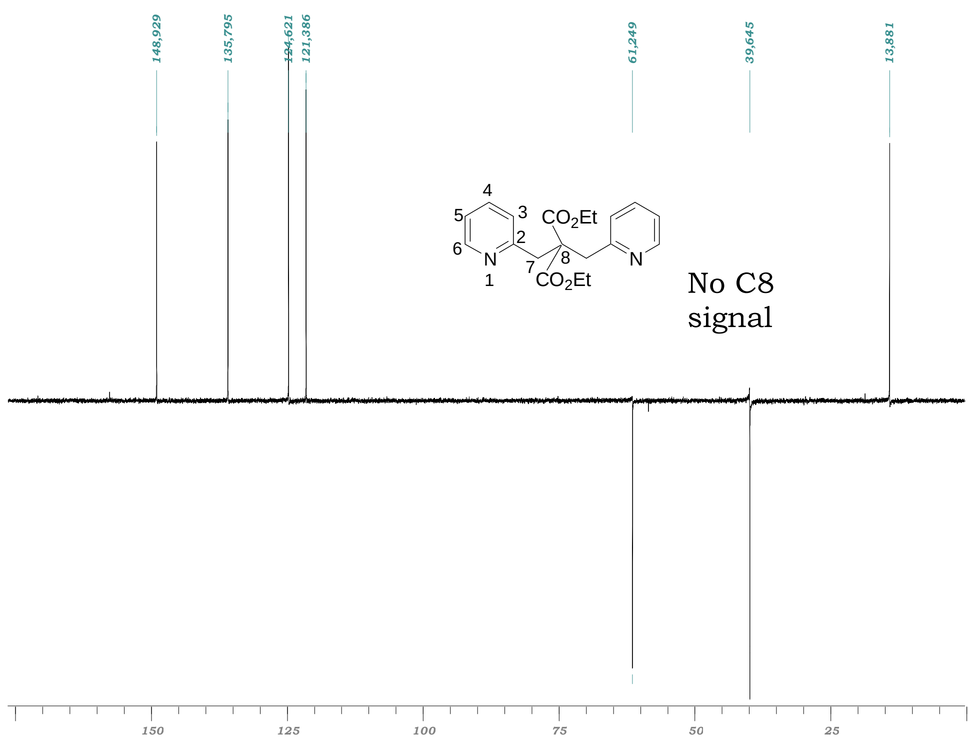

Figure 2.12. DEPT 135 spectrum of dialkylated diester **71** in $CDCl_3$.

The next challenge in the synthetic pathway was to hydrolyse the ester functionalities to give the diacid **64**. While this hydrolysis might seem to be a straight-forward textbook reaction, we expected difficulties in the work-up, owing to the presence of the basic pyridine moiety, tethered to the acidic dicarboxylate group. The challenge would be to ensure neutrality of the whole molecule so that it could be extracted into the organic phase. A slightly acidic aqueous phase could protonate the pyridine nitrogen, resulting in aqueous solubility of the resulting pyridinium salt. Conversely, a slightly basic aqueous phase could deprotonate the carboxylate functionalities, again resulting in the formation of aqueous soluble salts, and preventing the extraction of the desired product.

One means of overcoming this challenge would be to simultaneously hydrolyse the ester functionalities and form the thallium salt. The use of the thallium salt of a ligand is a common means of synthesizing Grubbs- and Hoveyda-type ruthenium complexes.[25,250] It would thus be advantageous to effect the hydrolysis and form the corresponding thallium salt **72** in one step (Scheme 2.10). This was achieved simply by heating the diester **69** in a solution of thallium carbonate in water at *ca.* 70°C for one hour.

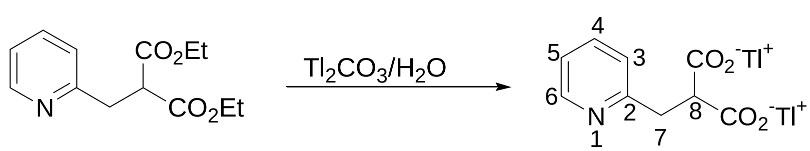

69 **72**

Scheme 2.10

Spectroscopic evidence for the formation of the desired salt was obtained from NMR analyses in D_2O. In the ^{1}H NMR spectrum (Figure 2.13), all four aromatic proton signals are evident in the aromatic region as well as the methylene doublet for H-7 at 3.05 ppm and the methine triplet for H-8 at 3.40 ppm. Significantly, however, neither of the two ethyl signals are present, in either the ^{1}H or ^{13}C NMR spectra, confirming hydrolysis of the ester groups. The carbonyl carbons resonate at 179.0 ppm in the ^{13}C NMR spectrum, as confirmed by the absence of this signal in the DEPT 135 spectrum. In the HSQC spectrum the carboxylate carbon signal does not correlate with any proton signals, but correlates with H-7 and H-8 in the HMBC spectrum, confirming its proximity to both (Figure 2.14). ICP analysis indicated a thallium content of 63% compared to the calculated value of 68%; the analysis was performed on the crude material and some deviation from the theoretical value is expected. The value obtained, however, clearly permits characterization of the product as the salt **72**.

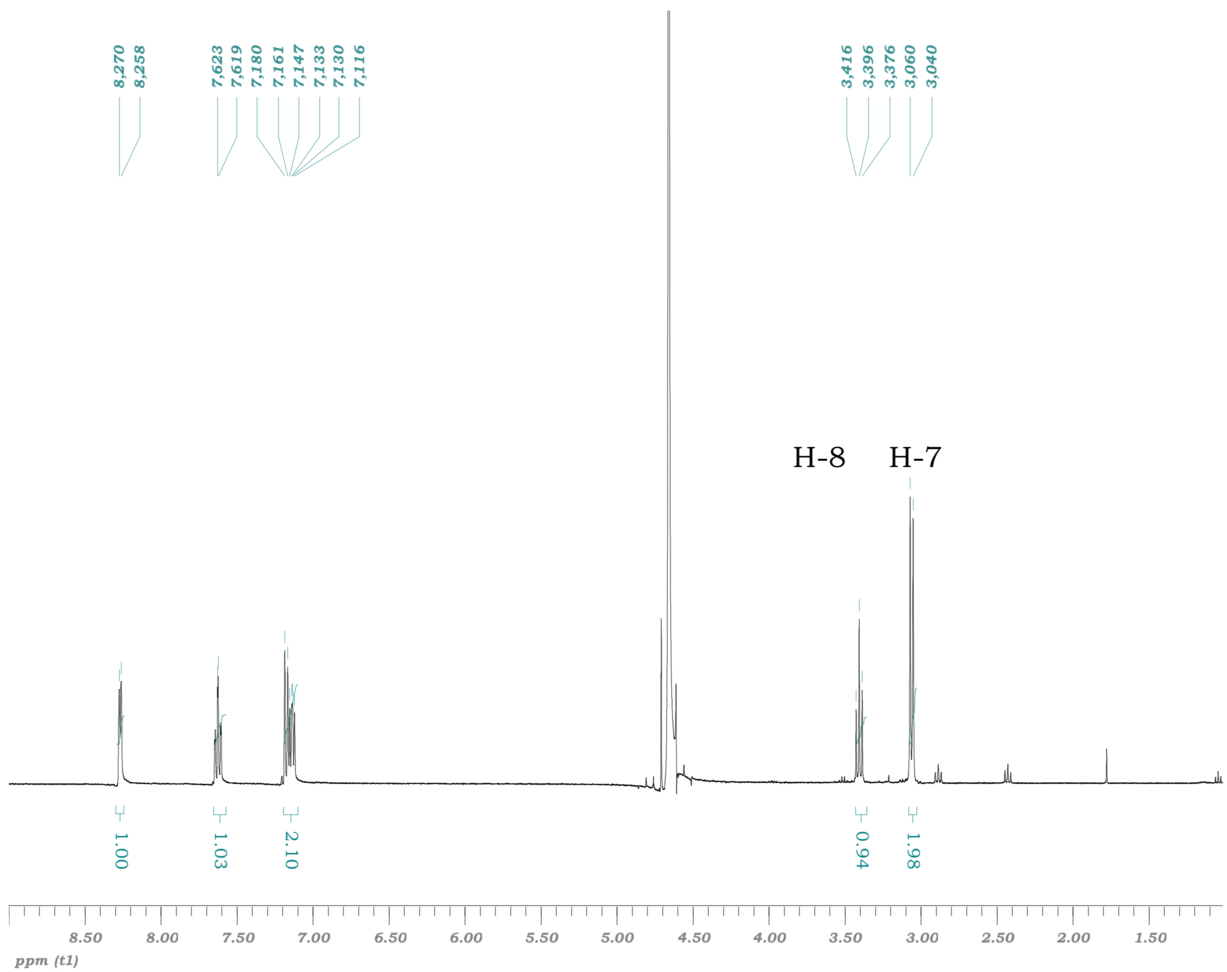

Figure 2.13. 400 MHz ^{1}H NMR spectrum of the thallium salt **72** in D_2O.

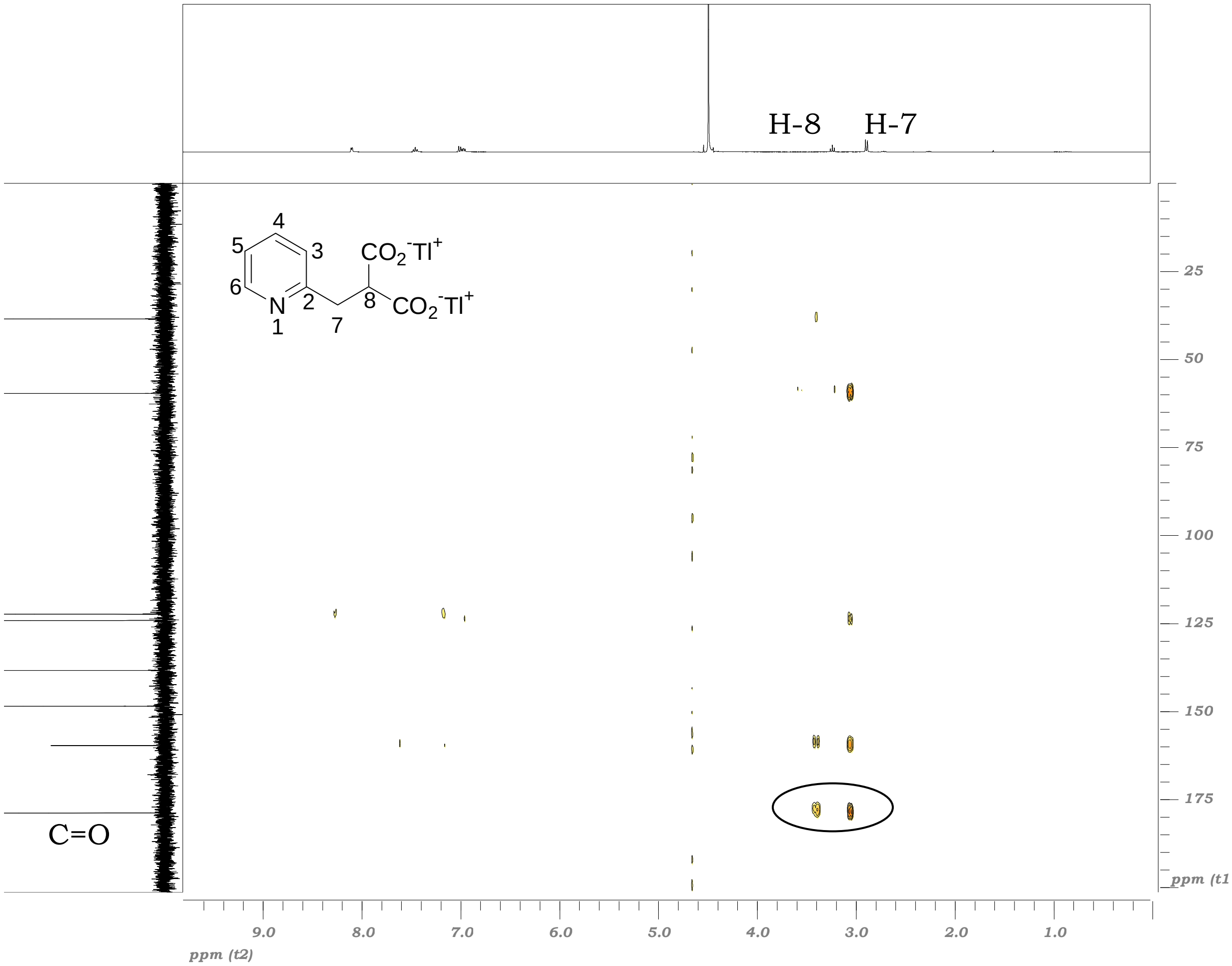

Figure 2.14. HMBC spectrum of the thallium salt **72** in D_2O, indicating the correlation between the carbonyl carbon and H8 + H7.

With the diester **69** successfully converted to one chelating ligand, it was thought that another potential ligand might be readily accessed by reducing the same diester **69** to the corresponding diol (Scheme 2.11). While alkoxide functionalities have received little attention as ligands for metathesis catalysts, a few reports are noted in the literature.[251-253]

This reduction was effected with DIBAL in dry THF, and was confirmed by the loss of the ethyl signals in the ^1H NMR spectrum in D_2O. However, aqueous NaOH was used to quench the highly reactive DIBAL on completion of the reaction, and it is presumed that the sodium salt of the diol **73** was isolated. This is supported by the limited solubility of the product in organic solvents, and the extremely high melting point of the solid product (> 320°C).

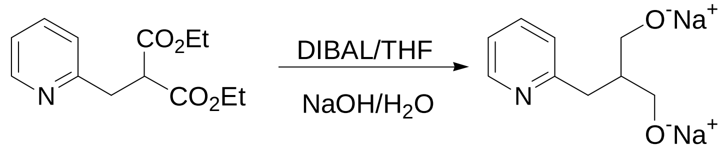

69 **73**

Scheme 2.11

The preparation of the longer-chained analogue **74** of diester **69** was a greater synthetic challenge, as the analogous starting material is not commercially available and therefore had to be synthesised. The first approach towards an equivalent starting material to 2-(bromomethyl)pyridine **70** was to synthesize 2-(chloroethyl)pyridine **74** *via* 2-vinylpyridine **76**. The method involved the *in situ* generation of HCl in a solution of 2-vinylpyridine **76** in ethanol, by the cautious addition of acetyl chloride (Scheme 2.12). As illustrated in Scheme 2.12, it was thought that the direct attack of Cl^- on the double bond of vinyl pyridine **76** would result in the formation of intermediate **77**, and that the restoration of aromaticity would favour spontaneous tautomerisation, affording the desired halide **74**.

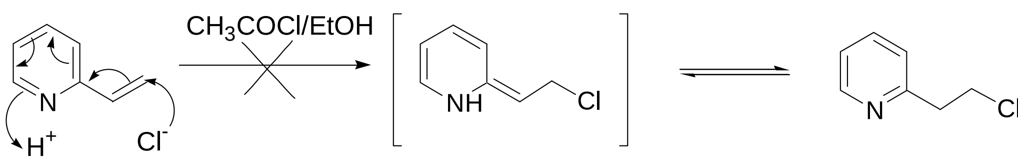

76 **77** **74**

Scheme 2.12

However, very broad signals were observed in the ^1H NMR spectrum of the crude material, in both DMSO-d_6 and $CDCl_3$. When the spectrum is overlaid with that of the starting material **76** (Figure 2.15), the broadness of the signals of the reaction material becomes starkly apparent. In addition to this, resolution is lost – multiplets become broad singlets – and there appears to have been a genuine shift of signals in the crude reaction product, relative to the starting material **76**. Notably, the $CDCl_3$ signal is not broad, and the phenomenon thus appears to be a genuine property of the crude and possibly polymeric material.

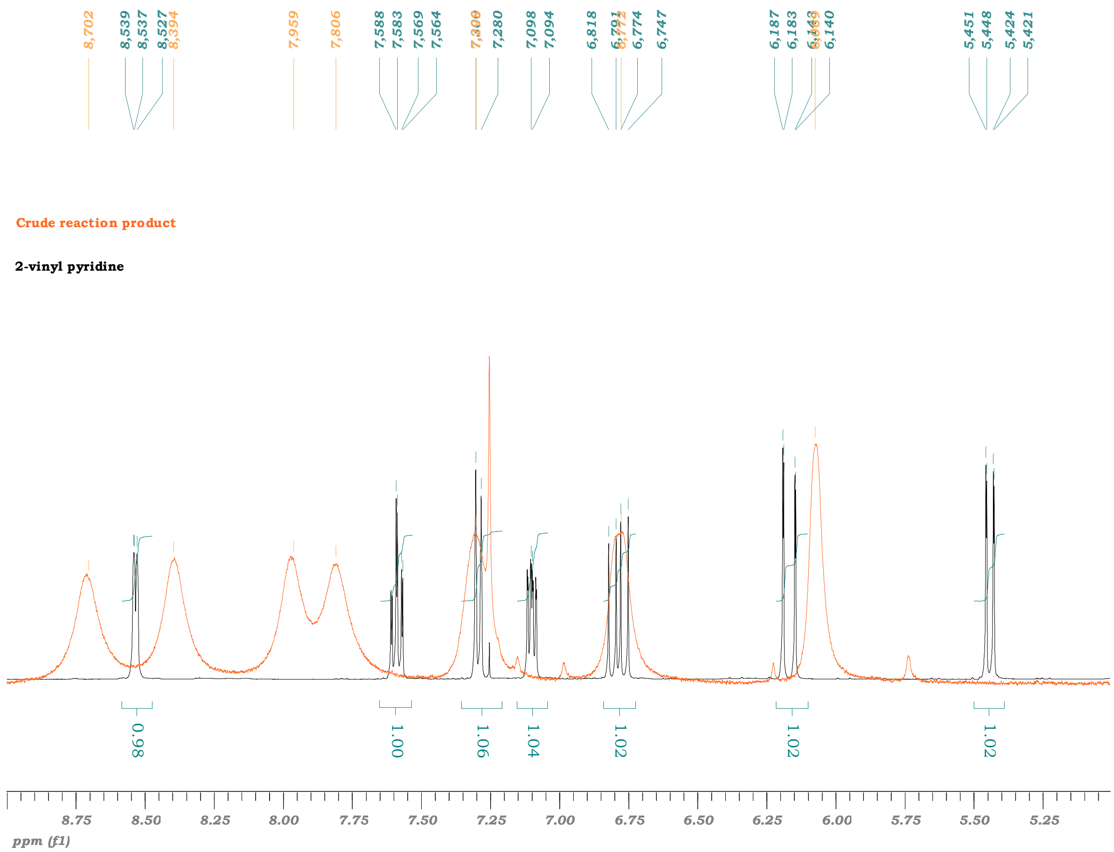

Figure 2.15. 400 MHz ^{1}H NMR spectrum of the crude product from reaction of 2-vinylpyridine **76** with HCl (orange) overlaid on the ^{1}H NMR spectrum of the starting material **76** (black); both spectra recorded in $CDCl_3$.

Due to the width of the signals in the ^{1}H NMR spectrum, characterization of this material by NMR analysis was not possible, and a different approach was explored. This involved the formation of the tosylate **78**, as illustrated in Scheme 2.13. Tosylation of the hydroxy group of 2-(2-hydroxyethyl)pyridine **79** was confirmed using NMR spectroscopy; the tosyl aromatic doublets and the methyl singlet at 2.46 ppm were observed in the ^{1}H NMR spectrum of the product **78**. However, as was the case with other tosyl-containing compounds in this work, purification of the tosylated **78** by chromatography proved difficult, suggesting decomposition or hydrolysis of the tosyl functional group.

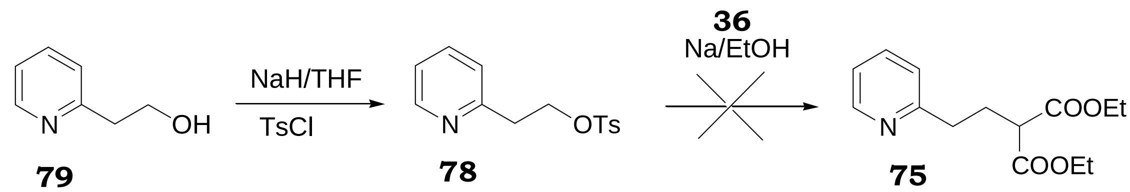

Scheme 2.13

The tosylate **78** was therefore used without purification in the next alkylation step (Scheme 2.13), but the reaction with diethyl malonate **36** and sodium ethoxide was unsuccessful.

2.3. BRANCHED TRIDENTATE PYRIDINE SYSTEMS

The third class of ligands examined in this work were the branched tridentate pyridine derivatives of the type illustrated below. In this class of ligand, two chains branch off the pyridine ring at positions 2 and 6. Chelation to ruthenium was expected to take place *via* suitable donor atoms (Y) located on each branch. There are two subtypes of ligand in this class – those where the chelating functionality is a carboxylate group (Section 2.3.1), and those where the donor atom Y is an amine functionality (Section 2.3.2).

These ligands differ from the malonate derivatives discussed in Sections 2.1 and 2.2, in that the ligand scaffold and all the donor atoms are expected to be co-planar. In the malonate derivatives, the carboxylate donor atoms are perpendicular to the plane of the NHC or pyridine rings. Hinderling *et al* report the operation of a swing-mechanism in the catalytic cycle, involving ligand rotation during metallacycle formation.[116] If this mechanism is accepted, the malonate-tethered systems of Sections 2.1 and 2.2 may have higher energies for the formation of the metallacycle due to their rotationally hindered ligand systems. This in turn may have negative implications for the activity of these complexes as metathesis catalysts. However, for the branched pyridine systems, this swing mechanism of the metallacyclobutane is unhindered by the donor atoms of the ligand scaffold, which could contribute to a higher overall catalytic activity.

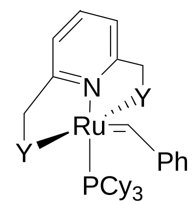

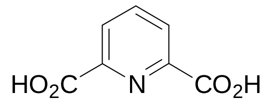

80

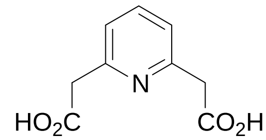

81

2.3.1. Branched carboxylate ligands

Firstly, as with the tethered pyridine ligands, it was thought that the length of the chain to the donor atom might affect chelation to the metal. Thus, ligands **80** and **81** were targeted.

2.3.1.1. Computational comparison

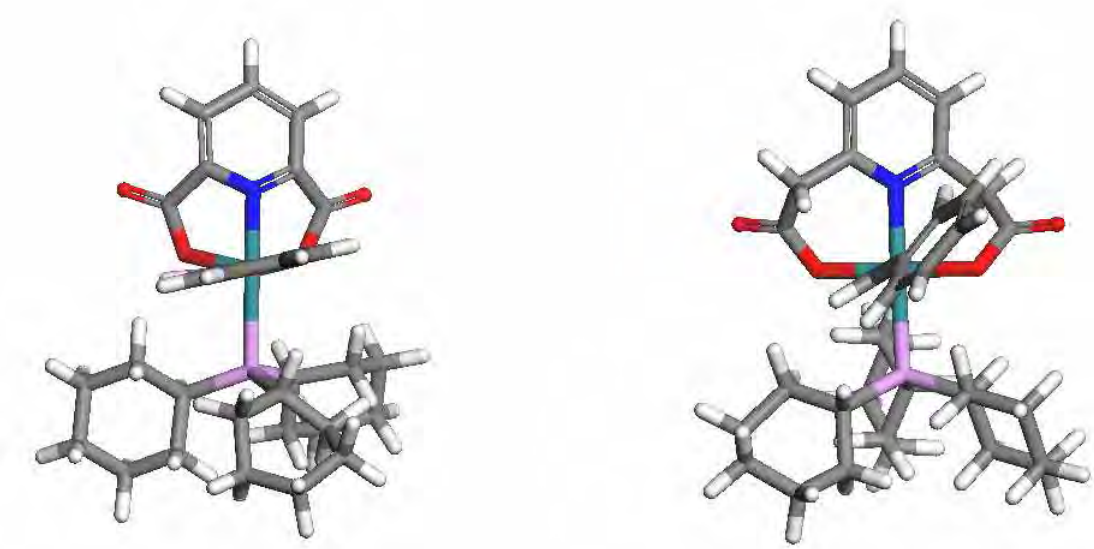

Figure 2.16. Complexes **80** (left) and **81** (right) with branched carboxylate ligands.

As with the tridentate malonate systems, it was thought that the size of the chelating ring could play a role in coordination to the metal, due to steric strain. The two systems were modelled as their ruthenium alkylidene complexes at the molecular mechanics and semi-empirical levels. Table 2.3 compares the geometries of the two structures obtained by a conformational search at the molecular mechanics level. From the data presented, it is clear that, as with the tridentate malonate systems, the Ru-PCy_3 bond is the weaker of the two axial bonds, and is thus more likely to dissociate from the ruthenium centre. It is also notable that the larger chelate **81** has a *trans* arrangement of the carboxylate donor groups with an O-Ru-O angle, θ = 179°, whereas in the smaller chelate **80** the arrangement is *cis* (θ = 94.7°). As mentioned previously, the *trans* geometry is more typical of anionic ligands in ruthenium alkylidene metathesis systems, and it appears that the longer chain permits the complex to adopt this geometry. Table 2.3 also indicates that the Ru-O bond lengths are slightly longer in the larger chelate **81** than in the smaller chelate **80**.

Table 2.3. Molecular mechanics geometrical data for ruthenium complexes containing branched dicarboxylates **80** and **81**.

Compound	Ru-PCy_3 (Å)	Ru-py (Å)	Ru-O (1) (Å)	Ru-O (2) (Å)	O-Ru-O (°)
80	2.61	2.062	2.048	2.054	94.7
81	2.587	2.119	2.07	2.064	179

2.3.1.2. Synthetic approach

The diacid **80** is commercially available, but had to be modified such that chelation would be encouraged with the Grubbs first-generation complex **4**. It was therefore readily converted to its thallium salt **82** by heating in methanol with thallium carbonate (Scheme 2.14). The structure of the thallium salt was confirmed by solubility differences, NMR analysis and ICP analysis. The product obtained was soluble only in D_2O, while the diacid **80** is soluble in DMSO-d_6, but not D_2O or $CDCl_3$. Since the starting material **80** and the product **82** were not soluble in the same solvents, their chemical shifts could not be directly compared by NMR analysis. The difference in solubility of each material was, however, an indication in itself that the reaction had been successful. In addition to this, ^{1}H NMR analysis of the crude product **82** in D_2O confirmed the presence of both aromatic protons, as a triplet at 8.12 ppm and a doublet at 8.17 ppm. ^{13}C NMR analysis confirmed the presence of the carbonyl carbon at 173.6 ppm (uncalibrated). IR analysis showed an asymmetric carboxylate [C$\overset{-}{=}$(O)$_2^-$] absorption band at 1561.6 cm^{-1}, while ICP analysis of the crude material **82** gave a thallium content of 68.8% (expect 71%).

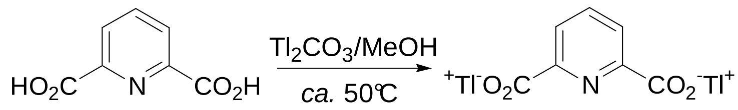

80 **82**

Scheme 2.14

The longer-chained diacid **81** is not commercially available, and the synthetic approach towards this ligand is illustrated in Scheme 2.15. The first attempt to react 2,6-bis(bromomethyl)pyridine **83** with cyanide followed a literature procedure,[254] using excess KCN in dry DMF. However, the reaction was not successful, and another approach was explored using trimethylsilyl cyanide (TMSCN) and tetrabutylammonium fluoride (TBAF).[255] With TBAF to cleave the silyl group, TMSCN proved to be a good source of the nitrile, and the dinitrile **84** was isolated in good yield (89%) after chromatography. In the ^{1}H NMR spectrum a shift in the CH_2 signal is observed relative to the starting material **83**, from 4.52 ppm to 3.93 ppm. The C≡N absorption band was also clearly visible at 2249 cm^{-1} in the IR spectrum.

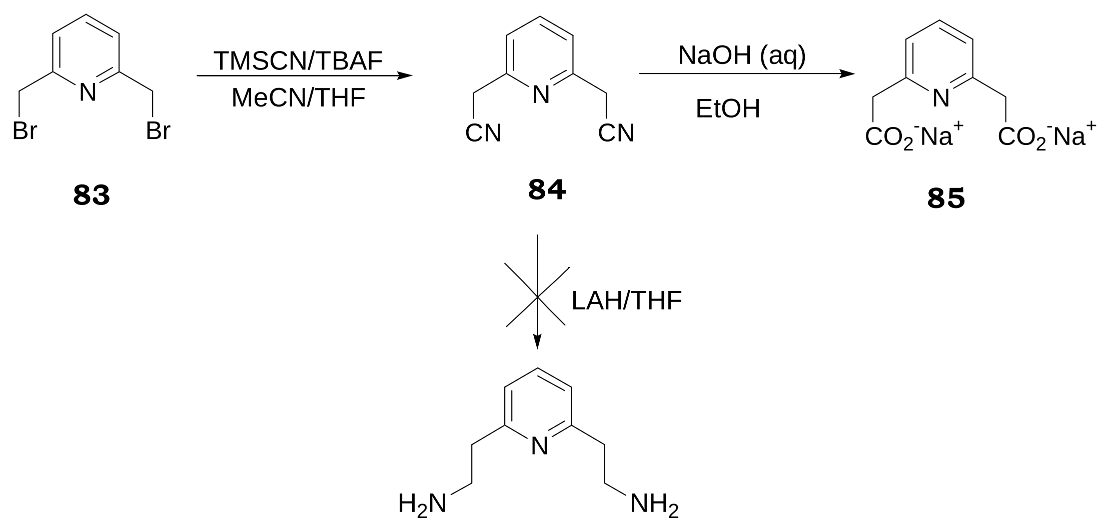

83 **84** **85** **86**

Scheme 2.15

The next step in the synthetic pathway was to hydrolyse the dinitrile **84** to the desired diacid **81**. However, as was the case with the malonate systems, the presence of both basic and acidic functionalities presented challenges in isolating the diacid. In light of these difficulties, we chose to isolate the desired acid as the sodium salt **85** (Scheme 2.15). A solution of the dinitrile **84** in ethanol and an aqueous solution of sodium hydroxide were combined and refluxed for four hours, by which time the reaction was perceived complete by TLC. After removing the ethanol *in vacuo*, the aqueous solution was passed through a cation exchange column, to replace the sodium ions with protons. The hydrolysis was supported by the absence of the C≡N signal (116.6 ppm in **84**) and the presence of a carbonyl carbon signal at 167.0 ppm in the ^{13}C NMR spectrum.

Reduction of the dinitrile **84** to the diamine **86** (Scheme 2.15) was attempted using a textbook LAH reaction[256] in THF, but ^{1}H NMR analysis of isolated material failed to indicate the presence of any aromatic protons. It is presumed that the desired amine species may have coordinated to the aluminium complexes present in the reaction mixture, rendering this method for reduction of the dinitrile ineffective. Time constraints prevented further experimentation with other reducing agents, and this reduction remains a challenge for future work.

2.3.2. Pyridine diamine (N_2py) systems

The second type of branched pyridine system to be explored was the pyridine diamine systems (N_2py) of the type illustrated below. This subtype also consists of a pyridine ring with two branches in positions 2 and 6. The branches each comprisse a methylene amino moiety, the substituents on the amine nitrogen being either alkyl or aromatic (see Table 2.4).

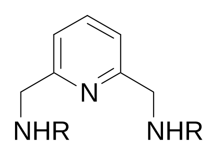

Such systems have been used as ligands in coordination chemistry, due to the chelating benefits offered by the ligand. In particular, multidentate nitrogen-donor ligands have been used increasingly in homogeneous catalysis.[257-260] For example, ligands **93** and **94** have been used for coordination to palladium,[261] while derivatives of **88** have been used to make macrocyclic lanthanide complexes for cell labelling and magnetic resonance imaging applications[262] and ligand **89** has been used extensively, as a precursor to a macrocyclic ligand for coordination to copper (II),[263] as well as a precursor for crown ethers and polyamide macrocycles.[264,265] One obvious advantage of these ligands is their potential for structural elaboration *via* the amine substituents, which could also provide a point of anchorage for immobilizing the catalyst on to a solid support. The range of substituents in Table 2.4 was chosen to reflect a range of electronic and steric properties.

Table 2.4. Alkyl and aromatic substituents in the N_2py systems.

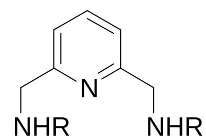

Type	R	Parent amine	Entry
Alkyl	H	Ammonia	**87**
	$(CH_2)_3CH_3$	Butylamine	**88**
	$CH_2(C_6H_5)$	Benzylamine	**89**
	$CH(CH_3)_2$	Isopropylamine	**90**
	$C(CH_3)_3$	*Tert*-butylamine	**91**
Aromatic	(C_6H_5)	Aniline	**92**
	$(C_6H_4)OCH_3$	Anisidine	**93**
	$(C_6H_4)CH_3$	*p*-Toluidine	**94**
	$(C_6H_4)Cl$	4-chloroaniline	**95**
	$(C_6H_4)NO_2$	4-nitroaniline	**96**

2.3.2.1. Computational studies

As discussed earlier, molecular mechanics and semi-empirical calculations have provided good approximations of the geometry of ruthenium metathesis systems. While discrepancies may be expected between results from these lower-level calculations and those obtained using higher-level *ab initio* and DFT methods, reported work has shown that, in some cases, sufficient geometrical accuracy may be obtained to warrant the use of molecular mechanics, rather than the time-consuming, higher-level theoretical methods.[245]

Here we examine the geometry of the N_2py-ruthenium systems at the molecular mechanics level, to make preliminary assessments of the conformational and energetic costs involved in chelation of the ligand to the metal centre. Two software packages were used to analyse the geometries of the N_2py ligands and their complexes, *viz.* Cerius^2 [266] and Spartan PC-Pro.[267]

For each ligand and its corresponding complex, a molecular dynamics search using the Cerius^2 package was performed, and the ten highest and ten lowest energy conformers obtained in this way were then energy-minimized. The lowest energy conformer(s) of these twenty structures was taken as the global minimum and used in the studies discussed below. Table 2.5 provides an indication of the conformational cost to the ligand involved on coordination. In this table, the chelated conformation of the ligand was assessed by correcting the hydrogen atoms on the amines, after removing the metal, and the PCy_3 and alkylidene ligands. Single-point energies were then calculated.

Table 2.5. Steric energies for selected free N_2py ligands, relative to their chelated conformations.[a]

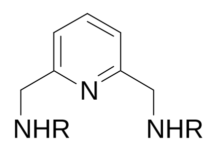

		Steric Energy (kcal/mol)		
Ligand	**R**	**Free ligand**	**Chelated ligand** [a]	**ΔE** [b]
90	$CH(CH_3)_2$	15.934	34.744	18.811
88	$(CH_2)_3CH_3$	59.333	82.820	23.487
89	$CH_2(C_6H_5)$	73.243	109.588	36.345
94	$(C_6H_4)CH_3$	33.793	76.476	42.683
95	$(C_6H_4)Cl$	28.091	76.539	48.448
93	$(C_6H_4)OCH_3$	71.447	124.990	53.543
96	$(C_6H_4)NO_2$	62.426	127.140	64.714
92	C_6H_5	59.350	129.827	70.477

[a] Following removal of the metal, PCy_3 and alkylidene ligands, and correcting the hydrogen atoms on the amines.
[b] $\Delta E = E_{\text{chelated ligand}} - E_{\text{free ligand}}$

From Table 2.5, it is clear that the amines with alkyl substituents have a lower conformational cost for chelation than their aromatic counterparts. In the case of ligand **88** (Table 2.6), rotation around the CH_2-NHR bond is required so that the amine nitrogen atoms are in a suitable position to coordinate to the ruthenium centre. Ligand **92** requires one phenyl ring to rotate away from the pyridine ring and it is possible that, in this process, interaction with the benzylidene system increases the steric cost for the required conformational change.

Table 2.6. Free ligand and corresponding complexes for ligands **88** and **92** with the lowest and highest conformational cost required for chelation.

Ligand	Free ligand	Chelated Ligand
88	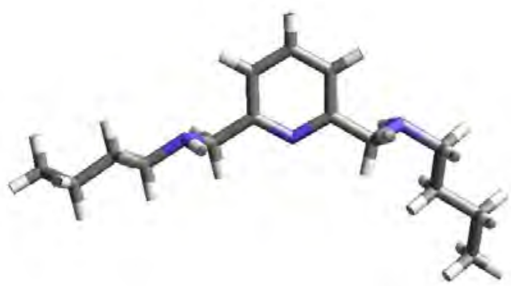	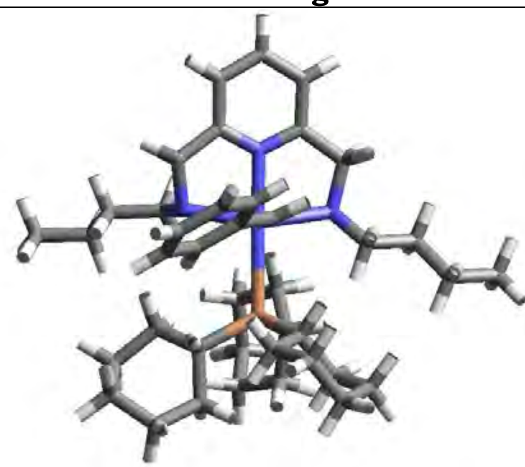
92	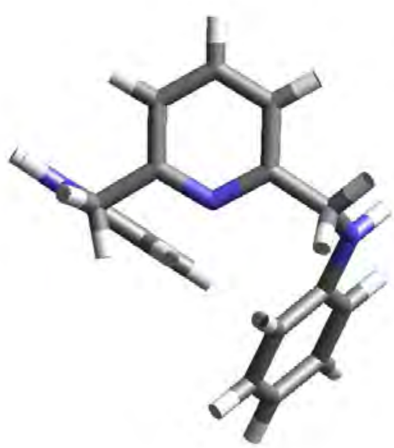	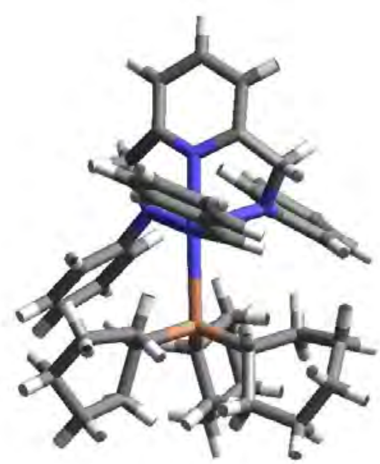

The aromatic ligands **92**-**94** all have similar geometries for the free ligand structure. In these structures (for example, as with **92** in Table 2.6) the aromatic rings are almost perpendicular to each other. This perhaps reflects the geometry assumed by benzene in the solid state; the rings align perpendicular to one another, owing to favourable electrostatic interactions between the π and σ systems.[273]

One interesting observation is the structure for the global minimum of ligand **96**. This structure differs from the other aromatic ligands in that its aromatic rings lie parallel to one another, but are slightly off-set, such that there is an interaction between the positively charged nitrogen of the nitro group of one aromatic ring, and the π system of the other (Figure 2.17). It is likely that the electron-rich aromatic system stabilizes the positive charge on the nitrogen of the other aromatic system.

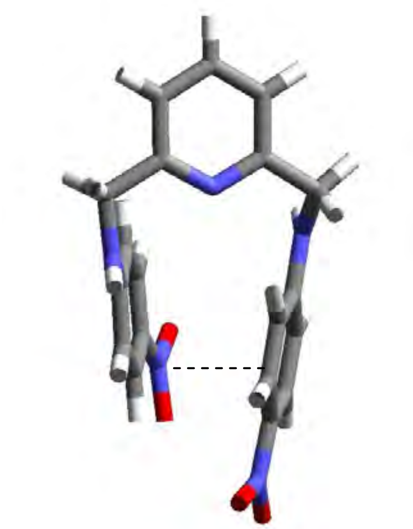

Figure 2.17. Conformation of the free ligand **96**, showing the proposed electrostatic interaction.

One structural feature common to all the N_2py ruthenium alkylidene complexes is the position of the benzylidene ring. DFT studies in the group of the Grubbs first-generation catalyst have shown that the benzylidene ring lies in the plane of the anionic ligands.[234] However, in the N_2py series of complexes, the benzylidene ring either bends up or down relative to this plane (See Table 2.6). This observation appears to be due to interaction with the bulky substituents on the amine moieties and may have important implications for the use of these complexes as metathesis catalysts. Further studies at a higher level of theory may be required to fully assess the potential of these complexes as metathesis catalysts, and to establish to what extent the sterically encumbered substituents may hinder the metathesis cycle.

The global minimum structures of the free ligands and complexes obtained using Cerius^2 were compared to those obtained using the Spartan PC-Pro package. A conformer distribution was performed on each of the ligands using this second software package, and the lowest energy conformation for each ligand was then geometry optimized. Owing to the greater length of time required, the corresponding complexes were simply geometry optimized and single point energy calculations were performed on these optimized structures.

Table 2.7 provides the steric energies for the free ligands, obtained from both Cerius^2 and Spartan PC-Pro, in order of increasing energy. It is not expected that the two software packages would provide the same steric energy values, as different force fields are utilized by each package. It was, however, hoped that the same trends might be observed between the two packages, but this is not the case. Ligand **89** appears to be an anomaly, with the highest energy in Cerius^2, but with intermediate energy in Spartan. Aside from this anomaly, ligands **96** and **93** have the highest energies in both packages, although their order relative to one another differs between the packages. More variation is obtained in the lower energy ligands, and a trend simply cannot be noted, despite the expectation that both sets of data represent the global minimum in each case.

Table 2.7. Steric energies obtained for the free ligands, from both Cerius^2 and Spartan modelling packages.

Steric Energy (kcal/mol)			
MM Cerius^2		**MM Spartan**	
Ligand	Free ligand	Ligand	Free ligand
95	28.091	**88**	46.180
94	33.793	**90**	49.488
87	57.270	**95**	80.569
88	59.333	**89**	81.224
92	59.350	**92**	86.555
96	62.426	**94**	91.260
93	71.447	**93**	92.911
89	73.243	**96**	150.766

Similarly, no clear trend is noted when comparing the steric energies of the complexes, where only single point energies were obtained using Spartan. Table 2.8 lists these energies, in increasing order of ΔE, the difference in energy between ligand

and complex. From the data presented by Tables 2.7 and 2.8, it must be concluded that the two modelling packages do not give comparable data.

Table 2.8. Steric energies obtained for the complexes, from both Cerius^2 and Spartan modelling packages.

Steric Energy (kcal/mol)					
MM Cerius^2			**MM Spartan**		
Ligand	Complex	ΔE	Ligand	Complex	ΔE
87	101.271	44.001	**93**	148.328	55.417
94	128.930	95.137	**95**	137.802	57.233
92	157.285	97.935	**92**	145.831	59.276
88	162.815	103.483	**96**	214.824	64.058
93	179.355	107.908	**94**	155.625	64.365
95	141.266	113.175	**88**	123.724	77.544
96	193.395	130.970	**89**	169.181	87.957
90	103.210	137.954	**90**	138.681	89.193
89	216.109	142.867	**87**	162.170	119.387

As with the steric energy, the geometrical data obtained using Spartan varies quite considerably relative to that obtained from Cerius^2 (Table 2.9). In most cases, Cerius^2 calculates wider N-Ru-N angles, more closely approximating the *trans* angles reported for anionic ligands in ruthenium alkylidene complexes,[123] compared to Spartan, which provides angles between *ca* 120° and 140°. These structures offered by Spartan may thus simply be local minima, rather than the global minima of the Cerius^2 structures. It must be noted, however, that in Cerius^2, two anomalies are observed, where ligands **87** and **92** present with a *cis* arrangement of the amine donor groups. Between the two modelling packages there is good approximation on the length of the Ru-PCy_3 bond, but in most cases, Spartan provides longer lengths for the Ru-py bond. This data indicates the need for caution when comparing data from different modelling packages.

Table 2.9. Geometrical data for complexes with N_2py ligands, using Cerius[2] and Spartan.

	L-Ru-L (°)		Ru-PCy_3 (Å)		Ru-N (Å)	
Ligand	Cerius[2]	Spartan	Cerius[2]	Spartan	Cerius[2]	Spartan
87	94.7	118.7	2.390	2.609	2.072	2.483
88	160.5	122.6	2.653	2.612	2.016	2.280
89	164.3	128.7	2.633	2.623	2.023	2.476
90	158.6	123.5	2.690	2.641	2.020	2.496
92	99.3	125.8	2.647	2.625	2.080	2.487
93	162.2	125.7	2.642	2.625	2.020	2.487
94	162.2	129.8	2.640	2.656	2.018	2.520
95	160.7	125.8	2.642	2.625	2.025	2.486
96	160.1	129.4	2.667	2.657	2.016	2.519

Zhang *et al.*[268] report the preparation of a ruthenium complex **97** incorporating ligands of similar geometry to those examined in this work, but with one phosphine moiety replacing an amine donor group. This complex has proved to be an efficient agent for the catalytic transformation of alcohols to esters, and preliminary modelling of ligands **91** and **92** afforded similar geometrical data to that reported by Zhang *et al.*[268] (Table 2.10). It must be noted that the modelling was conducted at the molecular mechanics level in Cerius[2] and that the structures have simply been energy-minimised rather than subjected to molecular dynamics routines.

Table 2.10. Geometrical data for complex **97** and analogous complexes with ligands **91** and **92**.

	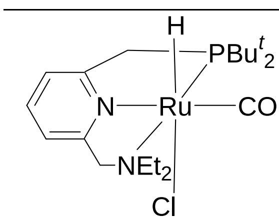	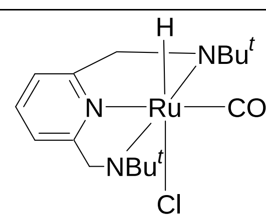	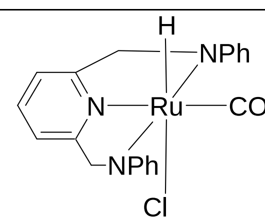
Ligand used	**97** [a]	**91**	**92**
N-Ru-P/N	159.1	165.3	163.4
Ru-py	2.103	1.994	2.01
Ru-N1	2.26	2.156	2.115
Ru-N2/P	2.273	2.166	2.115
Ru-C	1.834	2.192	2.192

[a] Data from crystal structure of complex **97** (Ref. 268)

2.3.2.2. Synthetic approach

In most cases (aside from that of the diamines **87** and **96**), a solution of 2,6-bis(bromomethyl)pyridine **83** and the amine (5 equivalents) in a suitable solvent (Table 2.8) was stirred overnight (Scheme 2.16). The reaction mixture was washed with Na_2CO_3 and extracted with $CHCl_3$. The success of the reaction was determined by the shift in the CH_2 signal in the ^1H NMR spectrum of the product, relative to the reactant **83** (Table 2.8).

Scheme 2.16

The N_2py systems with alkyl substituents (**88** – **92**) proved difficult to purify, with very poor separation on both reverse- and normal-phase TLC plates. However, as these are known compounds, rigorous purification was not required and it was hoped that on reaction with a metal system, the desired chelated complex would simply precipitate out of solution, leaving impurities behind.

Those compounds in the series with aromatic substituents were more readily purified by preparative TLC, on normal-phase silica gel. For R = C_6H_5, $C_6H_4OCH_3$, both the di- and mono-amines were isolated by this means, as (Figure 2.18) evidenced by the additional CH_2 signal present in the NMR spectra. In addition to this, the relative integrals of the aromatic protons support this conclusion. The diamines **92** and **95** appear to be novel compounds.

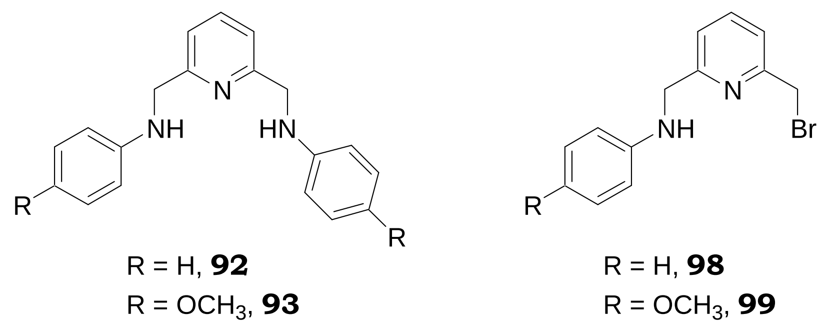

Figure 2.18. Di- and mono-amines isolated.

Table 2.11. Synthesis of N_2py compounds: Chemical shift (Δδ) of the CH_2 ^{1}H NMR signals of the productsin $CDCl_3$, relative to the reactant **83** (4.52 ppm).

Compound	R	Chemical shift (ppm)	Δδ (ppm)
87	H	-[a]	-
88	$(CH_2)_3CH_3$	3.95	-0.57
89	$CH_2(C_6H_5)$	3.94	-0.58
90	$CH(CH_3)_2$	3.86	-0.66
91	$C(CH_3)_3$	3.84	-0.68
92	(C_6H_5)	4.47	-0.05
93	$(C_6H_4)OCH_3$	4.41	-0.11
94	$(C_6H_4)CH_3$	4.44	-0.08
95	$(C_6H_4)Cl$	4.42	-0.1
96	$(C_6H_4)NO_2$	-	-

[a] Insoluble, possibly polymeric product.

In the case of the diamine **87** where R = H, an aqueous solution of ammonia (32%) was added to a solution of the starting material **83**. After stirring for 2 hours at room temperature, a heavy white precipitate had formed, which, upon filtration, appeared to have a slightly rubbery texture. Furthermore, the solid did not seem to be soluble in various organic solvents or in water, and it is thus assumed that the polymer **100** was formed (Scheme 2.17). Unfortunately, due to the solubility problems, this could not be confirmed by standard characterization techniques.

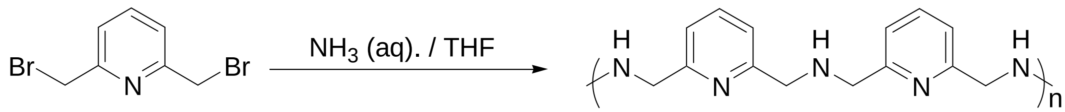

83 **100**

Scheme 2.17

The N_2py ligand where R = NO_2 presented a greater synthetic challenge than the other compounds in the series. Under the standard reaction conditions, only starting material was recovered. As illustrated in Figure 2.19, the nitro group is electron-withdrawing through both inductive and resonance effects, thus decreasing the nucleophilicity of 4-nitroaniline, relative to the other amines used in this series.

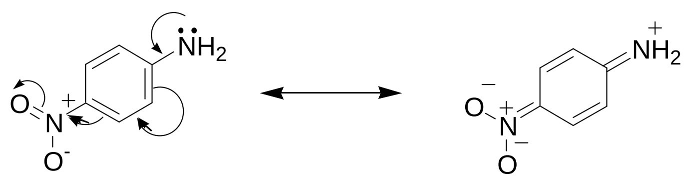

Figure 2.19. The electron-withdrawing effects of the nitro substituent, through resonance.

A microwave-assisted approach was consequently explored. Microwave energy is a very efficient source of energy, as it bypasses the need for the inefficient conductive heating typical of conventional heating methods. In microwave heating, the microwave radiation couples directly with the molecules in the reaction solution, allowing for more efficient and rapid heating.[269] Methanol was initially chosen as the solvent, as it is a good absorber of microwave energy.[269] Due to the low boiling point of this solvent, the temperatures for the microwave study were restricted to 75°C, and reactions were conducted in the microwave reactor for varying lengths of time. After about 10 minutes, a new spot became faintly visible on TLC analysis, although the parallel NMR data remained inconclusive, indicating the presence of starting material alone. This spot became more visible after 30 minutes of microwave irradiation at this temperature, and another spot also became apparent (Figure 2.20). The two spots were thought to correspond to both the di- and mono-amine species, **96** and **101** respectively. However, only starting material was extracted in the work-up process, suggesting that the desired reaction product(s) had limited solubility in organic solvents. Microwave irradiation at higher temperature (120°C) using DMF as solvent also failed to afford the desired product.

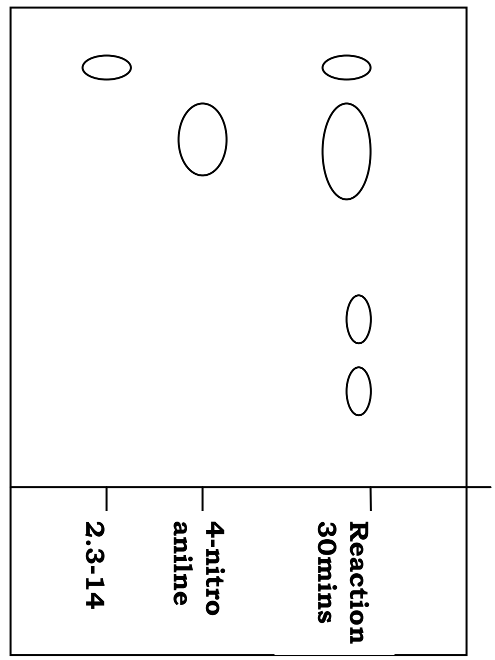

Figure 2.20. Re-drawn TLC plate of the reaction between 2,6-bis(bromomethyl)pyridine **83** and 4-nitroaniline, after 30 minutes of microwave irradiation, in methanol, at 75°C. Elution with hexane-ethyl acetate (1:1).

2.4. PRELIMINARY COMPLEXATION STUDIES

One means of halide displacement is through the use of silver salts. This method has been used extensively in the literature,[105,167,172,224] as the silver ions coordinate very readily with the halides. However, previous work in the group[234] using this method with the phosphine-containing Grubbs first-generation catalyst was not successful, owing to the formation of $AgClPCy_3$.

Sabbagh briefly investigated the use of the *tert*-butyldimethylsilyl ester **102** as a means of halide exchange with the phosphine-free Hoveyda-Grubbs complex **5**, and we decided to pursue the concept of using *O*-TBDMS esters with a cleaving agent such as AgF (Scheme 2.18). Hence, the *tert*-butyldimethylsilyl ester **102** was prepared quantitatively from *tert*-butyldimethylsilyl chloride (TBDMSCl) and malonic acid, using a textbook reaction.[256] Unfortunately, attempted alkylation of 3-

bromopropylamine with the TBDMS ester **102** was not successful, nor were attempts at the malonate-chloride exchange with the Grubbs first-generation catalyst **4**. It is possible that removal of the chloride ligands from the ruthenium centre in complex **4** results in rapid destabilization of the complex, resulting in accelerated decomposition. Another contributing factor may be the poor solubility of AgF in organic solvents. Super-dry, degassed ethanol was used, but the AgF nevertheless shows limited solubility.

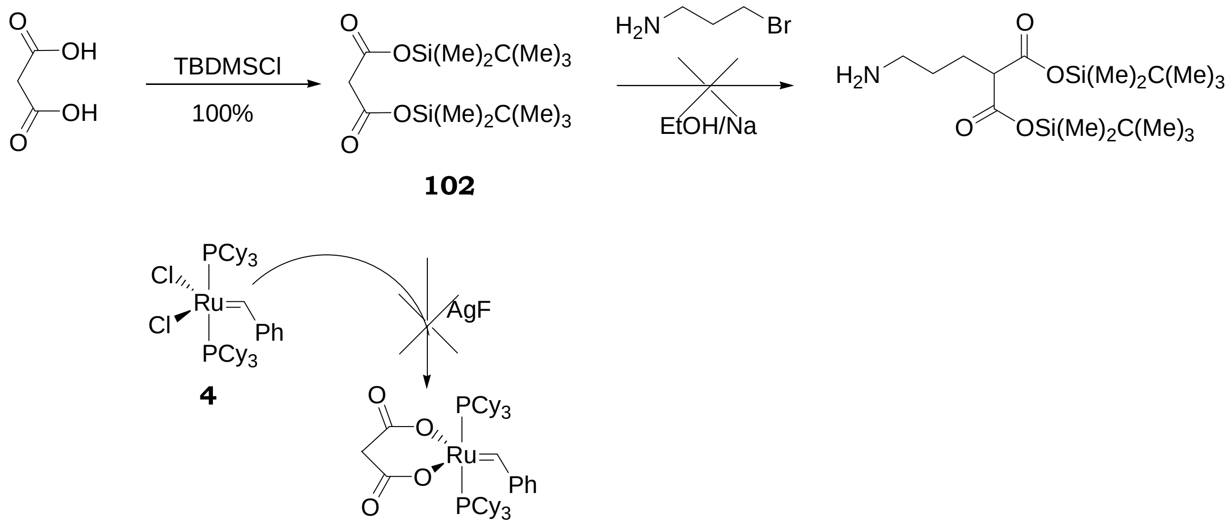

Scheme 2.18

As mentioned in Section 2.2.2, thallium salts are often used to prepare carboxylate-containing ruthenium complexes. Thallium salts are useful for halide exchange, as the electrophilic "pull" by the heavy-metal cation accelerates the rate of exchange.[248,250] The formation of complexes using either the thallium salt **82** or dithallium malonate **103**, generated by treating malonic acid with Tl_2CO_3 in methanol, proved more difficult than expected. Preliminary attempts to react the salts and the diamino ligand **91** with the Grubbs catalyst **4** were unsuccessful and will be explored in future studies, as part of our ongoing research programme.

2.5. CONCLUSIONS

A range of tridentate ligands have been prepared in this work, for possible complexation to ruthenium alkylidene complexes. The malonate-tethered pyridine ligand **64** has been successfully prepared as its thallium salt, establishing a possible means for accessing Grubbs-type complexes, but its longer-chained analogue **65** could not be accessed, due to difficulties encountered in the preparation of an intermediate alkyl halide **75** and the instability of the analogous tosylate prepared as a halide equivalent **78**. Numerous attempts to access the malonate-derived ligand **31** have been unsuccessful, but a promising route to the ligand has been established.

A branched, pyridine carboxylate ligand **81** has been successfully prepared, as have a range of branched pyridine diamine ligands **87**-**96**, where co-planarity of the ligand *and* the donor atoms is observed. The latter class of ligand employs a range of substituents, but preliminary modelling studies of these ligands have been inconclusive in terms of their potential as ligands for metathesis catalysts. The geometrical data obtained from these studies suggest that the bulky substituents on the amine donor groups would interfere with the benzylidene ring, pushing it out of the plane of the amine donor atoms. It is very likely that the bulky amine substituents may hinder the formation of the complex, and the effect of this must be modelled at a higher level of theory before further complexation studies with these ligands are undertaken. Preliminary modelling studies of these ligands with another ruthenium complex **97** have been explored, and the data suggest that the correct geometries may be obtained with this series of ligands.

Thallium carbonate-catalysed hydrolysis of diesters has provided convenient access to thallium salts **103** and **82**, but preliminary complexation studies employing these ligands and the TBDMS ester **102** have been unsuccessful.

Based on the results of this investigation, future research is expected to involve:-

i) completion of the preparation of ligand **31**, by following up on the final two steps required to prepare the precursor **60**,

ii) investigation of a different approach to the malonate-tethered pyridine ligand **65**, so that the effect of the chain length, if any, on the chelating ability of the ligands may be adequately assessed,

iii) further investigations into methods for halide exchange in Grubbs and Hoveyda-type complexes. Alternatively, attempts may be focussed on building the complex *ab initio* from a suitable precursor,

iv) investigations into the use of the N_2py series as ligands for analogues of the ruthenium complex **97**.

3. EXPERIMENTAL

3.1. SYNTHESIS

3.1.1. General

NMR spectra were recorded using a Bruker AMX400 spectrometer at 303 K in the specified deuterated solvents; NMR spectra were calibrated using residual protonated solvent signals ($CDCl_3$: 7.25 ppm for ^1H and 77.0 ppm for ^{13}C spectra; DMSO-d_6: 2.50 ppm for ^1H and 39.5 ppm for ^{13}C; and D_2O: 4.82 ppm for ^1H). Infra-red spectra were recorded using a Perkin Elmer FT-IR Spectrum 2000 spectrometer. Solid samples were analysed using KBr discs, and liquid samples using thin films on CsI discs. Low-resolution mass spectrometry was performed using a Finnigan MAT GCQ mass spectrometer, using the electron ionization EI mode. ICP analysis of thallium salts was performed using a Thermo Electron Corporation iCAP 6000 series ICP spectrometer. Wavelengths used for thallium analysis were 190.085, 276.787, 351.924 and 377.572 nm. All microwave experiments were conducted using a CEM Discover® System microwave reactor.

Thin layer chromatography was performed on Merck silica gel 60 PF_{254} plates. Flash chromatography was performed using Merck silica gel 60 (particle size 0.040 – 0.063 mm), preparative TLC plates were prepared using Merck silica gel 60 PF_{254} for preparative chromatography, and chromatatron plates were made with silica gel 60 PF_{254} containing $CaSO_4$. All melting points were determined using a Reichert 281313 hot-stage apparatus and are uncorrected.

Reagents were supplied by Aldrich, and were used without further purification, unless otherwise stated. Ethanol was dried according to the method described by Vogel[256] using magnesium turnings. All other solvents were dried by methods described by Perrin and Armagrego.[270] Ethanol was distilled from $Mg(OEt)_2$; methanol was distilled from $Mg(OMe)_2$; THF was distilled from sodium wire and benzophenone under nitrogen; DMF was fractionally distilled under reduced pressure after pre-drying with molecular sieves (4Å); and toluene, benzene, MeCN and CH_2Cl_2 were distilled from CaH_2.

All organometallic work was conducted using an Aldrich® AtmosBag or Schlenk techniques, under dry argon. All solvents for organometallic work were degassed by bubbling dry argon through the dry, freshly distilled solvent while stirring over molecular sieves (4 Å), for *ca.* 30 minutes. Thallium carbonate and thallium salts were handled using double glove and secondary containment procedures, owing to the extreme toxicity of thallium compounds.

3.1.2. Approaches to malonate derived system

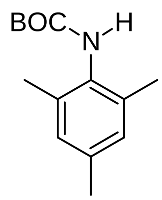

43

N-*(*tert*-Butyloxycarbonyl)-2,4,6-trimethylaniline* **43**[234]

2,4,6-Trimethylaniline **42** (7.5 mL, 53 mmol) was dissolved in dry THF (50 mL), in a two-necked round-bottomed flask, under nitrogen. A solution of di-*tert*-butyl dicarbonate (11.72 g, 53.5 mmol) in dry THF was added using a dropping funnel, under a flow of dry nitrogen. The resulting solution was then refluxed for 7 days, under nitrogen. The solvent was removed *in vacuo* and the resulting peach-yellow solid was dried under high vacuum, affording *N*-(*tert*-butyloxycarbonyl)-2,4,6-trimethylaniline **43** in quantitative yield, without requiring further purification; m.p. 68-70 ºC (lit. ref.[271] 66-68 ºC); δ_H (400 MHz; $CDCl_3$) 1.48 (9H, s, Bu^t), 2.21 (6H, s, *o*-CH_3), 2.24 (3H, s, *p*-CH_3), 5.78 (1H, br s, NH) and 6.86 (2H, s, ArH); δ_C (100 MHz; $CDCl_3$) 18.2 [C(*C*H_3)$_3$], 20.9 (*o*-CH_3), 28.3 (*p*-CH_3), 79.7 [*C*(CH_3)$_3$], 128.8, 133.7, 135.5, and 136.4 (ArC) and 152.2 (C=O); m/z 235 (M^+, 76%) and 135 (100).

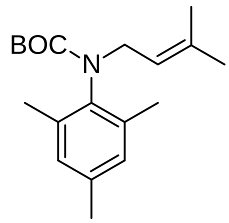

44

N-(tert-*Butyloxycarbonyl)*-N-*(3-methylbut-2-enyl)-2,4,6-trimethylaniline* **44**[234]

KH (*ca.* 1.5 g of a 30% mineral oil dispersion) was rinsed with dry hexane under dry nitrogen. The liquid was decanted, and dry DMF (40 mL) was added. The suspension was cooled to 0°C before adding a solution of *N*-(*tert*-butyloxycarbonyl)-2,4,6-trimethylaniline **43** (3.264 g, 13.87 mmol) in dry DMF (*ca.* 30 mL) by cannula. The resultant milky yellow solution was stirred at room temperature for two hours, before adding 3,3-dimethylallyl bromide (2.0 mL, 14 mmol). After stirring for a further 16 hours at room temperature, the mixture was transferred to a large separating funnel and H_2O (100 mL), saturated aq. $NaHCO_3$ (100 mL) and Et_2O (200 mL) were added. The aqueous phase was washed with Et_2O (2 x 150 mL), and the combined organic extracts were washed with an equal volume of saturated aq. NaCl and dried over $MgSO_4$. The solvent was removed *in vacuo* to afford *N*-(*tert*-butyloxycarbonyl)-*N*-(3-methylbut-2-enyl)-2,4,6-trimethylaniline **44**, a bronze-coloured oil (3.8 g, 90%), sufficiently pure by TLC and ^{1}H NMR analysis. In $CDCl_3$, at 303 K this compound exists as a 1:2.6 mixture of amide rotamers. Only the chemical shifts for the major rotamer are reported here. δ_H (400 MHz; $CDCl_3$) 1.31 (9H, s, Bu^t), 1.50 and 1.62 [6H, 2 x s, CH=(C*H*$_3$)$_2$], 2.12 (6H, s, *o*-CH_3), 2.24 (3H, s, *p*-CH_3), 4.04 (2H, d, NCH_2), 5.28 [1H, m, C*H*=C(CH_3)$_2$] and 6.80 (2H, s, ArH); δ_C (100 MHz; $CDCl_3$) 17.9 (*p*-CH_3), 18.6 (*o*-CH_3), 21.4 and 26.1 [CH=C(*C*H$_3$)$_2$], 28.7 [OC(*C*H$_3$)$_3$], 46.8 (NCH), 76.6 [C(*C*H$_3$)$_3$], 79.5 [CH=*C*(CH_3)$_2$], 120.5 [*C*H=C(CH_3)$_2$], 129.1, 135.5, 136.3 and 136.6 (ArC), and 155.4 (C=O); m/z 304 (MH^+, 100%).

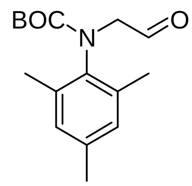

45

N-(tert-*Butyloxycarbonyl*)-N-(*formylmethyl)-2,4,6-trimethylaniline* **45**[234]

Ozone was bubbled through a solution of *N*-(*tert*-butyloxycarbonyl)-*N*-(3-methylbut-2-enyl)-2,4,6-trimethylaniline **44** (1.0445 g, 3.7659 mmol) in dichloromethane (30 mL) and methanol (10 mL) until the solution turned blue, indicating saturation of the solution with ozone. Nitrogen was then bubbled through the solution while warming to room temperature, and dimethyl sulfide (1.5 mL) was added. The solvent was removed *in vacuo* and the crude material purified by chromatography [flash chromatography on silica gel; elution with hexane-ethyl acetate (5:1)] to afford *N*-(*tert*-butyloxycarbonyl)-*N*-(formylmethyl)-2,4,6-trimethylaniline **45** (0.8 g, 80%) as a colourless oil. δ_H (400 MHz; $CDCl_3$) 1.35 (9H, s, Bu^t), 2.22 (6H, s, *p*-CH_3), 2.26 (3H, s, *o*-CH_3), 3.96 (2H, d, J = 1.6 Hz, NCH_2), 6.86 (2H, s, ArH) and 9.80 (1H, m, CHO); δ_C 12.7 (*o*-CH_3), 21.5 (*p*-CH_3), 28.7 [$C(CH_3)_3$], 65.6 (CH_2), 70.9 [$C(CH_3)_3$], 127.1, 129.4, 133.1 and 136.6 (ArC), 153.3 (Boc C=O), and 199.5 (C=O); m/z 235 (M^+, 76%) and 135 (100).

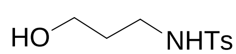

47

N-*(3-Hydroxypropyl)-4-methylbenzenesulfonamide* **47**

Sodium hydride (*ca.* 0.45 g, in a 60% mineral oil dispersion) was weighed into a round-bottomed flask, and rinsed 3 times with dry hexane. Dry THF (20 mL) was then added using a cannula under an atmosphere of dry nitrogen. 3-Amino-1-propanol **46** (1 mL, 13 mmol) in dry THF (7 mL), was slowly added to the NaH suspension using a pressure-equalized dropping funnel. The resultant mixture was stirred for 1 hour at room temperature, and a solution of *p*-toluenesulfonyl chloride

(2.516 g, 13.2 mmol) in THF (10 mL) was then introduced, using the dropping funnel. After stirring overnight, the THF was removed *in vacuo* and the white slurry diluted with water (50 mL) and ethyl acetate (50 mL). The aqueous layer was extracted with ethyl acetate (5 x 30 mL), and the combined organic solutions were dried ($MgSO_4$), and concentrated *in vacuo*, affording *N*-(3-hydroxypropyl)-4-methylbenzenesulfonamide **47**, a light yellow oil (2.7 g, 92%). No further purification was undertaken; ν/cm^{-1} 3288, br, OH and NH; δ_H (400 MHz; $CDCl_3$) 1.66 (2H, quintet, J = 6 Hz, CH_2), 2.39 (3H, s, $TsCH_3$), 3.04 (2H, t, J = 6 Hz, $NHCH_2$), 3.66 (2H, t, J = 6 Hz, CH_2OH), 7.26 (2H, d, J = 9.2, ArH) and 7.71 (2H, d, J = 8.4, ArH); δ_C (100 MHz; $CDCl_3$) 21.4 ($TsCH_3$), 31.5 (CH_2), 40.8 ($NHCH_2$), 60.3 (CH_2OH), 127.0, 129.6, 136.9 and 143.2 (ArC); m/z 230 (M+H, 71%) and 212 (100%).

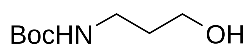

50

*3-Amino-3-(*tert*-butyloxycarbonyl)-1-propanol* **50**

In a round-bottomed flask equipped with a magnetic stirrer bar and a septum seal, di-*tert*-butyl dicarbonate (3.7773 g, 17.288 mmol) was dissolved in dichloromethane (*ca.* 40 mL). 3-Amino-1-propanol **46** (1.3 mL, 17 mmol) was introduced to this solution using a syringe, causing a gentle reflux. The solution was stirred for 3 hours, after which time the solvent was removed *in vacuo*. The desired 3-amino-3-(*tert*-butyloxycarbonyl)-1-propanol **50** was obtained in quantitative yield (3 g) as a clear oil, and no further purification was undertaken. δ_H (400 MHz; $CDCl_3$) 1.41 (9H, s, Bu^t), 1.64 (2H, q, J = 6 Hz, CH_2), 2.53 (1H, br s, OH), 3.24 (2H, q, J = 6 Hz. $NHCH_2$), 3.53 (2H, t, J = 5.2 Hz, CH_2OH), 4.85 (1H, br s, NH) δ_C (100 MHz; $CDCl_3$) 27.9 [$C(CH_3)_3$], 33.8 (CH_2), 40.3 ($NHCH_2$), 60.1 (CH_2OH), 71.2 [$C(CH_3)_3$] and 158.3 (C=O).

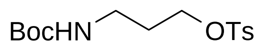

51

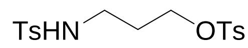

49

*3-Amino-3-(*tert*-butyloxycarbonyl)-1-tosyloxypropane* **51** and *3-amino-3-tosyl-1-tosyloxypropane* **49**

Sodium hydride (*ca.* 1 g, in a 60% mineral oil dispersion) was rinsed with dry hexane (2 x 10 mL), before adding dry THF (10 mL). A solution of 3-amino-3-(*tert*-butyloxycarbonyl)-1-propanol **50** (3 g, 17 mmol) in THF (10 mL) was added to the suspension drop-wise through a pressure-equalized dropping funnel, while stirring under nitrogen. After stirring at room temperature for 1 hour, a solution of *p*-toluenesulfonyl chloride (3.2g, 17 mmol) in THF (15 mL) was added to the suspension. The resulting mixture was stirred at room temperature overnight, after which time the THF was removed *in vacuo*. The slurry was taken up in water (50 mL) and ethyl acetate (50 mL), and the aqueous layer extracted further with two aliquots of ethyl acetate (2 x 30 mL). The combined organic fractions were dried ($MgSO_4$) and concentrated *in vacuo*, affording a white solid. Purification [preparative TLC on silica gel; elution with hexane-ethyl acetate (1:1)] afforded two fractions:

i) 3-Amino-3-(*tert*-butyloxycarbonyl)-1-tosyloxypropane **51**, as a yellow oil (2.6 g, 53%); δ_H (400 MHz; $CDCl_3$) 1.10 (9H, s, Bu^t), 1.94 (2H, m, CH_2), 2.33 (3H, s, $TsCH_3$), 3.32 (2H, t, *J* = 6 Hz, NCH_2), 4.27 (2H, t, *J* = 5.2 Hz, CH_2OTs), 6.24 (1H, s, NH), 7.14 (2H, d, *J* = 8.4 Hz, ArH) and 7.70 (2H, d, *J* = 8.0 Hz, ArH); δ_C (100 MHz; $CDCl_3$) 21.0 (CH_3), 21.3 [$C(\mathit{C}H_3)_3$], 27.3 (CH_2), 39.7 ($NHCH_2$), 60.2 (CH_2OTs), 66.8 [$\mathit{C}(CH_3)_3$], 125.8, 128.9, 140.4 and 141.5 (ArC), and 154.7 (C=O); and

ii) 3-Amino-3-tosyl-1-tosyloxy-propane **49** as an olive-green oil (0.6 g, 13%); δ_H (400 MHz; $CDCl_3$) 1.24 (1H, s, NH), 1.84 (2H, m, CH_2), 2.43 (3H, s, $TsCH_3$), 2.45 (3H, s, $TsCH_3$), 3.01 (2H, m, $NHCH_2$), 4.07 (2H, t, *J* = 5.6 Hz, CH_2OTs), 7.30 (2H, d, *J* = 8.0 Hz, Ts ArH), 7.35 (2H, d, *J* = 8.4 Hz, Ts ArH), 7.70 (2H, d, *J* = 8.0 Hz, Ts ArH), and 7.75 (2H, d, *J* = 8.4 Hz, Ts ArH); δ_C (100 MHz; $CDCl_3$); 21.5 (CH_3), 21. 7 (CH_3), 29.3 (CH_2), 39.2 ($NHCH_2$), 67.4 (CH_2OTs), 127.0, 127.9, 129.8, 130.0, 132.5, 136.6, 143.6 and 145.1 (ArC).

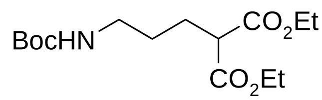

*Attempted synthesis of diethyl 2-{3-[(*tert*-butoxycarbonyl)amino]propyl}propane-1,3-dioate*

Small pieces of sodium metal (0.44 g, 19 mmol) were added to dry ethanol (*ca.* 30 mL), while stirring in a round-bottomed flask and cooling with ice. When all the sodium was consumed, diethyl malonate (2.3 mL, 15 mmol) was added, and the solution stirred at *ca.* 50°C for 1 hour. A solution of 3-amino-3-(*tert*-butyloxycarbonyl)-1-tosyloxypropane (4.25 g, 14.9 mmol) **51** in dry ethanol (*ca.* 15 mL) was added drop-wise, and the resulting solution stirred at reflux temperature for 7 hours, before stirring at room temperature overnight. The ethanol was then removed *in vacuo* and the slurry diluted with water (50 mL) and ethyl acetate (50 mL). The aqueous layer was extracted further with ethyl acetate (5 x 10 mL) and the combined organic fractions were dried ($MgSO_4$) and concentrated *in vacuo*, affording an orange oil, NMR analysis of which indicated the absence of the expected product.

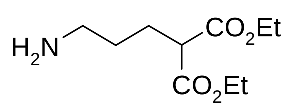

52

Diethyl 2-(3-aminopropyl)propane-1,3-dioate **52**

Small pieces of sodium metal (*ca.* 1.5 g, 65 mmol) were added to dry ethanol (30 mL) in a two-necked round-bottomed flask, fitted with a thermometer. When all the sodium had been consumed, freshly distilled diethyl malonate **36** (3.8 mL, 25 mmol) was added drop-wise, the flask fitted with a reflux condenser, and the solution heated at *ca.* 50°C for 30 minutes. 3-Bromopropylamine hydrobromide **53** (5.927 g, 27.1 mmol) was added and the mixture was refluxed overnight, resulting in precipitation of NaBr. After cooling, the precipitate was filtered off, and the filtrate concentrated *in vacuo.* The residue was purified [flash chromatography on silica gel; elution with hexane-ethyl acetate (5:1)] to afford diethyl 2-(3-aminopropyl)propane-1,3-dioate **52** as an ivory-coloured solid (1.8 g, 33%); m.p. 78-81°C (no lit. ref.

available); ν(C=O) 1658 cm^{-1}; δ_H (400 MHz; $CDCl_3$) 1.27 (2H, t, *J* = 7.2 Hz, CH_3), 1.74 (2H, m, CH_2), 1.93 (2H, m, CH_2CH), 2.09 (2H, m, NHCH_2), 3.37 (1H, t, *J* = 6.8 Hz, CH), and 4.20 (4H, q, *J* = 7.2 Hz, CH_2CH_3); δ_C (100 MHz; $CDCl_3$) 14.0 (CH_3), 20.2 (CH_2CH), 24.7 (CH_2), 42.0 ($NHCH_2$), 48.5 (CH), 61.3 (CH_2CH_3), and 170.8 (C=O); m/z 218 (MH^+).

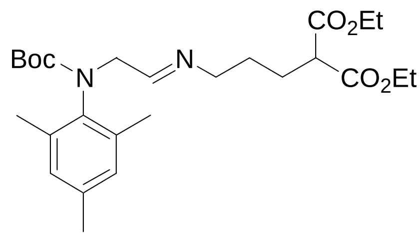

54

*Attempted synthesis of ethyl 9-(*tert*-butyloxycarbonyl)-2-carbethoxy-9-(2,4,6-trimethyl-phenyl)-6,9-diaza-6-nonenoate* **54**

Method 1

A solution of *N*-(*tert*-butyloxycarbonyl)-*N*-(formylmethyl)-2,4,6-trimethylaniline **45** (1.29 g, 4.64 mmol) and the ester **52** (1.513 g, 6.964 mmol) in dry ethanol (50 mL) was stirred overnight at room temperature, followed by heating at reflux temperature for 12 hours. The ethanol was removed *in vacuo* to afford an orange oil, but ^{1}H NMR analysis indicated the presence of only starting material.

Method 2

A dry two-necked round-bottomed flask was equipped with a nitrogen inlet, a magnetic stirrer, a Dean-Stark trap and a reflux condenser. The reaction vessel was purged with nitrogen, and charged with the ester **52** (0.8087 g, 3.722 mmol). A solution of *N*-(*tert*-butyloxycarbonyl)-*N*-(formylmethyl)-2,4,6-trimethylaniline **45** (1.02 g, 3.68 mmol) in dry toluene (*ca.* 10 mL) was added and the reaction refluxed for *ca.* 8 hours. After stirring overnight at room temperature the toluene was removed *in vacuo*. ^{1}H NMR analysis indicated the presence of only starting material

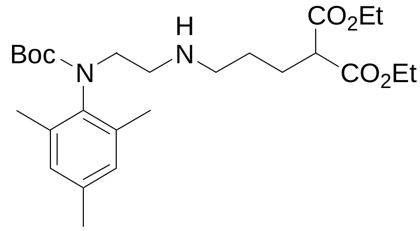

57

*Attempted synthesis of ethyl 9-(*tert*-butyloxycarbonyl)-2-carbethoxy-9-(2,4,6-trimethyl-phenyl)-6,9-diaza-6-nonanoate* **57**

Diethyl (3-aminopropyl)malonate **52** (0.7970 g, 3.668 mmol) was dissolved in dry ethanol (*ca.* 20 mL). A solution of *N*-(*tert*-butyloxycarbonyl)-*N*-(formylmethyl)-2,4,6-trimethylaniline **45** (0.7817 g. 2.991 mmol) in dry ethanol was added drop-wise, the flask was sealed, and the mixture stirred at room temperature for 1 hour. A solution of $NaBH_3CN$ (0.143 g, 2.27 mmol) in ethanol (*ca.* 10 mL) was added to the reaction mixture and stirring continued overnight. The ethanol was removed *in vacuo*, and the resultant slurry diluted with ethyl acetate (50 mL), water (30 mL) and saturated brine (20 mL). The aqueous layer was extracted with ethyl acetate (2 x 30 mL). The combined organic solutions were washed with 6M-HCl, dried over $MgSO_4$ and the solvent removed *in vacuo*. ^{1}H NMR analysis of this material indicated that only starting material **45** had been extracted. The remaining acidic aqueous fraction was basified to pH 12 using saturated aq. KOH, and then extracted with ethyl acetate, dried ($MgSO_4$) and concentrated *in vacuo*. ^{1}H NMR analysis of the residue indicated that only the starting material was present.

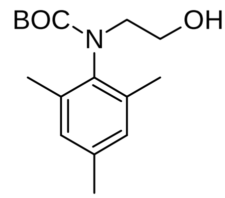

56

N-(tert-*Butyloxycarbonyl*)-N-(*2-hydroxyethyl)-2,4,6-trimethylaniline* **56**[256]

A solution of *N*-(*tert*-butyloxycarbonyl)-*N*-(formylmethyl)-2,4,6-trimethylaniline **45** (1.4923 g, 5.3798 mmol) in methanol (*ca.* 30 mL) was added to a solution of $NaBH_4$ (0.25 g, 6.6 mmol) in a 1 M NaOH (20 mL) solution drop-wise while stirring, under nitrogen. The temperature was maintained between 20° and 25°C, cooling with ice when necessary. After stirring for 3.5 hours the methanol was removed *in vacuo,* and the white emulsion was taken up in water (100 mL) and extracted twice with diethyl ether (2 x 100 mL). The combined organic solutions were dried over $MgSO_4$, and the solvent was removed *in vacuo*. Chromatography of the crude material [radial chromatography, on silica gel; elution with hexane-ethyl acetate (6:1)] afforded *N*-(*tert*-butyloxycarbonyl)-*N*-(2-hydroxyethyl*)-2,4,6*-trimethylaniline **56** as an ivory-coloured solid (0.9 g, 60%), m.p. 76-78°C; νOH 3461.2 cm^{-1}; δ_H (400 MHz; $CDCl_3$) 1.32 (9H, s, Bu^t), 1.32, (1H, s, OH), 2.18 (6H, s, *o*-CH_3), 2.26 (3H, s, *p*-CH_3), 3.60 (2H, t, J = 4.8 Hz, CH_2OH), 3.78 (2H, t, J = 4.8 Hz, NCH_2), and 6.85 (2H, s, ArH); δ_C (100 MHz; $CDCl_3$) 18.0 [$C(CH_3)_3$], 20.9 (*o*-CH_3), 28.2 (*p*-CH_3), 52.9 (CH_2OH), 62.8 (NCH_2), 80.4 [$C(CH_3)_3$], 129.0, 135.0, 136.7 and 138.1 (ArC), and 157.3 (C=O); m/z 280 (M+H, 100%). The presence of the hydroxy functionality was confirmed by proton exchange with D_2O in ^1H NMR analysis.

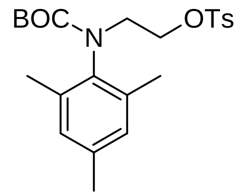

55

N-(tert-Butyloxycarbonyl)-N-[2-(tosyloxy)ethyl]-2,4,6-trimethylaniline **56**

Sodium hydride (*ca.* 0.5 g in a 60% mineral oil dispersion) was weighed into a round-bottomed flask and rinsed with dry hexane (4 x 10 mL). Dry THF (5 mL) was added and the suspension stirred under nitrogen. A solution of *N*-(*tert*-butyloxycarbonyl)-*N*-(2-hydroxyethyl)-2,4,6-trimethylaniline **56** (1.7475 g, 6.255 mmol) in dry THF (*ca.* 20 mL) was slowly added to the suspension using a pressure-equalised dropping funnel, producing a gentle reflux. The mixture was then stirred for 1 hour, after which time a solution of *p*-toluenesulfonyl chloride (1.8 g, 9.4 mmol) in dry THF (*ca.* 10 mL) was added *via* the dropping funnel, under nitrogen. After stirring for 12 hours at room temperature, the solution was diluted with water (50 mL) and extracted with ethyl acetate (3 x 50 mL). The combined organic fractions were dried over $MgSO_4$ and the solvent removed *in vacuo*, affording a brown, viscous oil (1.99 g, 74%). ^{1}H NMR analysis of the crude material indicated the presence of the desired product, *N*-(*tert*-butyloxycarbonyl)-*N*-[2-(tosyloxy)ethyl]-2,4,6-trimethylaniline **55** [δ_H (400 MHz; $CDCl_3$) 1.39 (9H, s, Bu^t), 2.33 (6H, s, *o*-CH_3), 2.36 (3H, s, *p*-CH_3), 2.49 (3H, s, Ts-CH_3), 3.82 (2H, t, J = 8 Hz, NCH_2), 4.54 (2H, t, J = 8.4 Hz, CH_2O), 6.86 (2H, s, ArH), 7.41 (2H, d, J = 8.4 Hz, ArH) and 7.93 (2H, d, J = 8.4 Hz, ArH); δ_C (100 MHz; $CDCl_3$) 12.7 (*o*-CH_3), 21.2 (Ts-CH_3), 22.1 (*p*-CH_3), 28.6 [$C(CH_3)_3$], 51.6 (NCH_2), 62.1 (CH_2O) 70.9 [$C(CH_3)_3$], 127.1, 127.7, 129.4, 130.2, 131.5, 133.9, 136.7 and 142.8 (ArC) and 163.2 (C=O)], which was used in the next step without further purification.

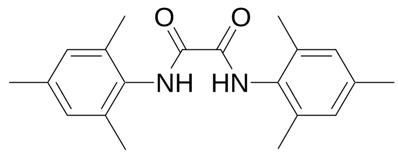

61

N,N*'-Bis(2,4,6-trimethylphenyl)oxalamide* **61**

A solution of 2,4,6-trimethylaniline **42** (4 mL, 29 mmol) and triethylamine (8.0 mL, 57 mmol) in dry THF (30 mL) was cooled to 0°C. Oxalyl chloride (3 mL, 34 mmol) was cautiously added to this solution while stirring under dry nitrogen, and the mixture left to stir overnight at room temperature. The resulting white precipitate was filtered off and, the filtrate diluted with water (40 mL) and extracted with ethyl acetate (4 x 40 mL). The combined organic fractions were washed with brine and dried ($MgSO_4$) before being concentrated *in vacuo* to afford as a white solid, *N,N'*-bis(2,4,6-trimethylphenyl)oxalamide **61** (1.2 g, 20%), m.p 232-235°C (no lit. ref. available); ν(C=O) 1687 cm^{-1}; δ_H (400 MHz; $CDCl_3$) 2.33 (12H, s, *o*-CH_3); 2.29 (6H, s, *p*-CH_3), 6.93 (4H, s, ArH), and 8.79 (2H, s, NH); δ_C (100 MHz; $CDCl_3$) 18.3 (*o*-CH_3), 21.0 (*p*-CH_3), 129.1, 129.6, 134.7 and 137.6 (ArC) and 158.2 (C=O); m/z 324 (M^+ 32%) and 135 (100).

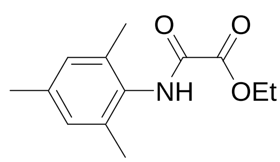

63

Ethyl N*-(2,4,6-trimethylphenyl)oxalamate* **63**

A solution of 2,4,6-trimethylaniline **43** (1 mL, 7 mmol) and triethylamine (2.0 mL, 14 mmol) in dry THF (5 mL) was cooled to 0°C. Ethyl chlorooxoacetate (0.8 mL, 7 mmol) was slowly added to this solution while stirring under dry argon. A white precipitate formed immediately, which, after stirring for an hour, was filtered off and washed with ethyl acetate (3 x 10 mL). The filtrate and washings were concentrated *in vacuo* and purified [preparative TLC; elution with hexane-ethyl acetate (1:1)] to afford ethyl *N*-(2,4,6-trimethylphenyl)oxalamate **63** as a caramel-coloured solid (3.53g, 56%); m.p 60-64°C (no lit. ref. available); ν (C=O)1676 and 1731 cm^{-1}; δ_H (400 MHz; $CDCl_3$) 1.43 (3H, t, *J* = 7.2 Hz, CH_2CH_3), 2.24 (6H, s, *o*-CH_3), 2.27 (3H, s, *p*-CH_3), 4.42 (2H, q, *J* = 7.2 Hz, CH_2), 6.90 (2H, s, ArH) and 8.34 (2H, s, NH); δ_C (100 MHz; $CDCl_3$) 14.0 (CH_2CH_3), 18.4 (*o*-CH_3), 20.9 (*p*-CH_3), 63.5 (CH_2), 128.8, 129.4, 135.0 and 137.4 (ArC), 154.7 and 160.0 (C=O); *m/z* 236 (MH^+, 43%) and 102 (100).

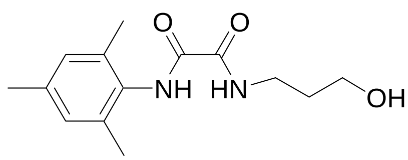

59

N-*(3-Hydroxypropyl)*-N'-*(2,4,6-trimethylphenyl)oxalamide* **59**

Ethyl N-(2,4,6-trimethylphenyl)oxalamate **63** (0.1847 g, 0.7820 mmol) was dissolved in 3-amino-1-propanol **46** (0.3 mL, 4 mmol), and the resulting solution stirred at 110° for 8 hours under dry nitrogen. Upon cooling, the material solidified and no further purification was undertaken. NMR analysis of the crude material (0.4329 g) confirmed the formation of *N*-(3-hydroxypropyl)-*N'*-(2,4,6-trimethylphenyl)oxalamide **59** as a caramel-coloured solid, m.p 129-132 °C (no lit. ref. available); δ_H (400 MHz; $CDCl_3$) 1.70 (2H, quintet, *J* = 6 Hz, CH_2), 2.07 (6H, s, *o*-CH_3), 2.18 (3H, s, *p*-CH_3), 3.39 (2H, t, *J* = 6.8 Hz, $NHCH_2$), 3.56 (2H, t, *J* = 5.6 Hz, OCH_2) and 6.80 (2H, s, ArH); δ_C (100 MHz; $CDCl_3$) 18.0 (*o*-CH_3), 20.7 (*p*-CH_3), 31.3 (CH_2), 37.0 ($NHCH_2$), 59.1 (CH_2OH), 128.7, 129.6, 134.5 and 137.2 (ArC), 158.2 and 160.0 (C=O).

3.1.2. Approaches to the malonate-tethered pyridine ligands

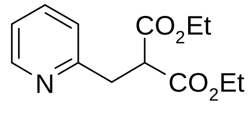

69

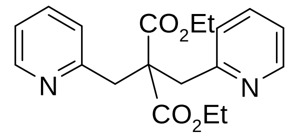

71

Diethyl [(2-pyridinyl)methyl]malonate **69** and *dietyl 2,2-bis-[2-pyridinyl)methyl]malonate* **71**

Small pieces of sodium metal (1.6 g, 79 mmol) were added to dry ethanol (40 mL), while stirring. Once all the sodium was consumed, freshly distilled diethyl malonate (4.2 mL, 2.7 mmol) was added, and the resulting solution heated at 50°C for 1 hour. 2-(Bromomethyl)pyridine hydrobromide **70** (6.9987 g, 27.7 mmol) was then added, and the solution turned a deep violet colour. The solution was heated at *ca.* 70°C for 6 hours, and stirred at room temperature overnight. The ethanol was removed *in vacuo* and the brown slurry taken up in ethyl acetate (50 mL) and water (50 mL). The aqueous layer was extracted with ethyl acetate (5 x 25 mL) and the combined organic solutions were dried ($MgSO_4$) and concentrated *in vacuo*. Chromatography of the crude dark brown oil [flash chromatography on silica gel; elution with hexane-ethyl acetate (3:1)] gave two fractions:

i) diethyl [(2-pyridinyl)methyl]malonate **69**, as a yellow oil (0.3 g, 50%); ν(C=O) 1733.5 cm^{-1}; δ_H (400 MHz; $CDCl_3$) 1.91 (6H, t, J = 7.2 Hz, CH_3), 3.35 (2H, d, J = 7.6 Hz, CH_2), 4.07 (1H, t, J = 8 Hz, CH), 4.14 (4H, q, J = 7.2 Hz, CH_2CH_3), 7.08 (1H, t, J = 5.2, ArH), 7.16 (1H, d, J = 7.6 Hz, ArH), 7.54 (1H, t, J = 8 Hz, ArH) and 8.47 (1H, d, J = 4.8 Hz, ArH); δ_C (100 MHz; $CDCl_3$) 13.9 (CH_2CH_3), 36.4 (CH_2), 51.2 (CH), 61.3 (CH_2CH_3), 121.5, 123.4, 136.2, 149.2 and 157.8 (ArC) and 169.1 (C=O); m/z 252 (MH^+, 100%); and

ii) 2,2-bis-[2-pyridinyl)methyl]malonate **71**, as a yellow oil (0.2 g, 20%); ν(C=O) 1733.5 cm^{-1}; δ_H (400 MHz; $CDCl_3$); 1.97 (6H, t, J = 7.2 Hz, CH_3), 3.44 (4H, s, CH_2), 4.18 (4H, q, J = 7.2 Hz, CH_3CH_2), 7.07 (1H, t, J = 2 Hz, ArH), 7.13 (1H, d, J = 8 Hz, ArH), 7.52 (1H, t, J = 8 Hz, ArH) and 8.48 (1H, d, J = 4 Hz, ArH); δ_C (100 MHz; $CDCl_3$) 13.8 (CH_3), 39.6 (CH_2CH_3), 58.0 [$C(CO_2Et)_2$], 61.7 (CH_2), 121.4, 124.5, 135.7, 148.9 and 157.6 (ArC) and 170.8 (C=O); m/z 343 (MH^+, 100%).

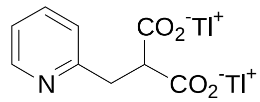

72

Thallium [(2-pyridin-2-yl)methyl]malonate **72**

Diethyl [(2-pyridinyl)methyl]malonate **69** (0.1730 g, 0.6885 mmol) was added to a solution of thallium carbonate (0.79 g, 1.7 mmol) in water (7 mL). After stirring overnight the suspension was heated at *ca.* 70°C to aid dissolution. After cooling, the crude material was freeze-dried, affording thallium [(2-pyridin-2-yl)methyl]malonate **72** as a white powder in quantitative yield (0.42 g), m.p 183-189°C (no lit. ref. available); ν(C=O) 1592 cm^{-1}; δ_H (400 MHz; D_2O) 3.06 (2H, d, J = 8 Hz, CH_2), 3.40 (1H, t, J = 8 Hz, CH), 7.13 (1H, t, J = 5.6 Hz, ArH), 7.17 (1H, d, J = 2 Hz, ArH), 7.62 (1H, t, J = 7.6 Hz, ArH), and 8.27 (1H, d, J = 5.2 Hz, ArH); δ_C (100 MHz; D_2O) 38.5 (CH_2), 59.7 (CH), 122.5, 124.3, 138.5, 148.7 and 159.8 (ArC) and 170.0 (C=O); ICP: Tl 63% (calculated 68%).

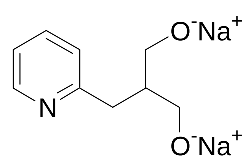

73

2-[2,2-Bis(hydroxymethyl)ethyl]pyridine **73**

A dry, 3-necked round-bottomed flask was equipped with a low-temperature thermometer, magnetic stirrer bar, condenser, rubber septum and nitrogen inlet. After flushing with dry nitrogen, the flask was charged with the diester **69** (1.509 g, 6.012 mmol) in dry THF and cooled to -78°C. DIBAL (9.5 mL of a 1M heptane solution) was added very slowly to this solution, using a syringe, such that the temperature did not rise above -60°C. The solution was stirred between -70 to -78°C for 45 minutes, after which time it was allowed to warm to room temperature and stirred overnight. Excess DIBAL was quenched by the drop-wise addition of methanol (1 mL), followed by saturated aq. NaOH (1 mL) and water (5 mL). The solvent was evaporated *in vacuo* and the solid residue dissolved in methanol and filtered. The filtrate was freeze-dried, affording the crude disodium salt of 2-[2,2-bis(hydroxymethyl)ethyl]pyridine **73** as a tan-coloured powder (0.8625 g, 86%), mp. > 320°C; ν(OH) 3409.5 cm^{-1}; δ_H (400 MHz; D_2O) 1.95 (1H, m, CH), 3.16 (2H, m, *C*H_2CH), 3.22 (CH_2O), 7.33 (2H, m, ArH), 7.81 (1H, t, *J* = 7.6 Hz, ArH), and 8.45 (1H, d, *J* = 7.2 Hz ArH); δ_C (100 MHz; D_2O) 38.6 (*C*H_2CH), 40.9 (CH), 60.2 (CH_2OH), 122.4, 138.4, 148.6, 159.9 and 161.0 (ArC).

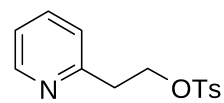

78

2-[2-(Tosyloxy)ethyl]pyridine **78**

Sodium hydride (0.24 g, 10 mmol, in a 60% mineral oil dispersion) was rinsed with dry hexane (2 x 10 mL), before adding dry THF (10 mL). While stirring, 2-(2-hydroxyethyl)pyridine **79** (1 mL, 9 mmol) was slowly added to the sodium hydride suspension, using a syringe. After stirring at room temperature for 1 hour, a solution of *p*-toluenesulfonyl chloride (1.7 g, 9.1 mmol) in THF (10 mL) was added using a pressure-equalized dropping funnel, under a flow of dry nitrogen. The resultant mixture was stirred overnight at room temperature, after which the caramel-coloured solution was concentrated *in vacuo*, and the residue diluted with water (50 mL) and ethyl acetate (50 mL). The aqueous layer was extracted further with aliquots of ethyl acetate (2 x 50 mL) and the combined organic fractions were dried with $MgSO_4$, and the solvent was removed *in vacuo*. The bronze-coloured oil was purified chromatographically [preparative TLC on silica gel; elution with hexane-ethyl acetate (1:1)] to yield the desired product as a bronze oil (1.8579 g, 74%); δ_H (400 MHz; $CDCl_3$) 2.48 (3H, s, CH_3), 3.22 (2H, t, *J* = 5.6 Hz, pyCH_2), 4.04 (1H, t, *J* = 5.6 Hz, ArH), 7.16 (1H, t, *J* = 5.6 Hz, ArH), 7.20 (1H, d, *J* = *7.6* Hz, ArH), 7.28 (2H, d, *J* = 8 Hz, ArH), 7.80 (1H, d, *J* = 8 Hz, ArH), 7.92 (2H, d, *J* = 8.4 Hz, ArH); δ_C (100 MHz; $CDCl_3$) 21.3 (CH_3) 36.2 (pyCH_2), 62.3 (CH_2OTs), 122.2, 124.9, 128.5, 130.7, 132.3, 139.1, 142.6, 148.2 and 160.6 (ArC); m/z 106 (MH^+, 100%).

3.1.3 Approaches to the branched tridentate pyridine systems

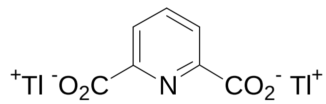

82

Thallium pyridine-2,6-dicarboxylate **82**

Thallium carbonate (0.9998 g, 2.133 mmol) was weighed into a 2-neck round-bottomed flask, equipped with a stirrer bar, reflux condenser and septum. Dry methanol (*ca.* 5 mL) was added to this *via* a cannula, followed by a solution of pyridine-2,6-dicarboxylic acid **80** (0.2009 g, 1.202 mmol) in dry methanol (*ca.* 10 mL). The resultant mixture was refluxed for 1 hour, and the ivory precipitate was filtered off, and dried *in vacuo*, affording the thallium salt of pyridine-2,6-dicarboxylate **82** in quantitative yield (0.6 g), m.p. 261-264°C; ν(C=O) 1561 cm^{-1}; δ_H (400 MHz; D_2O) 8.12 (2H, d, J = 8 Hz, ArH) and 8.18 (1H, t, J = 8 Hz, ArH); δ_C (100 MHz; D_2O) 127.8, 140.1 and 150.9 (ArC) and 173.6 (C=O); ICP: Tl 68.8% (calculated 71%).

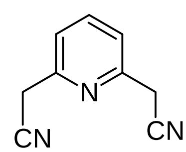

84

2,6-Bis(cyanomethyl)pyridine **84**

TMSCN (1.6 mL, 13 mmol) was added to a solution of TBAF (*ca.* 4 g, 15 mmol) in dry THF (*ca.* 15 mL), while stirring under dry nitrogen. A solution of 2,6-bis(bromomethyl)pyridine **83** (1.8539 g, 6.9969 mmol) in dry acetonitrile (15 mL) was added to the TBAF solution using a cannula, and the resulting solution stirred overnight. The dark reaction solution was quenched with 10 drops of deionised water and the solvent was then removed *in vacuo*, affording a dark oily residue. Purification of this crude material [flash chromatography on silica gel; elution with hexane-ethyl acetate (3:1)] afforded the desired 2,6-bis(cyanomethyl)pyridine **84** as brown crystals (0.9777 g, 89%), m.p. 94-96°C (lit. ref. [254] 96-97%); ν(C≡N) 2249 cm^{-1}; δ_H (400 MHz; $CDCl_3$) 3.93 (4H, s, CH_2), 7.42 (2H, d, J = 7.8 Hz, ArH), and 7.80 (1H, t, J = 7.7 Hz, ArH); δ_C (100 MHz; $CDCl_3$) 26.5 (CH_2), 116.6 (CN), 121.5, 138.8 and 151.0 (ArC).

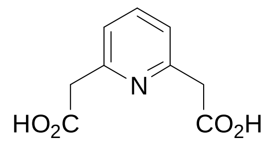

81

2,6-Bis(carboxymethyl)pyridine **81**

A solution of 2,6-bis(cyanomethyl)pyridine **84** (0.3542 g, 2.254 mmol) in ethanol (20 mL) was added to a 10M solution of sodium hydroxide (20 mL), and the mixture boiled under reflux for 4 hours. The reaction solution was then passed through a cation exchange column (Ag 50W-X2, H-form). The aqueous solution that was collected ranged in pH from 1-5, and was freeze-dried to afford 2,6-bis(carboxymethyl)pyridine **81** (0.26 g, 65 %), as a dark oil., δ_H (400 MHz; $CDCl_3$) 3.62 (4H, s, CH_2), 7.72 (2H, d, J = 7.2 Hz, ArH), and 7.91 (1H, t, J = 7.2 Hz, ArH); δ_C (100 MHz; $CDCl_3$) 40 (CH_2), 125.8, 139.1 and 151.8 (ArC), and 167.0 (C=O).

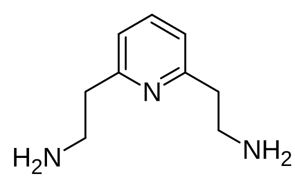

86

Attempted synthesis of 2,6-bis(2-aminoethyl)pyridine **86**

A dry, 2-neck round-bottomed flask was charged with lithium aluminium hydride (0.52 g, 14 mmol) and equipped with a reflux condenser, magnetic stirrer bar, and a pressure-equalized dropping funnel. Dry THF (2 mL) was added *via* the dropping funnel, under a flow of argon, and the resultant suspension cooled on ice. 2,6-bis(cyanomethyl)pyridine **84** (0.552 g, 3.51 mmol) was dissolved in dry THF (10 mL) and added to this cooled suspension using the dropping funnel, causing a gentle reflux. After stirring overnight at room temperature, the reaction was quenched [methanol (1 mL), followed by slow addition of 10 mL water]. Once quenched, the solution was diluted with ethyl acetate (30 mL) and water (30 mL). The aqueous layer was extracted twice more with ethyl acetate (2 x 20 mL), and the combined organic solutions dried over $MgSO_4$ and concentrated *in vacuo.* Neither this residue (20 mg) nor that obtained from drying the aqueous phase (358 mg) showed any evidence of a pyridine moiety from the ^1H NMR spectrum.

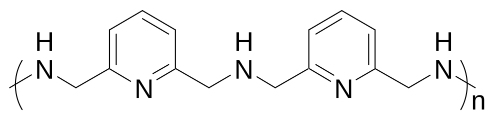

99

Poly-[2,6-bis(aminomethyl)]pyridine **99**

Aq. ammonia (3 mL of a 32% aqueous solution) was added to a solution of 2,6-bis(bromomethyl)pyridine **83** (1.0614 g, 4.006 mmol) in THF (*ca.* 10 mL), and the resultant emulsion stirred vigorously for 2 hours at room temperature. A heavy white precipitate had formed and the mixture was thus filtered and washed with ethyl acetate (5 x 20 mL), affording poly-2,6-bis(aminomethyl)pyridine **99** as a rubbery solid (0.6876 g, 93%). The precipitate did not seem to be soluble in common organic solvents or water, precluding detailed spectroscopic characterization. m.p. > 320°C.

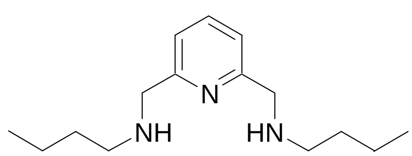

88

2,6-Bis(butylaminomethyl)pyridine **88**

A solution of butylamine (0.15 mL, 1.5 mmol) and 2,6-bis(bromomethyl)pyridine **83** (81.2 mg, 0.306 mmol) in toluene (1mL) was stirred overnight at room temperature. The solvent and excess butylamine were removed *in vacuo*, affording the crude 2,6-bis(butylaminomethyl)pyridine **88** as a peach-coloured oil (76 mg, 70%) [δ_H (400

MHz; $CDCl_3$) 0.87 (6H, s, CH_3), 1.34 (4H, m, CH_2CH_3), 1.67 (4H, m, CH_2), 2.73 (4H, t, J = 7.6 Hz, $NHCH_2$), 3.95 (4H, s, $pyCH_2$), 7.34 (2H, d, J = 7.6 Hz, ArH), and 7.75 (1H, t, J = 8 Hz, ArH); δ_C (100 MHz; $CDCl_3$) 13.5 (CH_3), 21.2 (CH_2CH_3), 33.8 (CH_2), 49.2 (CH_2NH), 56.5 ($pyCH_2$), 120.7, 135.8 and 157.6 (ArC); m/z 250 (MH^+ 54%) and 107 (100%)], which was used without further purification.

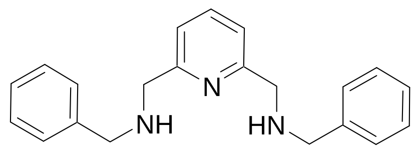

89

2,6-Bis(benzylaminomethyl)pyridine **89**

A solution of of benzylamine (0.2 mL, 1.8 mmol) and 2,6-bis(bromomethyl)pyridine **83** (0.1008 g, 0.3805 mmol) in toluene (1 mL) was stirred overnight at room temperature. The solvent was removed *in vacuo*, affording the crude 2,6-bis(benzylaminomethyl]pyridine **89** as a bronze-coloured oil (0.1911 g) [δ_H (400 MHz; $CDCl_3$) 3.79 (4H, s, $PhCH_2$), 3.94 (4H, s, $pyCH_2$), 7.12 (2H, d, J = 7.6 Hz, pyH), 7.25 (10H, m, ArH), and 7.52 (1H, t, J = 7.6 Hz, pyH); δ_C (100 MHz; $CDCl_3$) 53.9 ($PhCH_2$), 54.6 ($pyCH_2$), 120.7 (pyC), 126.9, 128.1, and 128.3 (PhC), 136.1 (pyC), 137.2 (PhC) and 156.7 (pyC); m/z 317 (M^+ 10%) and 91 (100%)], which was used without further purification.

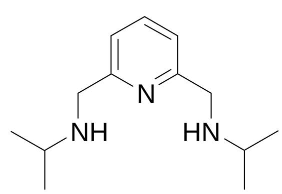

90

2,6-Bis(isopropylaminomethyl)pyridine **90**

A solution of 2,6-bis(bromomethyl)pyridine **83** (0.2404 g, 0.907 mmol) and excess isopropylamine (0.4 mL, 4.7 mmol) in THF (1 mL) was stirred overnight at room temperature. The reaction mixture was diluted with CH_2Cl_2 (2 mL) and washed with saturated aq. Na_2CO_3 (2 x 5 mL). After drying the organic solution with $MgSO_4$, the solvent and excess isopropylamine were removed *in vacuo,* thus affording the crude 2,6-bis[(isopropyl)aminomethyl]pyridine **90** as a white powder (0.1673 g 90%), m.p 100-102°C (no lit. ref. available); δ_H (400 MHz; $CDCl_3$) 1.08 (12H, m, CH_3), 2.40 (2H, s, NH), 2.84 (2H, q, *J* = 6.4 Hz, CH), 3.86 (4H, s, CH_2), 7.10 (2H, d, *J* = 7.6 Hz, ArH), 7.80 (1H, t, *J* = 7.6 Hz, ArH); δ_C (100 MHz; $CDCl_3$) 23.6 (CH_3), 46.9 (CH), 53.1 (CH_2), 119.7, 137.5 and 158.1 (py-C). m/z 221 (M^+, 25%) and 81 (100%)], which was used without further purification.

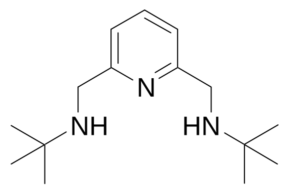

91

*2,6-Bis[(*tert*-butyl)aminomethyl]pyridine* **91**

A solution of 2,6-bis(bromomethyl)pyridine **83** (79.4 mg, 0.300 mmol) and *tert*-butylamine (0.16 mL, 1.5 mmol) in dry toluene (3 mL) was stirred overnight at room temperature, followed by heating at reflux temperature for 5 hours. After cooling, the solution was washed with saturated aq. Na_2CO_3 (10 mL) and extracted with CH_2Cl_2 (3 x 10 mL). The combined organic fractions were dried ($MgSO_4$) and then concentrated *in vacuo*, to afford crude 2,6-bis[(*tert*-butyl)aminomethyl]pyridine **91** as a clear oil (57.7 mg, 72%); δ_H (400 MHz; $CDCl_3$) 1.09 (18H, m, CH_3), 3.84 (4H, s, CH_2), 7.13 (2H, d, *J* = 7.6 Hz, ArH), 7.85 (1H, t, *J* = 7.6 Hz, ArH); δ_C (100 MHz; $CDCl_3$) 28.8 (CH_3), 47.2 [*C*($CH)_3$], 52.8 (CH_2), 119.8, 137.6, and 158.3 (py-C). m/z 250 (MH^+, 17%).

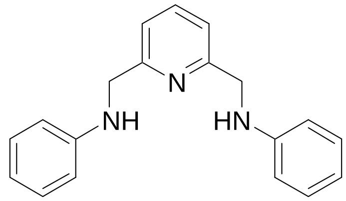

92

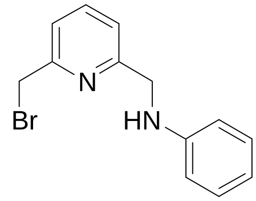

98

2,6-Bis(phenylaminomethyl)pyridine **92** and *2-bromomethyl-6-(phenylamino-methyl)-pyridine* **98**

A solution of 2,6-bis(bromomethyl)pyridine **83** (65.1 mg, 0.246 mmol) and aniline (0.11 mL, 1.2 mmol) in toluene (1 mL) was stirred overnight at room temperature, followed by heating for 1 hour at *ca.* 60°C. The solution was diluted with CH_2Cl_2 (2 mL) and washed with saturated aq. Na_2CO_3. After drying ($MgSO_4$) the solvent was removed *in vacuo*, affording an orange oil (72 mg). Purification, [preparative TLC; elution with hexane-ethyl acetate (1:1)], afforded two fractions:

i) 2,6-Bis(phenylaminomethyl)pyridine **92**, as a clear oil (25 mg, 35%); ν_{max} 3415 cm^{-1}; δ_H (400 MHz; $CDCl_3$) 4.47 (4H, s, CH_2), 4.73 (2H, s, NH), 6.67 (4H, d, *J* = 7.6 Hz, aniline-ArH), 6.73 (1H, t, *J* = 7.2 Hz, aniline-ArH), 7.19 (6H, m, py- and aniline-ArH), 7.59 (1H, t, *J* = 7.2 Hz, py-ArH); δ_C (100 MHz; $CDCl_3$) 49.2 (CH_2), 113.1 and 117.6 (Ph-C), 119.8 (py-C) 129.2 (Ph-C), 137.2 (py-C), 147.9 (Ph-C), and 158.1 (py-C); m/z 290 (MH^+ 62%); and

ii) 2-Bromomethyl-6-(phenylaminomethyl)pyridine **98**, an ivory solid (35 mg, 49%); m.p. 240-242°C; ν_{max} 3480 cm^{-1} (NH); δ_H (400 MHz; $CDCl_3$) 4.43 (2H, s, CH_2), 4.84 (2H, s, CH_2), 6.67 (2H, d, *J* = 3.6 Hz, aniline-ArH), 6.74 (1H, t, *J* = 6.8 Hz, aniline-ArH), 7.18 (4H, m, py+aniline-ArH), 7.56 (1H, t, *J* = 7.6 Hz, py-ArH); δ_C (100 MHz; $CDCl_3$) 49.2 (CH_2), 57.1 (CH_2), 113.1 and 117.5 (Ph-C), 119.2 and 119.9 (py-C), 129.2 (Ph-C), 137.3 (py-C), 147.9 (Ph-C), 158.2 (py-C) and 158.3 (py-C); m/z 278 (MH^+ 56%).

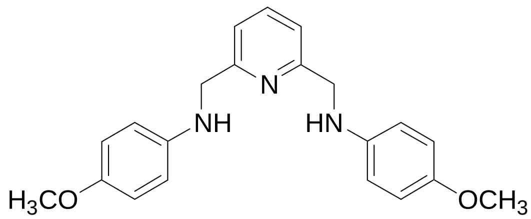

93

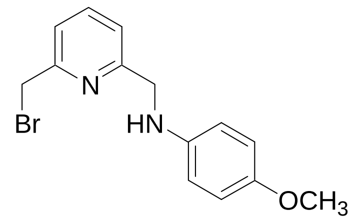

99

2,6-Bis[(4-methoxyphenyl)aminomethyl]pyridine **93** and *2-bromomethyl-6-[(4-methoxyphenyl)aminomethyl]pyridine* **99**

A solution of anisidine (0.2250 g, 1.827 mmol) and 2,6-bis(bromomethyl)pyridine **83** (0.1231 g, 0.4646 mmol) in THF (2 mL) was stirred overnight, diluted with CH_2Cl_2 (5 mL), and washed with saturated aq. Na_2CO_3 (5 mL). After extracting the aqueous layer with aliquots of CH_2Cl_2 (5 x 5 mL) the combined organic solutions were dried ($MgSO_4$) and concentrated *in vacuo*, yielding a brown oil. Chromatography [preparative TLC on silica gel; elution with hexane-ethyl acetate (1:1)] gave two fractions:

i) 2,6-Bis[(4-methoxyphenyl)aminomethyl]pyridine **93**, as a brown oil (34 mg, 21%); δ_H (400 MHz; $CDCl_3$) 3.74 (6H, s, CH_3), 4.41 (4H, s, CH_2), 6.63 (4H, d, J = 9.2 Hz, anisidine-ArH), 6.78 (4H, d, J = 8.8 Hz, anisidine-ArH), 7.19 (2H, d, J = 8 Hz, py-ArH) and 7.57 (1H, t, J = 8 Hz, py-ArH); δ_C (100 MHz; $CDCl_3$) 50.2 (CH_2), 55.7 (CH_3), 114.3, 114.9, 119.9, 137.2, 142.1, 152.2 and 158.3 (ArC); m/z 348 (M-1, 87%) and 123 (100%); and

ii) *2*-Bromomethyl-6-[(4-methoxyphenyl)aminomethyl]pyridine **99**, as a brown oil (26 mg, 19%); δ_H (400 MHz; $CDCl_3$) 3.73 (3H, s, CH_3), 4.38 (2H, s, CH_2), 4.77 (2H, s, CH_2), 6.62 (2H, d, J = 8.8 Hz, anisidine-ArH), 6.67 (1H, d, J = 9.2 Hz, py-ArH), 6.77 (1H, d, J = 9.2 Hz, py-ArH), 7.17 (2H, d, J = 8 Hz, anisidine-ArH), 7.55 (1H, t, J = 7.6 Hz, py-ArH); δ_C (100 MHz; $CDCl_3$) 50.1 (CH_2NH), 55. 8 (CH_3), 57.8 (CH_2), 114.3, 114.8, 119.3, 119.9, 137.3, 142.2, 152.2, 158.5 and 158.7 (ArC); m/z 306 (M+ 63%) and 140 (100%).

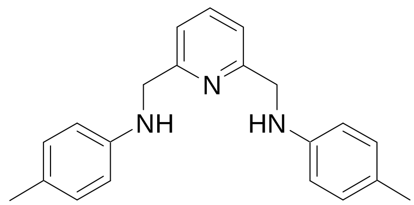

94

2,6-Bis[(4-methylphenyl)aminomethyl]pyridine **94**

A solution of 2,6-bis(bromomethyl)pyridine **83** (0.1401 g, 0.5288 mmol) and *p*-toluidine (0.2 g, 2 mmol) in THF (1 mL) was stirred at room temperature overnight. The reaction mixture was diluted with CH_2Cl_3 (3 mL) and saturated aq. Na_2CO_3 (3 mL). The aqueous layer was extracted with aliquots of CH_2Cl_3 (5 x 5 mL) and the combined organic extracts dried ($MgSO_4$) and the solvent removed *in vacuo.* The crude residue was purified [preparative TLC on silica gel; elution with hexane-ethyl acetate (1:1]], affording 2,6-bis[(4-methylphenyl)aminomethyl]pyridine **94** as a bronze oil (87.2 mg, 52%); δ_H (400 MHz; $CDCl_3$) 2.25 (6H, s, CH_3), 4.44 (4H, s, CH_2), 6.60 (4H, d, *J* = 8.4 Hz, Ph-ArH), 7.01 (4H, d, *J* = 8.4 Hz, Ph-ArH), 7.20 (2H, d, *J* = 7.6 Hz, py-ArH) and 7.57 (1H, t, *J* = 7.6 Hz, py-ArH); δ_C (100 MHz; $CDCl_3$) 20.4 (CH_3), 49.6 (CH_2), 113.2 (Ph-C), 119.8 (py-C), 126.8 and 129.7 (Ph-C), 137.2 (py-C), 145.6 (Ph-C) and 158.3 (py-C); m/z 318 (MH^+, 47%) and 106 (100%).

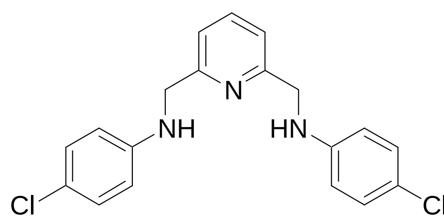

95

2,6-Bis[(4-chlorophenyl)aminomethyl]pyridine **95**

A solution of 2,6-bis(bromomethyl)pyridine **83** (80.3 mg, 0.303 mmol) and 4-chloroaniline (0.1980 g, 1.552 mmol) in toluene (2 mL) was stirred overnight, then diluted with CH_2Cl_2 (5 mL) and washed with saturated aq. Na_2CO_3 (2 x 5 mL). The combined aqueous solutions were further washed with aliquots of CH_2Cl_2 (5 x 5 mL) and the combined organic solutions were dried ($MgSO_4$) and concentrated *in vacuo,* affording a red-brown oil (0.2163 mg). Purification [preparative TLC; elution with hexane-ethyl acetate (1:1)] afforded 2,6-bis[(4-chlorophenyl)aminomethyl]pyridine **95** as a coppery solid (35.7 mg, 33%); mp. 124-127°C (no lit. ref. available); ν_{max} 1501 cm^{-1}; δ_H (400 MHz; $CDCl_3$) 4.42 (4H, s, CH_2), 4.75 (2H, s, NH), 6.57 (4H, d, *J* = 8.8 Hz, Ph-ArH), 7.12 (4H, d, *J* = 8.8 Hz, Ph-ArH), 7.18 (2H, d, *J* = 8.0 Hz, py-ArH), and 7.60 (1H, t, *J* = 7.6 Hz, py-ArH); δ_C (100 MHz; $CDCl_3$) 49.2 (CH_2), 114.1 (Ph-C), 120.0 (py-C), 122.3 and 129.1 (Ph-C), 137. 3 (py-C), 146.4 (Ph-C) and 157.6 (py-C); m/z 358 (MH^+, 63%) and 230 (100%).

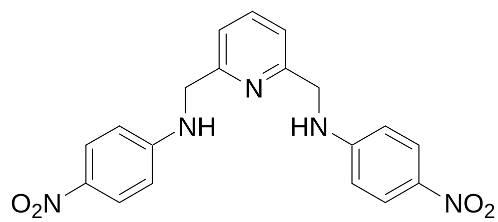

96

Attempted synthesis of 2,6-bis[(4-nitrophenyl)aminomethyl]pyridine **96**

2,6-Bis(bromomethyl)pyridine **83** (0.1105 g, 0.4171 mmol) and 4-nitroaniline (0.1202 g, 0.8702 mmol) were combined in a microwave vial, and DMF (2 mL) was added. Microwave irradiation was applied for 10 minutes, maintaining a temperature of *ca.* 165°C. After cooling the mixture was poured into ice water, causing the precipitation of a brown material (5.8258 g). This was then freeze-dried, but NMR analysis of the residue showed only unconverted 4-nitroaniline.

3.1.5. Preliminary complexation studies

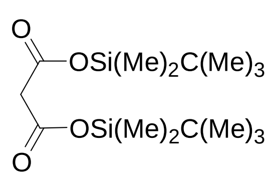

102

*Bis(*tert-*butyldimethylsilyl) malonate* **102**[256,272]

Malonic acid (4.5148 g, 43.34 mmol), imidazole (6.2091g, 91.2 mmol) and *tert*-butyldimethylsilyl chloride (13.3 g, 88.2 mmol) were dissolved in dry DMF (*ca.* 50

mL). The resulting solution was heated at *ca.* 50°C for one hour while stirring and then left to cool to room temperature. The reaction mixture was diluted with water (50 mL) and extracted with petroleum ether (40°-60°) (2 x 50 mL). After drying with $MgSO_4$, the combined organic solutions were concentrated *in vacuo*, affording a colourless oil. Distillation under reduced pressure afforded the silyl ester **102** as a colourless oil (13.9014 g, 98%). δ_H (400 MHz; $CDCl_3$) 0.27 (12H, s, $Si(CH_3)_2$, 0.91 [18H, s, $C(CH_3)_3$] and 3.34 (2H, s, CH_2); δ_C (100 MHz; $CDCl_3$) -5.0 [$Si(CH_3)_2$], 15.2 [$\mathit{C}(CH_3)_2$], 25.3 [$C(\mathit{C}H_3)_3$], 45.0 (CH_2) and 166.9 (C=O); m/z 333 (MH^+, 100%).

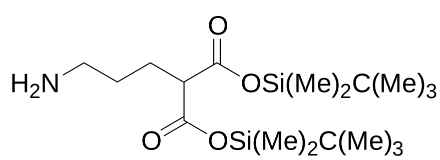

104

*Attempted synthesis of 1-amino-3,3-di[(*tert*-butyldimethylsilyl)ester]* **104**

Sodium hydride (*ca.* 0.3 g in a 60% mineral oil dispersion) was rinsed with dry hexane (3 x 10 mL) before adding dry THF (*ca.* 20 mL). The suspension was cooled on ice before adding a solution of bis(*tert*-butyldimethylsilyl) malonate **102** (1.0103 g, 3.0750 mmol) in THF (10 mL) drop-wise, while stirring under dry nitrogen. After stirring at room temperature for 1 hour, a solution of 3-aminopropyl bromide **53** (0.6757 g, 3.0865 mmol) in THF (10 mL) was added, and the resulting solution heated at reflux temperature for 16 hours. The solution was cooled to room temperature and diluted with water (50 mL) and ethyl acetate (50 mL). The aqueous solution was extracted further with aliquots of ethyl acetate (3 x 30 mL) and the combined organic solutions were dried ($MgSO_4$) and concentrated *in vacuo*, affording unconverted starting material, as evidenced by NMR analysis.

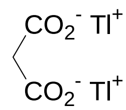

103

Thallium malonate **103**

A dry round-bottomed flask was charged with thallium carbonate (1.2467 g, 2.660 mmol) and dry methanol (8 mL). A solution of malonic acid (0.14 g, 1.3 mmol) in methanol (15 mL) was added to the thallium carbonate solution, and the resulting solution heated at *ca.* 70°C under argon, for 1 hour. The solvent was removed *in vacuo* to afford thallium malonate **103** as a white powder, in quantitative yield (0.41 g). The product was pure by NMR analysis and no further purification steps were thus undertaken. m.p 149-151°C (no lit. ref. available); ν(C=O) 1563 cm^{-1}; δ_H (400 MHz; D_2O) 3.13 (2H, s, CH_2); δ_C (100 MHz; D_2O) 48.6 (CH_2), 177.9 (C=O); % Tl 66% (calculated 79%).

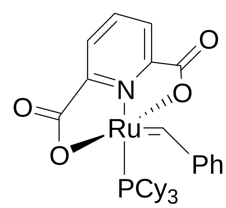

105

Attempted synthesis of the ruthenium complex **105**

Method 1

The Grubbs first-generation catalyst **4** (55.8 mg, 0.0678 mmol) was transferred to a Schlenk flask under a flow of dry nitrogen, and dry toluene (5 ml) was added *via* a cannula, while stirring. Solid thallium pyridine-2,6-dicarboxylate **82** (46.1 mg, 0.0802 mmol) was added, and the sides of the flask rinsed with dry toluene. The resulting mixture was stirred overnight, under argon, and filtered through celite, using a cannula, to remove the insoluble material. The filtrate was concentrated *in vacuo*, affording a purple solid. NMR and IR analysis confirmed this to be the Grubbs complex **4**.

Method 2

The Grubbs first-generation catalyst **4** (56.1 mg, 0.0682 mmol) was transferred to a Schlenk flask under a flow of dry nitrogen, and dry toluene (10 ml) was added, while stirring. Solid thallium pyridine-2,6-dicarboxylate **82** (46.1 mg, 0.0802 mmol) was added, and the suspension heated at 80-100°C for 1 hour. After this time the solution had changed colour from purple to brown, and was filtered and concentrated *in vacuo*. However, NMR and IR analysis confirmed this to be the Grubbs complex **4**.

Method 3

The Grubbs first-generation catalyst **4** (29.9 mg, 0.0363 mmol) and thallium pyridine-2,6-dicarboxylate **82** (26.0 mg, 0.0452 mmol) were combined in a microwave tube, fitted with a septum and a magnetic stirrer bar. Dry, degassed toluene (1 mL) was added to the mixture and was irradiated at 120°C for 10 minutes in the microwave reactor. The brown suspension was filtered and concentrated *in vacuo*, but NMR analysis confirmed the presence of only the Grubbs complex **4**.

Method 4

The Grubbs first-generation catalyst **4** (31.4 mg, 0.0382 mmol) and thallium pyridine-2,6-dicarboxylate **82** (35 mg, 0.061 mmol) were combined in a crucible, and heated with a heat-gun, while grinding intermittently. Heating was halted upon colour change of the mixture from purple to brown, but NMR and IR analysis confirmed this to be the Grubbs complex **4**.

Method 5

The Grubbs first-generation catalyst **4** (34.1 mg, 0.0414 mmol) and thallium pyridine-2,6-dicarboxylate **82** (27.1 mg, 0.0471 mmol) were combined in a microwave tube, fitted with a septum and a magnetic stirrer bar. The mixture was irradiated for 10 minutes in the microwave reactor, at 120°C. However, NMR and IR analysis confirmed this to be the Grubbs complex **4**.

Method 6

The Grubbs first-generation catalyst **4** (25.7 mg, 0.0312 mmol) and thallium pyridine-2,6-dicarboxylate **82** (21.2 mg, 0.0367 mmol) were combined in a microwave tube, fitted with a septum and a magnetic stirrer bar. DMSO-d_8 (1 mL) was added to the mixture, and the tube was irradiated at 120°C for 10 minutes in the microwave reactor. However, no identifiable products were observed in NMR analysis.

3.2. COMPUTATIONAL

Molecular mechanics simulations were performed using both the Accelerys[269] Cerius^2 modelling platform on an SGI O^2 unix-based platform, and the Wavefunction[270] Spartan PC-Pro software package on a windows-based PC. The general purpose universal force-field was used for all calculations, using Cerius^2, and charges were included using the charge equilibration method. The Qeq_charged 1.0 parameter was employed, and structures were minimised to convergence using the conjugate gradient method. Isothermal molecular dynamics methods were used to search for the lowest energy conformers. Annealed dynamics simulations employed a mid-cycle temperature of 1000 K and included 300 anneal cycles. The lowest energy structure was obtained for each compound examined by minimising the ten highest and ten lowest energy conformers; the structure with the lowest energy was saved as the global minimum structure. Geometry optimizations with the Spartan software package were performed at the molecular mechanics level using the MMFF force-field, following the conformer search and equilibrium options.

4. REFERENCES

(1) Frennet, A.; Hubert, C. *J. Mol. Cat.: A* **2000***, 163*, 163-188.

(2) Somorjai, G. A.; McCrea, K. *Appl. Catal., A* **2001***, 222*, 3-18.

(3) Taylor, H. S. *Proc. R. Soc. A.* **1925***, 108*, 105-111.

(4) Marcilly, C. *J. Catal.* **2003***, 216*, 47-62.

(5) Cavani, F.; Trifirò, F. *Catal. Today* **1997***, 34*, 269-279.

(6) Widegren, J. A.; Finke, R. G. *J. Mol. Cat.: A* **2003***, 198*, 317-341.

(7) Cornils, B.; Herrmann, W. A. *J. Catal.* **2003***, 216*, 23-31.

(8) Pariya, C.; Jayaprakash, K. N.; Sarkar, A. *Coord. Chem. Rev.* **1998***, 168*, 1-48.

(9) Zhao, X. S.; Bao, X.; Guo, W.; Lee, F. *Mater. Today* **2006***, 9*, 32-39.

(10) Olivier, H. *J. Mol. Cat.: A* **1999***, 146*, 285-289.

(11) Goetheer, E. L. V.; Verkerk, A. W.; van den Broeke, L.J.P.; de Wolf, E.; Deelman, B.; van Koten, G.; Keurentjies, J. T. F. *J. Catal.* **2003***, 219*, 126-133.

(12) Chaudhari, R. V.; Jayasree, S. S. *Catal. Today* **2001***, 66*, 371-380.

(13) Stone, F. S. *J. Catal.* **2003***, 216*, 2-11.

(14) Castarlenas, R.; Fischmeister, C.; Bruneau, C.; Dixneuf, P. H. *J. Mol. Cat.: A* **2004**, *213*, 31-37.

(15) Crabtree, R. H. *Chem. Commun.* **1999**, 1611-1616.

(16) Armor, J. N. *Appl. Catal., A* **2000***, 194-195*, 3-11.

(17) Blaser, H.; Pugin, B.; Spindler, F. *J. Mol. Cat.: A* **2005***, 231*, 1-20.

(18) Barrault, J.; Pouilloux, Y.; Cacens, J. M.; Vanhove, C.; Bancquart, S. *Catal. Today* **2002***, 75*, 177-181.

(19) McMorn, P.; Hutchings, J. *Chem. Soc. Rev.* **2004***, 33*, 108-122.

(20) Calderon, N. *Acc. Chem. Res.* **1972***, 5*, 127-132.

(21) Trnka, T. M.; Grubbs, R. H. *Acc. Chem. Res.* **2001***, 34*, 18-29.

(22) Yao, Q.; Motta, A. M. *Tetrahedron Lett.* **2004***, 45*, 2447-2451.

(23) Grubbs, R. H.; Chang, S. *Tetrahedron* **1998***, 54*, 4413-4450.

(24) Blackwell, H. E.; O'Leary, D. J.; Chatterjee, A. K.; Washendfelder, R. A.; Bussmann, D. A.; Grubbs, R. H. *J. Am. Chem. Soc.* **2000***, 122*, 58-71.

(25) Allaert, B.; Dieltiens, N.; Ledoux, N.; Vercaemst, C.; Van Der Voort, P.; Stevens, C. V.; Linden, A.; Verpoort, F. *J. Mol. Cat.: A* **2006***, 260*, 221-226.

(26) Mol, J. C. *J. Mol. Cat.: A* **2004***, 213*, 39-45.

(27) Grubbs, R. H. *Tetrahedron* **2004***, 60*, 7117-7140.

(28) Feast, W. J.; Khosravi, E. *J. Fluor. Chem.* **1999***, 100*, 117-125.

(29) Calderon, N.; Chen, H.Y.; Scott, K.W. *Tetrahedron Lett.* **1967***, 8*, 3327-3329.

(30) Rouhi, A. M. *C&EN* **2002***, 80*, 29-33.

(31) Banks, R. L.; Bailey, G. C. *Ind. Eng. Chem. Prod. Res. Dev.* **1964***, 3*, 170-173.

(32) Tebbe, F. N.; Parshall, G. W.; Ovenall, D. W. *J. Am. Chem. Soc.* **1979***, 101*, 5075-5078.

(33) Wengrovius, J. H.; Schrock, R. R. *J. Am. Chem. Soc.* **1980***, 102*, 4515-4516.

(34) Lu, S.; Quale, P.; Heatley, F.; Booth, C.; Yeates, S. G.; Padget, J. C. *Macromolecules* **1992***, 25*, 2692-2697.

(35) France, M. B.; Grubbs, R. H.; McGrath, D. V. *Macromolecules* **1993***, 26*, 4742-4747.

(36) Nguyen, S. T.; Johnson, L. K.; Grubbs, R. H. *J. Am. Chem. Soc.* **1992***, 114*, 3974-3877.

(37) Johnson, L. A.; Grubbs, R. H.; Ziller, J. W. *J. Am. Chem. Soc.* **1993**, *115*, 8130-8190.

(38) Fu, G. C.; Nguyen, S. T.; Grubbs, R. H. *J. Am. Chem. Soc.* **1993**, *115*, 9856-9857.

(39) Armstrong, S. K. *J. Chem. Soc., Perkin Trans.1* **1998**, 371-388.

(40) Diver, S. T.; Giessert, A. J. *Chem. Rev.* **2004**, *104*, 1317-1382.

(41) Dragutan, V.; Dragutan, I. *J. Organomet. Chem* **2006**, *691*, 5129-5147.

(42) Courchay, F. C.; Sworen, J. C.; Coronado, A.; Wagener, K. B. *J. Mol. Cat.: A* **2006**, *254*, 111-117.

(43) Joo, S.; Yun, Y.; Jin, J.; Kim, D.; Zin, W. *Macromolecules* **2000**, *33*, 6704-6712.

(44) De Clercq, B.; Verpoort, F. *Tetrahedron Lett.* **2002**, *43*, 9101-9104.

(45) Lynn, D. M.; Kanaoka, S.; Grubbs, R. H. *J. Am. Chem. Soc.* **1996**, *118*, 784-790.

(46) Lynn, D. M.; Mohr, B.; Grubbs, R. H. *J. Am. Chem. Soc.* **1998**, *120*, 1627-1628.

(47) Webster, O. W. *Science* **1991**, *251*, 887-893.

(48) Hillmyer, M. A.; Lepetit, C.; McGrath, D. V.; Novak, B. M.; Grubbs, R. H. *Macromolecules* **1992**, *25*, 3345-3350.

(49) France, M. B.; Paciello, R. A.; Grubbs, R. H. *Macromolecules* **1993**, *26*, 4739-4741.

(50) Novak, B. M.; Grubbs, R. H. *J. Am. Chem. Soc.* **1988**, *110*, 7542-7543.

(51) Kanaoka, S.; Grubbs, R. H. *Macromolecules* **1995**, *28*, 4707-4713.

(52) Nguyen, S. T.; Grubbs, R. H.; Ziller, J. W. *J. Am. Chem. Soc.* **1992**, *114*, 3974-3975.

(53) Nguyen, S. T.; Grubbs, R. H. *J. Am. Chem. Soc.* **1993**, *115*, 9858-9859.

(54) Grigg, R.; Martin, W.; Morris, J.; Sridharan, V. *Tetrahedron Lett.* **2003**, *44*, 4899-4901.

(55) Banfi, L.; Basso, A.; Guanti, G.; Riva, R. *Tetrahedron Lett.* **2003**, *44*, 7655-7658.

(56) Van de Weghe, P.; Aoun, D.; Boiteau, J.; Eustache, J. *Org. Lett.* **2002**, *4*, 4105-4108.

(57) Kirkland, T. A.; Grubbs, R. H. *J. Org. Chem.* **1998**, *63*, 9904-9908.

(58) Doodeman, R.; Rutjes, F. P. J. T.; Hiemstra, H. *Tetrahedron Lett.* **2000**, *41*, 5979-5983.

(59) Fürstner, A.; Langerman, K. *J. Org. Chem.* **1996**, *61*, 3942-3943.

(60) Basu, K.; Cabral, J. A.; Paquette, L. A. *Tetrahedron Lett.* **2002**, *43*, 5453-5456.

(61) Kirkland, T. A.; Grubbs, R. H. *J. Org. Chem.* **1997**, *62*, 7310-7318.

(62) Chatterjee, A. K.; Choi, T.; Sanders, D. P.; Grubbs, R. H. *J. Am. Chem. Soc.* **2003**, *125*, 11360-11370.

(63) Chatterjee, A. K.; Grubbs, R. H. *Org. Lett.* **1999**, *1*, 1751-1753.

(64) O'Leary, D. J.; Blackwell, H. E.; Washenfelder, R. A.; Grubbs, R. H. *Tetrahedron Lett.* **1998**, *39*, 7427-7430.

(65) O'Leary, D. J.; Blackwell, H. E.; Washenfelder, R. A.; Miura, K.; Grubbs, R. H. *Tetrahedron Lett* **1999**, *40*, 1091-1094.

(66) Feher, F. J.; Soulivong, D.; Eklund, A. F.; Wyndham, K. D. *Chem. Commun.* **1997**, 1185-1186.

(67) Wybrow, R. A. J.; Johnson, L. A.; Auffray, B.; Moran, W. J.; Adams, H.; Harrity, J. P. A. *Tetrahedron Lett.* **2002**, *43*, 7851-7854.

(68) La, D. S.; Sattely, E. S.; Ford, J. G.; Schrock, R. R.; Hoveyda, A. H. *J. Am. Chem. Soc.* **2001**, *123*, 7767-7778.

(69) Hagiwara, H.; Katsumi, T.; Endou, S.; Hoshi, T.; Suzuki, T. *Tetrahedron* **2002**, *58*, 6651-6654.

(70) Dragutan, I.; Drajutan, V. *Platinum Metals. Rev.* **2006**, *50*, 81-94.

(71) Valenti, D. J.; Wagener, K. B. *Macromolecules* **1998**, *31*, 2764-2773.

(72) Walba, D. M.; Keller, P.; Shao, R.; Clark, N. A.; Hillmyer, M.; Grubbs, R. H. *J. Am. Chem. Soc.* **1996**, *118*, 2740-2741.

(73) Courchay, F. C.; Baughman, T. W.; Wagener, K. B. *J. Organomet. Chem* **2006**, *691*, 585-594.

(74) Opstal, T.; Verpoort, F. *J. Mol. Cat.: A* **2003**, *200*, 49-61.

(75) Randl, S.; Connon, S. J.; Blechert, S. *Chem. Commun.* **2001**, 1796-1797.

(76) Tonzetich, Z. J.; Lam, Y. C.; Müller, P.; Schrock, R. R. *Organometallics* **2007**, *26*, 475-477.

(77) Sashuk, V.; Grela, K. *J. Mol. Cat.: A* **2006**, *257*, 59-66.

(78) Tsai, Y.; Diaconescu, P. L.; Cummins, C. C. *Organometallics* **2000**, *19*, 5260-5262.

(79) Fürstner, A.; Mathes, C.; Lehmann, C. W. *J. Am. Chem. Soc.* **1999**, *121*, 9453-9454.

(80) Zhang, W.; Kraft, S.; Moore, J. S. *J. Am. Chem. Soc.* **2004**, *126*, 329-335.

(81) Cho, H. M.; Weissman, H.; Wilson, S. R.; Moore, J. S. *J. Am. Chem. Soc.* **2006**, *128*, 14742-14743.

(82) Jafarpour, L.; Nolan, S. P. *J. Organomet. Chem* **2001**, *617-618*, 17-27.

(83) Hong, S. H.; Grubbs, R. H. *J. Am. Chem. Soc.* **2006**, *128*, 3508-3509.

(84) Feher, F. J.; Tajima, T. L. *J. Am. Chem. Soc.* **1994**, *116*, 2145-2146.

(85) Funk, T. W.; Berlin, J. M.; Grubbs, R. H. *J. Am. Chem. Soc.* **2006**, *128*, 1840-1846.

(86) Singh, R.; Czekelius, C.; Schrock, R. R.; Müller, P.; Hoveyda, A. H. *Organometallics* **2007**, *26*, 2528-2539.

(87) Fujimura, O.; Grubbs, R. H. *J. Am. Chem. Soc.* **1996**, *118*, 2499-2500.

(88) Fujimura, O.; Fu, G. C.; Grubbs, R. H. *J. Org. Chem.* **1004**, *59*, 4029-4031.

(89) Sattely, E. S.; Cortez, G. A.; Moebius, D. C.; Schrock, R. R.; Hoveyda, A. H. *J. Am. Chem. Soc.* **2005**, *127*, 8526-8533.

(90) Patton, J. T.; Boncella, J. M.; Wagener, K. B. *Macromolecules* **1992**, *25*, 3862-3867.

(91) Blosch, L. L.; Abboud, K.; Boncella, J. M. *J. Am. Chem. Soc.* **1991**, *113*, 7066-7068.

(92) Lefebvre, F.; Leconte, M.; Pagano, S.; Mutch, A.; Basset, J. *Polyhedron* **1995**, *14*, 3209-3226.

(93) Wengrovius, J. H.; Sancho, J.; Schrock, R. R. *J. Am. Chem. Soc.* **1981**, *103*, 3932-3934.

(94) Castarlenas, R.; Esteruelas, M. A.; Oñate, E. *Organometallics* **2007**, *26*, 2129-2132.

(95) Castarlenas, R.; Esteruelas, M. A.; Onate, E. *Organometallics* **2005**, *24*, 4343-4346.

(96) Grubbs, R. H. *J. Mol. Struct.* **1994**, *A31*, 1829-1833.

(97) Bazan, G. C.; Shrock, R. R.; O'Regan, M. B. *Organometallics* **1991**, *10*, 1062-1067.

(98) Kress, J.; Osborn, J. A.; Greene, R. M. E.; Irvin, K. J.; Rooney, J. J. *J. Am. Chem. Soc.* **1987**, *109*, 899-901.

(99) Schrodi, Y.; Pederson, R. L. *Aldrichimica Acta* **2007**, *40*, 45-52.

(100) Colacino, E.; Marinez, J.; Lamaty, F. *Coord. Chem. Rev.* **2007**, *251*, 126-764.

(101) Sanford, M. S.; Love, J. A.; Grubbs, R. H. *J. Am. Chem. Soc.* **2001**, *123*, 6543-6554.

(102) Dias, E. L.; Nguyen, S. T.; Grubbs, R. H. *J. Am. Chem. Soc.* **1997**, *119*, 3887-3897.

(103) Lynn, D. M.; Mohr, B.; Grubbs, R. H.; Henling, L. M.; Day, M. W. *J. Am. Chem. Soc.* **2000**, *122*, 6601-6609.

(104) Conrad, J. C.; Snelgrove, J. L.; Eeelman, M. D.; Hall, S.; Fogg, D. E. *J. Mol. Cat.: A* **2006**, *254*, 105-110.

(105) Vehlow, K.; Maechling, S.; Köhler, K.; Blechert, S. *Tetrahedron Lett.* **2006**, *47*, 8617-8620.

(106) Jacobsen, H. *J. Chem. Soc., Dalton Trans.* **2006**, 2214-2224.

(107) Ulman, M.; Grubbs, R. H. *Organometallics* **1998**, *17*, 2484-2489.

(108) Adlhart, C.; Hinderling, C.; Baumann, H.; Chen, P. *J. Am. Chem. Soc.* **2000**, *122*, 8204-8214.

(109) Sanford, M. S.; Ulman, M.; Grubbs, R. H. *J. Am. Chem. Soc.* **2001**, *123*, 749-750.

(110) Adlhart, C.; Chen, P. *Helv. Chim. Acta.* **2000**, *83*, 2192-2196.

(111) Correa, A.; Cavallo, L. *J. Am. Chem. Soc.* **2006**, *128*, 13352-13353.

(112) Jordaan, M.; van Helden, P.; van Sittert, C. G. C. E.; Vosloo, H. C. M. *J. Mol. Cat.: A* **2006**, *254*, 145-154.

(113) Ung, T.; Hejl, A.; Grubbs, R. H.; Schrodi, Y. *Organometallics* **2004**, *23*, 5399-5401.

(114) Benitez, D.; Goddard, W. A. *J. Am. Chem. Soc.* **2005**, *127*, 12218-12219.

(115) Anderson, D. R.; Hickstein, D. D.; O'Leary, D. J.; Grubbs, R. H. *J. Am. Chem. Soc.* **2006**, *128*, 8386-8387.

(116) Hinderling, C.; Adlhart, C.; Chen, P. *Angew. Chem. Int. Ed.* **1998***, 37*, 2685-2689.

(117) Occhipinti, G.; Bjørsvik, H.; Jensen, V. R. *J. Am. Chem. Soc.* **2006***, 128*, 6952-6964.

(118) Cavallo, L. *J. Am. Chem. Soc.* **2002***, 124*, 8965-8973.

(119) Costabile, C.; Cavallo, L. *J. Am. Chem. Soc.* **2004***, 126*, 9592-9600.

(120) Aagaard, O. M.; Meier, R. J.; Buda, F. *J. Am. Chem. Soc.* **1998***, 120*, 7174-7182.

(121) Fomine, S.; Vargas, S. M.; Tlenkopatchev, M. A. *Organometallics* **2003***, 22*, 93-99.

(122) Suresh, C. H.; Koga, N. *Organometallics* **2004***, 23*, 76-80.

(123) Huang, J.; Stevens, E. D.; Nolan, S. P.; Petersen, J. L. *J. Am. Chem. Soc.* **1999***, 121*, 2674-2678.

(124) Adlhart, C.; Chen, P. *J. Am. Chem. Soc.* **2004***, 126*, 3496-3510.

(125) Louie, J.; Grubbs, R. H. *Organometallics* **2002***, 21*, 2153-2164.

(126) Burdett, K. A.; Harris, L. D.; Margl, P.; Maughon, B. R.; Mokhtar-Zadeh, T.; Saucier, P. C.; Wasserman, E. P. *Organometallics* **2004***, 23*, 2027-2047.

(127) Bernardi, F.; Bottoni, A.; Miscione, G. P. *Organometallics* **2003***, 22*, 940-947.

(128) Janse van Rensburg, W.; Steynberg, P. J.; Kirk, M. M.; Meyer, W. H.; Forman, G. S. *J. Organomet. Chem* **2007***, 691*, 5312-5325.

(129) Forman, G. S.; McConnell, A. E.; Hanton, M. J.; Slawin, A. M. Z.; Tooze, R. P.; van Rensburg, W .J.; Meyer, W. H.; Dwyer, C.; Kirk, M. M.; Serfontein, D. W. *Organometallics* **2004***, 23*, 4824-4827.

(130) Forman, G. S.; McConnell, A. E.; Tooze, R. P.; Janse van Rensburg, W.; Meyer, W. H.; Kirk, M. M.; Dwyer, C. L.; Serfontein, D. W. *Organometallics* **2005***, 24*, 4528-4542.

(131) Bourissou, D.; Guerret, O.; Gabbai, F. P.; Bertrand, G. *Chem. Rev.* **2000***, 100*, 39-92.

(132) Volland, M. A. O.; Rominger, F.; Eisentrager, F.; Hofmann, P. *J. Organomet. Chem* **2002***, 641*, 220-226.

(133) Nieczypor, P.; Van Leeuwen, P. W. N. M.; Mol, J. C.; Lutz, M.; Spek, A. L. *J. Organomet. Chem* **2001***, 625*, 58-66.

(134) Schwab, P.; Grubbs, R. H.; Ziller, J. W. *J. Am. Chem. Soc.* **1996***, 118*, 100-110.

(135) Wu, Z.; Benedicto, A. D.; Grubbs, R. H. *Macromolecules* **1993***, 26*, 4975-4977.

(136) Wijmans, C. M. *Macromolecules* **1996***, 29*, 789-791.

(137) Fu, G. C.; SonBinh T.N.; Grubbs, R. H. *J. Am. Chem. Soc.* **1993***, 115*, 9856-9857.

(138) Miller, S. J.; Kim, S.; Chen, Z.; Grubbs, R. H. *J. Am. Chem. Soc.* **1995***, 117*, 2108-2109.

(139) Miller, S. J.; Grubbs, R. H. *J. Am. Chem. Soc.* **1995***, 115*, 5855-5856.

(140) Kim, S.; Bowden, N.; Grubbs, R. H. *J. Am. Chem. Soc.* **1994***, 116*, 10801-10802.

(141) Zuercher, W. J.; Hashimoto, M.; Grubbs, R. H. *J. Am. Chem. Soc.* **1996***, 118*, 6634-6640.

(142) Borer, B. C.; Deerenberg, S.; Bieräugel, H.; Pandit, U. K. *Tetrahedron Lett.* **1994***, 35*, 3191-3194.

(143) Andrade, R. B.; Plante, O. J.; Melean, L. G.; Seeberger, P. H. *Org. Lett.* **1999***, 1*, 1811-1814.

(144) Nicola, T.; Brenner, M.; Donsbach, K.; Kreye, P. *Org. Process Res. Dev.* **2005***, 9*, 513-515.

(145) Arduengo, A. J. I. *Acc. Chem. Res.* **1999***, 32*, 913-921.

(146) Huang, J.; Schanz, H.; Stevens, E. D.; Nolan, S. P. *Organometallics* **1999**, *18*, 5375-5380.

(147) Ackerman, L.; Fürstner, A.; Weskamp, T.; Kohl, F. J.; Hermann, W. A. *Tetrahedron Lett.* **1999**, *40*, 4787-4790.

(148) Weskamp, T.; Kohl, F. J.; Hieringer, W.; Gleich, D.; Herrmann, W. A. *Angew. Chem. Int. Ed.* **1999**, *38*, 2416-2419.

(149) Lord, R. L.; Wang, H.; Vieweger, M.; Baik, M. *J. Organomet. Chem* **2006**, *691*, 5505-5512.

(150) Scholl, M.; Trnka, T. M.; Morgan, J. P.; Grubbs, R. H. *Tetrahedron Lett.* **1999**, *40*, 2247-2250.

(151) Garbaccio, R. M.; Stachel, S. J.; Baeschlin, D. K.; Danishefsky, S. J. *J. Am. Chem. Soc.* **2001**, *123*, 10903-10908.

(152) Scholl, M.; Ding, S.; Lee, C. W.; Grubbs, R. H. *Org. Lett.* **1999**, *1*, 953-956.

(153) Ritter, T.; Hejl, A.; Wenzel, A. G.; Funk, T. W.; Grubbs, R. H. *Organometallics* **2006**, *25*, 5740-5745.

(154) Vehlow, K.; Maechling, S.; Blechert, S. *Organometallics* **2006**, *25*, 25-28.

(155) Dinger, M. B.; Nieczypor, P.; Mol, J. C. *Organometallics* **2003**, *22*, 5291-5296.

(156) Van Veldhuizen, J. J.; Garber, S. B.; Kingsbury, J. S.; Hoveyda, A. H. *J. Am. Chem. Soc.* **2002**, *124*, 4954-4955.

(157) Seiders, T. J.; Ward, D. W.; Grubbs, R. H. *Org. Lett.* **2001**, *3*, 3225-3228.

(158) Amundsen, L. H.; Nelson, L. S. *J. Am. Chem. Soc.* **1954**, *73*, 242-244.

(159) Fürstner, A.; Thiel, O. R.; Ackermann, L.; Schanz, H.; Nolan, S. P. *J. Org. Chem.* **2000**, *65*, 2204-2207.

(160) Schanz, H.; Jafarpour, L.; Stevens, E. D.; Nolan, S. P. *Organometallics* **1999**, *18*, 5187-5190.

(161) Love, J. A.; Sanford, M. S.; Day, M. W.; Grubbs, R. H. *J. Am. Chem. Soc.* **2003**, *125*, 10103-10109.

(162) Pruhs, S.; Lehmann, C. W.; Furstner, A. *Organometallics* **2004**, *23*, 280-287.

(163) Jafarpour, L.; Heck, M.; Baylon, C.; Lee, H. M.; Mioskowski, C.; Nolan, S. P. *Organometallics* **2002**, *21*, 671-679.

(164) Yao, Q.; Zhang, Y. *J. Am. Chem. Soc.* **2004**, *126*, 74-75.

(165) Kuriyama, T.; Schmidt, T. J.; Okuyama, E.; Ozoe, Y. *Biorg. & Med. Chem.* **2002**, *10*, 1873-1881.

(166) Dowden, J.; Savović, J. *Chem. Commun.* **2001**, 37-38.

(167) Verlow, K.; Maechling, S.; Köhler, K.; Blechert, S. *J. Organomet. Chem* **2006**, *691*, 5267-5277.

(168) Hoveyda, A. H.; Gillingman, D. G.; Van Veldhuizen, J. J.; Katoaka, O.; Garber, S. B.; Kingsbury, J. S.; Harrity, J. P. A. *Org. Biomol. Chem.* **2004**, *2*, 8-23.

(169) Nguyen, S. T.; Grubbs, R. H. *J. Organomet. Chem* **1995**, *497*, 195-200.

(170) Nieczypor, P.; Buchowicz, W.; Meester, W. J. N.; Rutjies, F. P. J. T.; Mol, J. C. *Tetrahedron Lett.* **2001**, *42*, 7103-7105.

(171) Ahmed, M.; Barrett, A. G. M.; Braddock, D. C.; Cramp, S. M.; Procopiou, P. A. *Tetrahedron Lett.* **1999**, *40*, 8657-8562.

(172) Halback, T. S.; Mix, S.; Fishcer, D.; Maechling, S.; Krause, J. O.; Sievers, C.; Blechert, S.; Nuyken, O.; Buchmeiser, M. R. *J. Org. Chem.* **2005**, *70*, 4687-4694.

(173) Kingsbury, J. S.; Hoveyda, A. H. *J. Am. Chem. Soc.* **2005**, *127*, 4510-4517.

(174) Garber, S. B.; Kingsbury, J. S.; Gray, B. L.; Hoveyda, A. H. *J. Am. Chem. Soc.* **2000**, *122*, 8168-8179.

(175) Schoeller, W. W.; Schroeder, D.; Rozhenko, A. B. *J. Organomet. Chem* **2005**, *690*, 6079-6088.

(176) Garbaccio, R. M.; Danishefsky, S. J. *Org. Lett.* **2000**, *2*, 3127-3129.

(177) Fürstner, A.; Müller, C. *Chem. Commun.* **2005**, *44*, 5583-5585.

(178) Lee, C. W.; Grubbs, R. H. *J. Org. Chem.* **2001**, *66*, 7155-7158.

(179) Van de Weghe, P.; Bisseret, P.; Blanchard, N.; Eustache, J. *J. Organomet. Chem* **2006**, *691*, 5078-5108.

(180) Chao, W.; Weinreb, S. M. *Org. Lett.* **2003**, *5*, 2505-2507.

(181) Garber, S. B.; Kingsbury, J. S.; Gray, B. L.; Hoveyda, A. H. *J. Am. Chem. Soc.* **2001**, *123*, 3186-3186.

(182) Khidekel, N.; Hsieh-Wilson, L. C. *Org. Biomol. Chem.* **2004**, 1-7.

(183) Gessler, S.; Randl, S.; Blechert, S. *Tetrahedron Lett.* **2000**, *41*, 9973-9976.

(184) Van Veldhuizen, J. J.; Campbell, J. E.; Giudici, R. E.; Hoveyda, A. H. *J. Am. Chem. Soc.* **2005**, *127*, 6877-6882.

(185) Bujok, R.; Bieniek, M.; Masnyk, M.; Michrowska, A.; Sarosiek, A.; Stępowska, H.; Arlt, D.; Greia, K. *J. Org. Chem.* **2004**, *69*, 6894-6896.

(186) Yao, Q.; Sheets, M. *J. Organomet. Chem* **2005**, *690*, 3577-3584.

(187) Kingsbury, J. S.; Harrity, J. P. A.; Bonitatebus, P. J.; Hoveyda, A. H. *J. Am. Chem. Soc.* **1999**, *121*, 791-799.

(188) Bieniek, M.; Bujok, R.; Cabaj, M.; Lugan, N.; Lavigne, G.; Arit, D.; Grela, K. *J. Am. Chem. Soc.* **2006**, *128*, 13652-13653.

(189) Zaja, M.; Connon, S. J.; Dunne, A. M.; Rivard, M.; Buschmann, N.; Jiricek, J.; Blechert, S. *Tetrahedron* **2003**, *59*, 6545-6558.

(190) Michrowska, A.; Bujok, R.; Harutyunyan, S.; Sashuk, V.; Dolgonos, G.; Grela, K. *J. Am. Chem. Soc.* **2004**, *126*, 9318-9325.

(191) Tsuji, J.; Hashiguchi, S. *Tetrahedron Lett.* **1980**, *21*, 2955-2958.

(192) Itô, S.; Fujise, Y.; Sato, M. *Tetrahedron Lett.* **1969**, *10*, 691-694.

(193) Camps, P.; Muñoz-Torrero, D. *Tetrahedron Lett.* **1994***, 35*, 3187-3190.

(194) Fürstner, A.; Kindler, N. *Tetrahedron Lett.* **1996***, 37*, 7005-7008.

(195) Kim, S. H.; Figueroa, I.; Fuchs, P. L. *Tetrahedron Lett.* **1997***, 38*, 2601-2604.

(196) Dyatkin, A. B. *Tetrahedron Lett.* **1997***, 38*, 2065-2066.

(197) Linderman, R. J.; Siedlecki, J.; O'Neill, S. A.; Sun, H. *J. Am. Chem. Soc.* **1997***, 119*, 6919-6920.

(198) Heron, N. M.; Adams, J. A.; Hoveyda, A. H. *J. Am. Chem. Soc.* **1997***, 119*, 6205-6206.

(199) Visser, M. S.; Heron, N. M.; Didiuk, M. T.; Sagal, J. F.; Hoveyda, A. H. *J. Am. Chem. Soc.* **1996***, 118*, 4291-4298.

(200) Martinez, L. E.; Nugent, W. A.; Jacobsen, E. N. *J. Org. Chem.* **1996***, 61*, 7963-7966.

(201) Crimmins, M. T.; King, B. W. *J. Org. Chem.* **1996***, 61*, 4192-4193.

(202) Miller, S. J.; Blackwell, H. E.; Grubbs, R. H. *J. Am. Chem. Soc.* **1996***, 118*, 9606-9614.

(203) Clark, T. D.; Ghadiri, M. R. *J. Am. Chem. Soc.* **1995***, 117*, 12364-12365.

(204) Garro-Hélion, F.; Guibé, F. *Chem. Commun.* **1996**, 691-692.

(205) Barrett, A. G. M.; Baugh, S. P. D.; Gibson, V. C.; Giles, M. R.; Marshall, E. L.; Procopiou, P. A. *Chem. Commun.* **1996**, 2231-2232.

(206) Barrett, A. G. M.; Baugh, S. P. D.; Gibson, V. C.; Giles, M. R.; Marshall, E. L.; Procopiou, P. A. *Chem. Commun.* **1997**, 155-156.

(207) Hammer, K.; Undheim, K. *Tetrahedron* **1997***, 53*, 2309-2322.

(208) Hammer, K.; Undheim, K. *Tetrahedron* **1997***, 53*, 5925-5936.

(209) Sweeney, W. A. USA Patent 5057638, 1991.

(210) Oikawa, T.; Ookoshi, T.; Tanaka, T.; Yamamoto, T.; Onaka, M. *Microporous and Mesoporous Materials* **2004**, *74*, 93-103.

(211) http://www.materia-inc.com/index.html. Accessed August 2007.

(212) Grubbs, R. H.; Pederson, R. L. USA Patent 6696597, 2004.

(213) Taylor, R. E.; Haley, J. D. *Tetrahedron Lett.* **1997**, *38*, 2061-2064.

(214) Meng, D.; Su, D.; Balog, A.; Bertinato, P.; Sorensen, E. J.; Danishefsky, S. J.; Zheng, Y.; Chou, T.; He, L.; Horwitz, S. B. *J. Am. Chem. Soc.* **1997**, *119*, 2733-2734.

(215) Zaminer, J.; Stapper, C.; Blechert, S. *Tetrahedron Lett.* **2002**, *43*, 6739-6741.

(216) Overkleeft, H. S.; Pandit, U. K. *Tetrahedron Lett.* **1996**, *37*, 547-550.

(217) Hirama, M.; Oishi, T.; Uehara, H.; Inoue, M.; Maruyama, M.; Oguri, H.; Satake, M. *Science* **2001**, *294*, 1904-1907.

(218) Inoue, M.; Miyazaki, K.; Ishihara, Y.; Tatami, A.; Ohnuma, Y.; Kawada, Y.; Komano, K.; Yamashita, S.; Lee, N.; Hirama, M. *J. Am. Chem. Soc.* **2006**, *128*, 9352-9354.

(219) Inoue, M.; Miyazaki, K.; Uehara, H.; Maruyama, M.; Hirama, M. *PNAS* **2004**, *101*, 12013-12018.

(220) Nicolaou, K. C.; Postema, M. H. D.; Claiborne, C. F. *J. Am. Chem. Soc.* **1996**, *118*, 1565-1566.

(221) Nicolaou, K. C.; Postema, M. H. D.; Yue, E. W.; Nadin, A. *J. Am. Chem. Soc.* **1996**, *118*, 10335-10336.

(222) Fournier, P. A.; Collins, S. K. *Organometallics* **2007**, *26*, 2945-2949.

(223) Fujimura, O.; de la Mata, F.J.; Grubbs, R. H. *Organometallics* **1996**, *15*, 1865-1871.

(224) Wu, Z.; Nguyen, S. T.; Grubbs, R. H.; Ziller, J. W. *J. Am. Chem. Soc.* **1995**, *117*, 5503-5511.

(225) Courchay, F. C.; Sworen, J. C.; Ghiviriga, I.; Abboud, K. A.; Wagener, K. B. *Organometallics* **2006**, *25*, 6074-6086.

(226) Kirkland, T.A. Lynn, D.M.; Grubbs, R. H. *J. Org. Chem.* **1998**, *63*, 9904-9909.

(227) Burton, S. G. Ph.D. Thesis, Rhodes University, **1993**.

(228) Wellington, K. W. Ph.D. Thesis, Rhodes University, **1999**.

(229) Hagemann, J. P. *Ph.D.* Thesis, Rhodes University, **1997**.

(230) Daubinet, A. Ph.D. Thesis, Rhodes University, **2001**.

(231) Tshikudo, T. R. MSc Thesis, Rhodes University, **2002**.

(232) Gxoyiya, B. MSc Thesis, Rhodes University, **2003**.

(233) Magqi, N. MSc Thesis, Rhodes University, **2007**.

(234) Sabbagh, I. T. Ph.D. Thesis, Rhodes University, **2005**.

(235) Magqi, N. *MSc Thesis, Rhodes University* **2007**.

(236) Amoroso, D.; Yap, G. P. A.; Fogg, D. E. *Organometallics* **2002**, *21*, 3335-3343.

(237) Conrad, J. C.; Amoroso, D.; Czechura, P.; Yap, G. P. A.; Fogg, D. E. *Organometallics* **2003**, *22*, 3634-3636.

(238) Ulman, M.; Grubbs, R. H. *J. Org. Chem.* **1999**, *64*, 7202-7207.

(239) Chang, S.; Jones, L.; Wang, C.; Henling, L. M.; Grubbs, R. H. *Organometallics* **1998**, *17*, 3460-3465.

(240) Coalter, J. N.; Bollinger, J. C.; Eisenstein, O.; Caulton, K. G. *New. J. Chem* **2000**, *24*, 925-927.

(241) Buchowicz, W.; Mol, J. C.; Lutz, M.; Spek, A. L. *J. Organomet. Chem.* **1999**, *588*, 205-210.

(242) Hahn, F.; Paas, M.; Fröhlich, R. *J. Organomet. Chem.*, **2005**, *690*, 5816-5821.

(243) Wilkinson, G.; In *Comprehensive Coordination Chemistry;* Pergamon Press: Oxford, 1987; Vol. 2, pp 443.

(244) Braddock, D. C.; Tanaka, K.; Chadwick, D.; Böhm, V. P. W.; Roeper, *Tetrahedron Lett.* **2007**, *48*, 5301-5303.

(245) Sabbagh, I. T.; Kaye, P. T. *J. Mol. Struct., THEOCHEM.* **2006**, *763*, 37-42.

(246) CambridgeSoft.Com **2000**, *6.02*.

(247) Vougioukalakis, G. C.; Grubbs, R. H. *Organometallics* **2007**, *26*, 2469-2472.

(248) Clavier, H.; Petersen, J. L.; Nolan, S. P. *J. Organomet. Chem* **2006**, *691*, 5444-5447.

(249) McMurry, J. In *Organic Chemistry;* Brooks/Cole Publishing Company: Pacific Grove, California, 1992.

(250) Conrad, J. C.; Camm, K. D.; Fogg, D. E. *Inorg. Chim. Acta* **2006**, *359*, 1967-1973.

(251) Chang, S.; Jones, L.; Wang, L. M.; Henling, M.; Grubbs, R. H. *Organometallics* **1998**, *17*, 3460.

(252) Conrad, J. C.; Snelgrove, J. L.; Eeelman, M. D.; Hall, S.; Fogg, D. E. *J. Mol. Catal.: A,* **2006**, *254*, 105-110.

(253) Straub, B. F. *Adv. Synth. Catal.* **2007**, *349*, 204-214.

(254) Binyamin, I.; Pailloux, S.; Duesler, E. N.; Rapko, B. M.; Paine, R. T. *Inorg. Chem.* **2006**, *45*, 5886-5892.

(255) Soli, E. D.; Manoso, A. S.; Patterson, M. C.; DeShong, P.; Favor, D. A.; Hirschmann, R.; Smith, A. B. *J. Org. Chem.* **1999**, *64*, 3171-3177.

(256) Furniss, B. S.; Hannaford, A. J.; Smith, A. B.; Tatchell, A. R. In *Vogel's Textbook of Practical Organic Chemistry,* Longman Scientific and Technical: New York, **1989**.

(257) Fache, F.; Schulz, E.; Tommasino, M. L.; Lemaire, M. *Chem. Rev.* **2000**, *100*, 2159-2232.

(258) Miller, K. J.; Kitagawa, T. T.; Abu-Omar, M. M. *Organometallics* **2001**, *20*, 4403-4412.

(259) Rodriguez, M.; Romero, I.; Llobet, A.; Deronzier, A.; Biner, M.; Parella, T.; Stoeckli-Evans, H. *Inorg. Chem.* **2001**, *40*, 4150-4156.

(260) Matsuo, Y.; Mashima, K.; Tani, K. *Organometallics* **2001**, *20*, 3510-3518.

(261) Arnáiz, A.; Cuevas, J. V.; García-Herbosa, G.; Carbayo, A.; Casares, J. A.; Cutierrez-Puebla, E. *J. Chem. Soc., Dalton Trans.* **2002**, 2581-2586.

(262) Zheng, C.; Dai, H.; Merritt, M. E.; Malloy, C.; Pan, C. Y.; Li, W. *J. Am. Chem. Soc.* **2005**, *127*, 16178-16188.

(263) Scrimin, P.; Tecilla, P.; Toellato, U.; Valle, G.; Veronese, A. *Tetrahedron* **1995**, *51*, 527-538.

(264) Chen, X.; Du, D.; Hua, W. *Tetrahedron: Asym.* **2003**, *14*, 999-1007.

(265) Marchand, A. P.; Chong, H.; Alihodžić, S. *Tetrahedron* **1999**, *55*, 9687-9696.

(266) Cerius^2® Molecular Simulations, San Diego **2000**, *4.5.*

(267) Wavefunction, Inc., 18401 Von Karman Avenue, Suite 370, Irvine, CA 92612.

(268) Zhang, J.; Leitus, G.; Ben-David, Y.; Milstein, D. *J. Am. Chem. Soc.* **2005**, *127*, 10840-10841.

(269) Hayes, B. L. In *Microwave Synthesis: Chemistry at the Speed of Light;* CEM Publishing: Matthews, USA, **2002**.

(270) Perrin, D. D.; Armarego, L. F. In *Purification of Laboratory Chemicals;* Pergamon Press: Oxford, **1988**.

(271) Rybak-Akimova, E. V.; Nazarenko, A. Y.; Chen, L.; Krieger, P. W.; Herrera, A. M.; Tarasov, V. V.; Robinson, P. D. *Inorg. Chim. Acta* **2001**, *324*, 1-15.

(272) Gemel, C.; Folting, K.; Caulton, K. G. *Inorg. Chem.* **2000**, *39*, 1593-1597.

(273) Hehre, W.J. In *A Guide To Molecular Mechanics And Quantum Chemical Calculations;* Wavefunction, Inc. Irvine, CA, **2003**.